HYDROGENERATION REPRESENTATION IN PRODUCTION COST MODELING OF LONG-TERM TRANSMISSION STUDIES

By Christie M. Dennis

A Thesis

Submitted in Partial Fulfillment

of the Requirements for the Degree of

Master of Science

in Engineering

Northern Arizona University

May 2011

Approved:

_____

Thomas Acker, Ph.D., Chair

_____

Allison Kipple, Ph.D.

_____

Peter Vadasz, Ph.D.

ABSTRACT

HYDROGENERATION REPRESENTATION IN PRODUCTION COST MODELING OF LONG-TERM TRANSMISSION STUDIES

Christie M. Dennis

Transmission planning in the US is more important today than it has ever been. In today's deregulated power industry, there is often no single entity that is responsible for installing and maintaining transmission lines, and there is little incentive to invest in them. Long-term transmission planning is therefore key in utilizing the current transmission system as efficiently as possible, as well as for determining the most cost-effective options, ahead of time, when new transmission is needed. The Western Electricity Coordinating Council, recognizing the importance of interconnection-wide transmission planning, formed the Transmission Expansion Planning Policy Committee (TEPPC) in 2006. TEPPC utilizes the production cost model (PCM) PROMOD IV© to model the Western Interconnection for these studies. In certain geographic regions, a high level of hydropower penetration necessitates careful consideration of hydrogeneration models used in the PCM to produce the most realistic system results. Realistic system simulations, in this work, are those in which the hydrogeneration responds to system load variations as well as system energy price variations, as would occur in "real-time". This study first details the hydro modeling methods (Proportional Load Following (PLF) and Hydrothermal Co-optimization (HTC)) utilized by TEPPC for improving hourly hydrogeneration time series representations in transmission planning studies, and demonstrates the effectiveness of these models over those traditionally used by performing a 2019 transmission simulation study. In addition, two simulation test cases with different wind penetration levels were performed to determine how well the PLF and HTC were able to respond to increased levels of renewable generation. The results of this study indicate that the PLF-modeled hydrogeneration of applicable plants is able to follow load variations more effectively than historical data modeling or peak shave modeling, and that

HTC-modeled hydrogeneration is able to respond to energy price fluctuations more effectively than other models. Furthermore, the wind penetration comparisons demonstrated that the use of PLF and HTC hydromodeling in a PCM resulted in simulation results capable of reflecting realistic modifications to hydropower dispatch expected with wind integration.

ACKNOWLEDGEMENTS

First, I would like to thank Tom Chisholm from the Bonneville Power Administration for providing the PLF model and data for the PLF analysis, and for providing much insight into the Northwest hydrogeneration system, as well as serving on the thesis committee. Next, I would like to thank Heidi Pacini from the Western Electricity Coordinating Council for running the PCM simulations in PROMOD for the 2019 simulation study analyzed herein, and being willing to answer any and all questions. I would also like to thank Dr. Tom Acker for his support and advising throughout the entire process. Finally, thanks go to Dr. Allison Kipple and Dr. Peter Vadasz for serving on this thesis committee.

Table of Contents

LIST OF TABLES

LIST OF FIGURES

LIST OF ACRONYMS

AI	Alaskan Interconnection
AVA	Avista
BA	Balancing Authority
BPA	Bonneville Power Administration
CC	Correlation Coefficient
CEM	Coordination Equation Method
CHPD	Chelan County Public Utility District
COI	California Oregon Intertie
DCOPF	DC Optimized Power Flow
DOPD	Douglas County Public Utility District
DP	Dynamic Programming
DTC	Data Test Case
EHV	Extra-High Voltage AC
EI	Eastern Interconnection
ERCOT	Electric Reliability Council of Texas
ERO	Electric Reliability Organization
EWITS	Eastern Wind Integration and Transmission Study
FERC	Federal Energy Regulatory Commission
GSF	Generation Shift Factor
HC	Hourly Chronological
HCHP	Hourly Chronological Hydrogeneration Profile
HD	Historical Data
HTC	Hydrothermal Co-Optimization
HS	Hydrothermal Scheduling
HVDC	High Voltage Direct Current

LC	Load Cost
LMP	Locational Marginal Price
LP	Linear Programming
LTHS	Long-Term Hydrothermal Scheduling Problem
MIP	Mixed Integer Program
MILP	Mixed Integer Linear Programming
MNW	Montana Northwest
NERC	North American Electric Reliability Corporation
NJD	North of John Day
NLP	Non-Linear Programming
NREL	National Renewable Energy Laboratory
NW	Northwest
NWPP	Northwest Power Pool
O&M	Operation and Maintenance
OTC	Operational Transfer Capability
PCM	Production Cost Model
PDCI	Pacific DC Intertie
PGN	Portland General Electric
PLA	Piecewise Linear Approximation
PLF	Proportional Load Following
PS	Peak Shaving
QI	Quebec Interconnection
RMATS	Rocky Mountain Area Transmission Study
RPS	Renewable Portfolio Standards
RS	Reliability Standards
SA	Simulated Annealing
SCOPF	Security Constrained Optimal Power Flow
SCED	Security Constrained Economic Dispatch

SCL	Seattle City and Light
SCUC	Security Constrained Unit Commitment
STHS	Short-Term Hydrothermal Scheduling Problem
TEP	Transmission Expansion Planning
TEPPC	Transmission Expansion Planning Policy Committee
TTC	Total Transfer Capability
TVA	Treasure Valley
WCN	West of Cascades North
WCS	West of Cascades South
WECC	Western Electricity Coordinating Council
WI	Western Interconnection

1 INTRODUCTION

1.1 U.S. Power System and WECC

The United States electrical system is a complicated entity that attempts to balance the demand of electricity from the public with operating cost-, security-, and transmission-optimized energy generation from a multitude of sources. It consists of three distinct "grids" made up of a network of transmission lines: the Western Interconnection (WI), the Eastern Interconnection (EI), and the Electric Reliability Council of Texas (ERCOT). These grids are connected to each other as well as to other North American grids such as the Quebec Interconnection (QI), and Alaskan Interconnection (AI), as depicted in Figure 1.1. The operation of each of the U.S. grids is overseen by the North American Electric Reliability Corporation (NERC) in order to "maintain and improve the reliability of North America's bulk power system" (About NERC: Company Overview, 2011). NERC was formed as the electric reliability organization (ERO) designated by the Energy Policy Act of 2005, that is certified by the Federal Energy Regulatory Commission (FERC) to generate and enforce electricity reliability standards (North American Electric Reliability Corporation, 2011). There are eight regional reliability entities that manage the three U.S. grids as delegated by NERC (Figure 1.1); these entities, or councils, are made up of representatives from all areas of the electricity operating system, including those from transmission operators, generators, utilities, governments, and consumers. These regional entities work to ensure that the grid delivers secure and reliable electricity to consumers, adhering to the Reliability Standards (RS) set by NERC, through work with many balancing authorities located within the region. Balancing authorities (BA) (white circles, Figure 1.1) oversee the day-to-day operations of the utilities present under their control, ensuring that NERC standards are met.

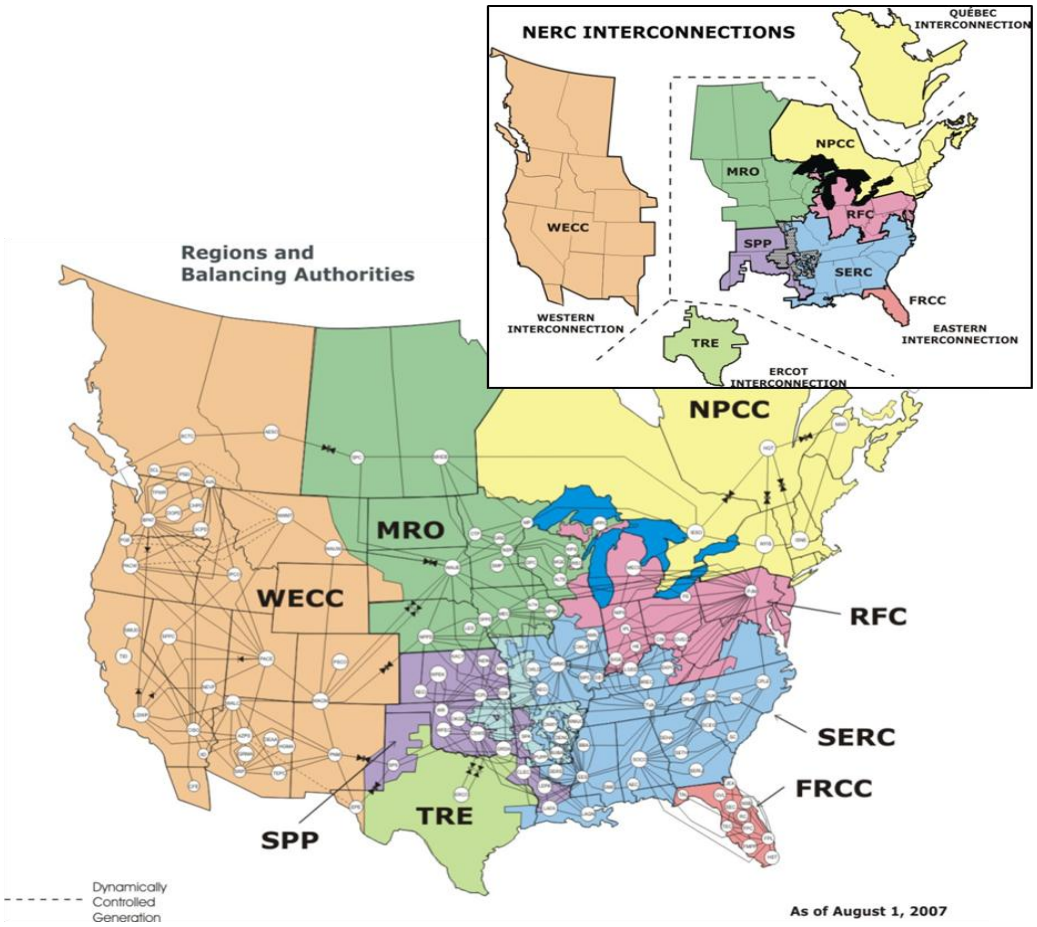

Figure 1.1: Graphical representation of North American Interconnection regions, and the associated regional entities[1]

The regional entity that oversees the operation of the WI is the Western Electricity Coordinating Council (WECC), and its mission is to assure a reliable bulk electric power system in the WI (About WECC, 2011). The WI encompasses an area of nearly 1.8 million square miles. It includes the provinces of Alberta and British Columbia, the northern portion of Baja California, Mexico, and all or parts of 14 Western states. Transmission lines span long distances connecting the Pacific Northwest, with its hydroelectric resources, to the Southwest,

[1] (http://www.nerc.com/fileUploads/File/AboutNERC/maps/NERC_Regions_BA.jpg))

with its large coal-fired and nuclear resources. The WI provides electricity to over seventy-one million customers.

One important aspect of the regional entities' function is to conduct transmission expansion planning studies. WECC, recognizing the need for a regional approach to transmission expansion planning, organized the Transmission Expansion Planning Policy Committee (TEPPC) to provide transmission expansion planning coordination and leadership across the WI. TEPPC works in close coordination with sub-regional planning groups, transmission operators, and others to perform regional economic transmission expansion planning studies in the WI. One of TEPPC's primary responsibilities is to guide the analyses and modeling for the WI's economic transmission expansion planning. As part of this responsibility, TEPPC develops an annual study program that details the transmission system expansion studies they will perform. Studies and analyses performed by TEPPC focus on plans with interconnection-wide implications and include a high-level assessment of transmission congestion and operational impacts.

TEPPC operates with a limited staff, and has limited access to hydrological data, individual plant characteristics, and specific hourly generation data due to confidentiality agreements. In order to fulfill its responsibilities with regard to regional transmission expansion planning, TEPPC has undertaken system simulation modeling of the WI using a commercial Production Cost Model (PCM), PROMOD IV©, which dispatches generation resources based on the variable cost of operation and within the operating constraints of the system. Constraints present in the operating system include those of transmission (line capacities, transfer limits), generation (plant capacities and availabilities, ramp rates, operating costs), and security (power quality regulations, reserve regulations). Inputs to the system model then consist of a load model, generation model, and a transmission model. A PCM simulation produces a cost- and security-optimized unit commitment and dispatch schedule based on these inputs. Additional simulation outputs can include transmission utilization, locational marginal pricing (LMP) valuation, and system operational costs. By simulating the power system under different

operating conditions, long-term transmission studies can investigate future transmission bottlenecks, line utilization, effects on LMP, the adequacy of resources for future loads, and the economic impacts of transmission expansion.

1.2 TEPCC Transmission Studies, Hydrogeneration Modeling

In using a PCM for transmission expansion planning, accurate inputs are necessary to achieve a realistic system simulation. PCM packages were originally designed for thermal power dominated systems; in most cases, hydrogenation dispatch is not cost optimized, therefore PCMs are often not suitable for representing the complexities that can be met in systems with significant levels of hydropower production (Nordlund, Sjelvgren, Pereira, & Bubenko, 1987). The Pacific Northwest region of the WI is just such a system; as of 2008, hydrogeneration makes up approximately 54% of the Northwest Power Pool (NWPP) operating area generation, as opposed to 29% of the generation in the entire WECC region (WECC, 2011). At this level of hydrogeneration penetration, it is essential that it be carefully modeled in order to effectively represent the impact on future transmission simulations.

Hydrogeneration differs from thermal generation in that it is not only limited by plant capacity, but also by water supply, and therefore resource availability. Hydrogeneration plants also have dispatchability constraints due to environmental or other operational factors (i.e. irrigation water deliveries, flood control, environmental release) that are sometimes unpredictable. However, in many cases hydropower plants have significant generation flexibility arising from their particular operating regime; this may include reservoir storage, consistency of resource, and minimal environmental constraints.

There are numerous methods available for modeling hydrogenation; these methods vary in data, computing, and manpower requirements. In general, the most accurate hydrogeneration models require large sets of data to account for multiple variables and multiple water

availability scenarios, which leads to the need for extensive computing resources. As mentioned previously, TEPPC has limited access to plant hydrogeneration data, therefore is presently unable to use extensive hydrogeneration modeling in their transmission studies. Additionally, the representation of hydrogeneration in a PCM is limited. Due to these limitations, hydrogeneration modeling is needed that effectively represents hydrogeneration in planning studies without requiring extensive, unit specific hydro data, providing WECC with accurate future transmission congestion conditions. TEPPC has endeavored to maximize long-term planning efficiency by developing or incorporating new hydro modeling methods that accomplish this objective.

Traditionally, TEPPC has modeled hydrogeneration using historical generation data (HD) time series. This method assumes that future generation will be similar to past generation given similar loads. Historical generation patterns reflect constraints on the hydropower system in the year from which the data was taken. However, they do not reflect constraints that may be present in future operating conditions. If loads and generation are correlated, then generation must be updated whenever loads change. In addition, load or generation discrepancies in the data year are carried forward as predictions of future discrepancies. As discussed previously, one function of TEPPC is to carry out annual transmission expansion studies, and the forecast year is set based on the requests of TEPPC's stakeholders. This can be a 10- or 20-year forecast time frame; consequently, the lack of accuracy is an issue, particularly if the flexibility of certain hydro plants is not properly factored in.

Another common hydrogeneration model used in PCM packages, and by TEPPC, is peak shaving (PS). The PS method assumes plants dispatch energy during times of highest loads subject to minimum and maximum generation constraints. In this way, the resource-limited hydrogeneration is dispatched to reduce the total operating cost of the thermal system (Simopoulos, Kavatza, & Vournas, 2007).

Two methods used by TEPPC for better integrating hydrogeneration into a PCM-based transmission planning scenario have been developed. One of these, proportional load following (PLF), is a method for improving the modeling of hydrogeneration for plants whose operation is primarily governed by load variability. PLF modeling uses as inputs monthly plant minimum and maximum operating capacity, the allowable monthly energy, and an assigned proportionality constant ("K" value) determined by the plant's ability to follow load. This greatly reduces the hydro plant data requirements compared to HD or dynamic programming, as will be discussed in a later section. Additionally, wind power generation can be incorporated into the model by adjusting the load profile used to produce the hydro shape.

The second method is the hydrothermal co-optimization (HTC) model within PROMOD. HTC allows for a portion of the generation capacity of suitable hydro plants to be cost optimized within the system constraints as are the thermal generators. In this way, the flexible portion of the plant capacity is at the disposal of the system, and more accurate transmission simulation results can be obtained. As TEPPC utilizes it, HTC relies upon a PLF-modeled hydro shape and a "p" factor, which describes the fraction of a plant's generation that is able to be cost-optimized within the full system constraints in the PCM. The use of HTC modeling has the potential to better represent the impacts that renewable generation has on a future system, since the hydrogeneration would respond to the resulting system energy price variations.

1.3 Renewables and Transmission Planning

Accurate representation of future systems in transmission and congestion studies is essential, since operational flexibility will become increasingly important with the anticipated implementation of Renewable Portfolio Standards (RPS), resulting in significant penetrations of non-dispatchable, intermittent renewable power. Most renewables are price takers (first to

be dispatched); therefore greater flexibility in the system can result in more efficient grid transmission operation, potentially reducing transmission congestion and operational costs.

Increasingly in the last decade, coordinating the operation of wind power and hydro power has been discussed as a way to offset the technical difficulties that wind power imposes on the power system (Jaramillo, Borja, & Huacuz, 2004) (Cohen, Lafrance, Krau, & Saulnier, 2003) (Pete, 2010) (Acker, Buechler, Knitter, & Conway, 2007) (Acker & Pete, Western Wind and Solar Integration Study: Hydropower Analysis, 2011). Wind power is a growing source of energy across the United States, and many policies and initiatives have been added on state, regional, and national levels. There are, however, many challenges associated with integrating wind-generated power into the power grid. The main technical difficulty encountered when wind is introduced into a power system grid is the variability of the resource and uncertainty in its prediction. Conventional grid management is challenged by the variability and uncertainty, since it relies upon predictable power output for the hours ahead, days ahead, weeks ahead, or years ahead power dispatch schedule. Variations in the power output predictions from wind facilities can cause power reliability to decrease at higher levels of wind penetration, generally those higher than 5% (Georgilakis, 2008). Hydro power is also reliant upon a variable natural resource, and has the additional operational constraints described previously. Due to the natural variations of the respective resources, and the operational constraints, both wind and hydro operate at 50% capacity or below (Acker T. , Characterization of Wind and Hydropower, 2005) (Acker T. , 2010) (Acker T. , Hydroelectric Industry's Role in Integrating Wind Energy, 2010). Hydro resource variability is on the scale of seasons to years, while wind resource variability has a scale of minutes to weeks. In coordinating the operation of wind and hydro power operations, hydro power facilities have the potential to provide virtual storage for the excess power that wind generation may produce in times of low demand, and also to provide additional ancillary services that may arise from higher levels of wind penetration. Operating wind and hydro power in concert can have the overall effect of increasing the overall flexibility of both systems, resulting in overall lower operational costs (Ancona D. ,

Krau, Lafrance, & Bezrukikh, 2003). This coordinated operation may be reflected in long-term transmission studies, resulting in more realistic system simulation.

1.4 Thesis Overview and Objectives

This thesis presents an analysis of the two hydrogeneration models developed for use in TEPPC PCM transmission simulations, PLF and HTC. These methods were developed to provide a more accurate representation of hydrogeneration, in comparison to other models used in their PCM simulations. In order to determine if these methods are effective in this regard, a 2019 case study was conducted to demonstrate the effects of utilizing these hydrogeneration models. The goal in analyzing the results of the case study is to provide an answer to the following questions:

- What constitutes a realistic system simulation?
- How is this verified?

PCM outputs such as generation, transmission flows, and LMP values are used to qualitatively and quantitatively ascertain if PLF and HTC improve the veracity of a PCM simulation.

The objectives this thesis intends to accomplish are:

1. Evaluate current literature pertaining to transmission planning, PCMs, hydrogeneration modeling in PCMs, and wind integration
2. Demonstrate the need for improving hydrogeneration modeling in PCMs used for transmission studies
3. Present two new hydrogeneration models and present a model error analysis on the novel modeling methods

4. Demonstrate improvements in the representation of hydrogeneration due to the utilization of these modeling methods in a PCM-simulated transmission study (see analysis goals above)
5. Discuss the effects of increasing wind integration in a PCM-simulated transmission study utilizing these methods
6. Discuss how the results impact the field of transmission planning

In order to evaluate the effectiveness of the PLF model as compared to the traditional HD and PS hydro modeling methods, a forecast error comparison study of 2009 data for a large hydro plant in the Pacific Northwest, Grand Coulee, was conducted. The generation forecast created for the plant using PLF and HD was compared to that of actual 2009 generation. Demonstrative results of this comparison, as well as the derivation of the *K* value, are discussed in the modeling section of this report. The HTC method is then presented, including methods for calculating the *p* factor.

The 2019 PROMOD simulation of the WI focused on varying the hydrogeneration modeling of twelve key plants in the Northwest (NW). Three scenarios were run in PROMOD to facilitate a comparison of the methods:

1. 2019 base case, standard hydrogeneration modeling[2], with 2019 wind generation levels
2. 2019 base case, with the addition of PLF hydrogeneration modeling for the 12 plants, with 2019 wind generation levels
3. 2019 base case as above, with HTC dispatch optimization of the 12 plants, with 2019 wind generation levels

In addition, the effects of renewable energy on the hydrogeneration outputs were determined by repeating three scenarios with wind capacity penetration levels decreased by 5,600 MW, the

[2] The use of HD or PS is hydro plant dependent; the specific method used in this scenario is defined in the case study description in Chapter 4.

current level of wind generation present in the NW. The results of these runs, in terms of hydrogeneration, transmission, and LMP, are discussed and compared. Finally, the advantages and disadvantages in utilizing HTC and PLF in PCM-based transmission planning are discussed, as well as the applications they may have in integrating renewable resources.

1.5 Relevance to Transmission Planning Community

The goal of a power system transmission planning study is to produce a reasonable portrayal of the system in the future, under forecasted system conditions, so that transmission needs may be identified. Once these needs are known, decisions concerning transmission system adjustments are planned for well in advance of any critical impediments to the quality of the power. The efficacy of the system simulation ultimately depends on the accuracy of the inputs. Any improvements made to the accuracy of these inputs are therefore significant in making informed decisions regarding system transmission requirements.

The research results presented in this thesis can assist power system planners by providing more tools to realistically represent the hydrogeneration resources present in a system under future conditions, thus improving the quality of a transmission simulation conducted with a PCM. In providing transmission planning entities with results obtained in this manner, well-informed long-term transmission expansion plans can be formulated; with the ultimate goal of the continuous provision of affordable, reliable, and high quality electricity to the consumer.

1.6 Thesis Organization

This thesis from this point on is organized as follows. In Chapter 2, the literature background is presented, with sections on PCMs, transmission planning, hydrogeneration modeling, and wind integration. Chapter 3 details the hydrogeneration models, PROMOD methodology, TEPPC transmission planning with PCM simulations, and PCM simulation results analysis

methods. Chapter 4 presents the 2019 simulation study, and the results are analyzed and discussed in Chapter 6. Chapter 5 contains the manuscript for a paper published in the Proceedings of the IEEE Power and Energy Society conference in March, 2011 (Dennis, Walish, Pacini, Chisholm, & Acker, 2011). This conference paper summarizes a portion of the content of this thesis, therefore some redundancy is present. Finally, Chapter 7 discusses the objectives of the thesis, summarizes the results of the 2019 simulation study, and forms conclusions based on these results. In addition, the implications of the results to transmission planning and further research are addressed. The Appendix contains additional reference material, as well as 2019 simulation study input information and additional 2019 results.

2 BACKGROUND/LITERATURE REVIEW

This chapter addresses the first objective, which is to provide a background based on a literature review of the topics covered in this thesis. This includes literature in the areas of PCMs, long term transmission planning, hydrogeneration modeling and its incorporation in PCMs, and wind power integration.

2.1 Production Cost Modeling

Production cost modeling equates total generation with the total load at each point in time, while minimizing operational costs within the constraints of the transmission system. In a deregulated power system, transmission planning has become more complicated, due to the addition of generators by independent power providers, a constantly increasing load, and a lack of investment in new transmission lines. In a regulated power market, an electric utility is responsible for the three main duties of generation, transmission, and distribution, or some subset of these. The electricity prices are set by the state utility commission and are based on average costs of electricity generation. In contrast, deregulated power markets have a mix of

utility and non-utility producers. In this scenario, electricity prices are set by the marginal cost, or the cost of meeting the last increment of demand, resulting in much greater variations in price. The end result is a higher level of power generation competition, with the end benefit of lower costs to the electric consumer (in theory) (Leevongwat, Rastgoufard, & Kaminsky, 2008). In order to facilitate planning, there are many market-based software packages available such as MAPS™, PROMOD® IV, GridView™, and LCG UPLAN. These packages have some basic similarities in function that include, but are not limited to: generation model, transmission system power flow model, emissions model, reliability (forced outage) model, and hourly chronological security constrained unit commitment (SCUC) and security constrained economic dispatch (SCED) with LMP bus pricing and ancillary services (Li, Yuan, & Tomsovic, Integrated Generation and Transmission Planning Tools under Competitive Energy Markets: An Academic Perspective, 2009). Li et al. (2009) have identified potential new functions that they feel should be integrated into generation and transmission planning packages, based on challenges that are present, such as bidding strategy and system dynamics models. These authors also feel that the linearized DC optimal power flow (DCOPF) power flow transmission model typically used may result in less accuracy than a non-linear programming (NLP) AC solution method. Additionally, another possible improvement may be to implement statistical models to develop a system simulation based on historical data inputted into such processes as artificial neural networks.

The over-riding objective of production cost modeling is to minimize the operating cost of the system such that the generation of the system is equal to the total required load and the total losses of the system, within system constraints. A simplified outline of the problem can be described by the following:

$$OC = \sum_{k=1}^{K} C_k \times G_k \tag{2.1}$$

where *OC* is the operating cost of the system, *K* is the number of generators, G_k is the generation of the *k-th* unit, and C_k is the generation cost for the *k-th* unit. This is subject to:

$$\sum_{k=1}^{K} G_k = D + P_{loss} + RA \quad (2.2)$$

$$\sum_{k=1}^{K} G_k \times GSF_{k-j} \leq TC_j^{max} \quad (2.3)$$

$$G_k^{min} \leq G_k \leq G_k^{max} \quad (2.4)$$

where D is the load demand, P_{loss} is the amount of system power loss, RA is the reserve amount at time *t*, GSF_{k-j} is the generation shift factor[3] (GSF) of generator *k* to line *j*, and TC_j^{max} is the maximum transmission capability of line *j*. For the remainder of this discussion, the indices are as follows:

$$k - K = Generator\ index, total\ K\ generators$$

$$j - J = Line\ index, total\ J\ lines$$

$$i - I = Bus\ (node)\ index, total\ I\ buses$$

$$L = total\ generators\ to\ line\ j$$

In a full solution set, C_k is also constrained by individual generator start up and shutdown costs, failure outages, operation and maintenance outages, and fuel costs. Expansion of Equations 2.1 – 2.4 with these constraints leads to the formulation of the complete SCUC/SCED problem on the level of the **generators** (Carrion & Arroyo, 2006) (Li F. , DCOPF-Based LMP Simulation: Algorithm, Comparison with ACOPF, and Sensitivity, 2007).

In a nodal solution method, used by many PCMs, Equations 2.1 – 2.4 are solved at the bus level, with a bus index of *i*. The additional equation is then needed:

[3] GSFs are a measure of what fraction of a generator's output goes through a particular line, or flowgate, in the transmission system, from the point of a reference bus.

$$P_i = G_i - D_i;\ G_i = \sum_k^{k-i} G_{k-i} \tag{2.5}$$

where P_i is the net injection at bus *i*, G_i is the generation input to bus *i* (sum of output from generators *k* connected to bus *i*), and D_i is the load demand at bus *i*. Combining Equation 2.5 with Equations 2.1 – 2.4 expanded with constraints results in the **nodal** system solution of the SCUC/SCED.

Many PCMs, including PROMOD, utilize a DC power flow to model the transmission in Equation 2.5. A DC power flow is a linear approximation of the actual AC flow in the entire system, with the assumptions that there are small voltage angle differences between the lines, the line resistance is considered to be negligible, and there is a flat voltage or all voltage magnitudes are equal or close to unity. Overbye et al. (2004) reviewed the two methods and compared their performance, in terms of accuracy and computational requirements, for obtaining a security constrained optimal power flow (SCOPF) and resulting LMP values. The authors concluded from simulating two different networks with both the AC SCOPF and the DC SCOPF models that the DC SCOPF performed nearly as well as the full AC SCOPF, but with a substantially faster computational time.

The DC power flow problem at each bus is:

$$P_i = B'_i \theta_i \tag{2.6}$$

where P is the vector of real injections of generation at the bus, the B' matrix represents the relation of generation injections to the angles of the bus voltage phasors[4], and θ is the angle vector (Overbye, Cheng, & Sun, 2004). Combining Equations 2.1-2.6 results in a DC optimal power flow (DCOPF) model. This model may be solved with numerous solution methods,

[4] This matrix is only dependent upon the transmission make-up of the system, and is therefore constant as long as the topology remains the same. If the network topology changes due to scenario, a new B' matrix would need to be formulated.

including mixed integer programming (MIP), dynamic programming (DP), Bender's decomposition, Lagrangian relaxation, and others (Salam, 2007).

Equations 2.1 and 2.2 represent a minimization problem with a single inequality constraint, therefore a method of Lagrange multipliers may be used for its solution (Stewart, 2005). This is described by:

$$\nabla f(x,y) = \lambda \nabla g(x,y) \tag{2.7}$$

$$g(x,y) = k \tag{2.8}$$

where λ is the Lagrange multiplier, and *f* is the function to be minimized, subject to the constraint expressed in Equation 2.8. In terms of Equations 2.1 and 2.2, the following may then be defined:

$$OC - \lambda(\sum_{k=1}^{K} G_k - D - P_{loss} - RA) = L \tag{2.9}$$

$$\nabla L = 0 \tag{2.10}$$

$$\nabla OC - \lambda(\sum_{k=1}^{K} G_k - D - P_{loss} - RA) = 0 \tag{2.11}$$

This results in a set of linear equations, the solution of which yields the Lagrange multiplier, which represents the system incremental cost. The system incremental cost, or shadow cost, is then used in the LMP calculation, described in a paragraph to follow.

The LMP value at a bus, or node, is defined as the cost to produce the next MW of energy needed to meet the load. A bus is a physical location on the grid where energy is input by generators and output to meet the load. The LMP at that bus can be summarized as:

$$LMP_i = \lambda + LF_i + MLC_i \tag{2.12}$$

where λ is the shadow cost of the energy (Equation 2.9), *LF*, or loss factor, is the cost of congestion at the node, and MLC is the marginal loss from delivery at the node. The shadow cost, or λ (Equation 2.9), is simply the least amount it will cost to produce the next increment of power to serve the load demand at the node; the higher the demand, typically the higher the cost of energy. When there is congestion, the power will have to come from another, possibly less cost efficient source, so the price of energy will increase (or decrease, in the case of obtaining less expensive power). The LF is the difference between the cost to generate and transmit the energy in the most transmission-effective way, and the actual cost due to congestion constraints. Lastly, MLC, also called the delivery factor, is the cost incurred by the energy lost in transmission lines; this will be higher the further away the generation is from the power delivery.

In order to calculate the bus LMP, the LF and *MLC* must be determined. LF can be considered as the change in total system loss in response to a 1MW injection at bus *i*:

$$LF_i = \frac{\partial P_{loss}}{\partial P_i} \tag{2.13}$$

where P_{loss} is the total loss of the system. Since $MLC_i$is the cost of a delivery of 1MW to serve the load at the bus, it can be defined as:

$$MLC_i = 1 - LF_i \tag{2.14}$$

P_{loss} is defined as:

$$P_{loss} = \sum_{j=1}^{J} F_j^2 \times R_j \tag{2.15}$$

where *F* is the current flow and *R* is the resistance of line *j* with total lines *J*. The flow in line j is calculated as the sum of all generation to that line:

$$F_j = \sum_{k=1}^{L} GSF_{k-j} \times P_j \tag{2.16}$$

$$P_j = \sum_{k=1}^{L} G_{k-j} - D_j \tag{2.17}$$

where P_j is the net power for the line, with the *k* index indicating the generators (*L* total generators to line) and load demand for line *j*. Equation 2.13 is then expressed as:

$$\frac{\partial P_{loss}}{\partial P_i} = \sum_{j=1}^{J} \frac{\partial}{\partial P_i} \left[\left(\sum_{k=1}^{L} GSF_{k-j} \times P_j \right)^2 \times R_j \right] \tag{2.18}$$

and then:

$$\frac{\partial P_{loss}}{\partial P_i} = \sum_{j=1}^{J} \left[2 \times GSF_{i-j} \times \left(\sum_{k=1}^{L} GSF_{k-j} \times P_j \right) \times R_j \right] \tag{2.19}$$

Substituting this expression into Equations 2.13, 2.14, and then back into Equation 2.12, the bus LMP is calculated.

Li et al. (2007) has developed a possible improvement in the calculation of LMP, termed continuous LMP. In an article detailing the method, two case study results are used to illustrate the benefits of the new method. The LMP curve is typically formulated within the optimal power flow model, and undergoes a step change issue when the load increases or decreases, which can lead to inaccurate LMP signals at these discrete points. The algorithm proposed by the author smoothes the curve at these discrete points and interpolates a single value. The algorithm introduces a fourth component to the LMP value, the Future Limit Risk price, which succeeds in smoothing the LMP curve with respect to load variation. Implementation of this algorithm may reduce the risk of a sudden step change in electricity price, and provide market participants with a more accurate, continuous price charge function (Li F. , 2007).

The PCM packages contain modules for modeling generation, load, transmission, and power market pricing. Long-range planning and transmission decisions can be facilitated by running the PCM software as a system transmission simulation with varying conditions to identify future load, generation, or transmission issues that should be addressed before they arise. In looking at the transmission system as a whole, areas of congestion and bottlenecks can be identified. This can aid planners in decision-making for new or upgraded transmission lines. In addition, system configuration changes can be analyzed in advance to determine the economic impacts of such issues as increased renewables penetration, transmission line additions, decommissioning of plants, or fuel market fluctuations.

2.2 Long Term Transmission Planning

Transmission planning is important at every level of the electrical system; this includes transmission providers, generating companies, load serving entities, regulatory agencies, investors, and finally the consumers. Long term transmission planning is at the head of electric energy policy, with the objectives of making the best possible transmission expansion decisions based on anticipated future conditions, and ensuring that transmission designs contain enough flexibility to adapt to any unforeseen future conditions (WECC, 2009). Prior to deregulation, transmission planning had the ultimate goals of meeting NERC and regional reliability standards and ensuring the transport of electricity to all consumers. Transmission expansion was done by generators to improve the transport of their product to consumers. However, in a deregulated electricity market, competition for energy sales and removing the centralized responsibilities of construction and maintenance in the transmission system greatly decreases the incentives for generators to take on the costs of new transmission. This is graphically represented in Figure 2.1, which shows the average annual U.S. growth rates of summer peak loads and transmission for the last three decades. From 1979 to 2009, transmission expansion rates have declined drastically in comparison to load growth rates (Hirst & Kirby, 2001). This unbalance results in greater congestion, leading to increases in congestion costs. The more congestion there is in a system, the more it costs to move energy

from either remote locations or more expensive energy sources. Some portion of this decline can be attributed to the increased construction of natural gas fueled generators in the 1990s due to decreased natural gas prices. Since these generators produce energy in a relatively clean fashion, they were able to be built close to load centers, thus reducing the length of new transmission needed.

Figure 2.2 illustrates the effect of congestion by looking at the incidence data for transmission loading relief (TLR) in the Eastern Interconnection for the years 1998 to 2001. TLRs are procedures designated by NERC to mitigate regulatory exceedances on transmission lines; these are reported and recorded in logs (NERC, 2011). Any TRL call above a level two[5] indicates that an actual mitigation process was needed to reduce transmission congestion. The number of times increased more than 200 percent between 1999 and 2000, as compared to a 10 percent increase between 1998 and 1999. The costs of congestion on California's Path 15 in the last four months of 2000 were $169 million, showing just how much congestion can cost electrical systems, and ultimately the electric consumer.

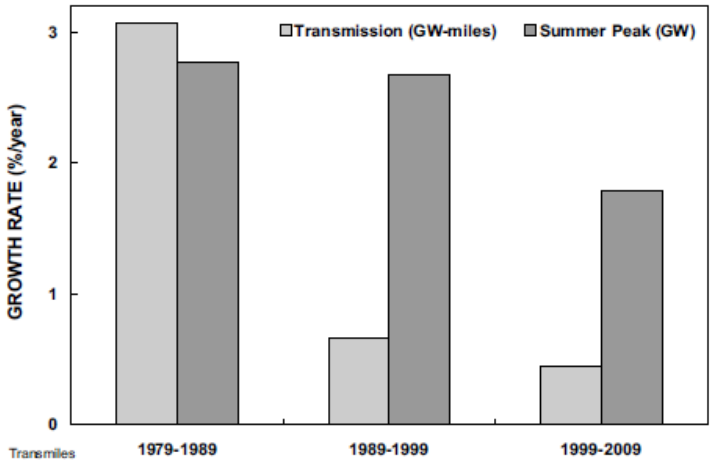

Figure 2.1: Average annual growth rates in U.S. transmission and summer peak demand (Hirst & Kirby, 2001)

[5] The TLR levels are (in order of least to worst) 1, 2, 3a. 3b, 4, 5a, 5b, and 6. Each level requires a different TRL mitigation procedure based on the needs of the system.

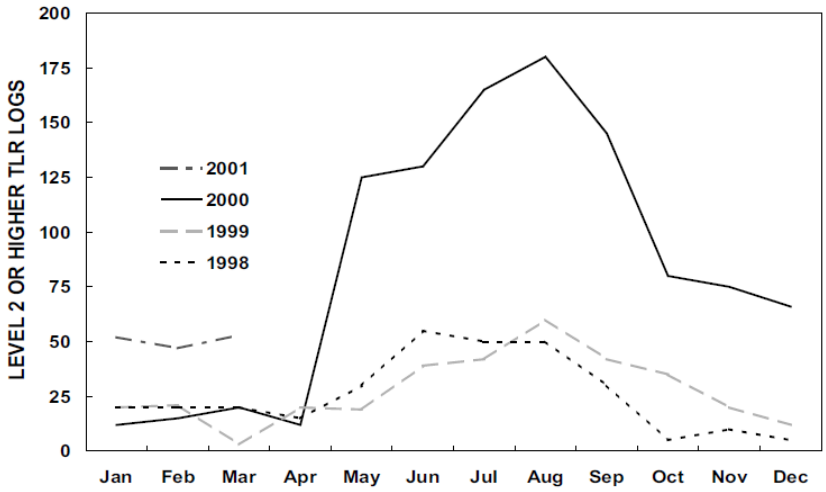

Figure 2.2: Number of transmission loading relief calls in the Eastern Interconnection (Hirst & Kirby, 2001)

In addition, as a response to deregulation, there are many more associated system uncertainties such as energy prices, fuel costs, generator expansion, and load growth that can greatly affect the feasibility of long term transmission plans.

In order to address the challenges posed to transmission expansion planning (TEP), some authors have come up with some guidelines for improving the transmission planning process, from the models used to determine optimal expansion to the decision making processes. In Drayton et al. (2004), the authors describe improvements to the transmission planning process (models, databases, and decision-support systems) used in the WI and some planning models that may address these (Drayton, McCoy, Pereira, Cazalet, Johannis, & Phillips, 2004). In terms of the planning process, the authors feel that the following issues need to be addressed:

- Who pays and who benefits from expansion projects?
- What is the reliability of different TEP scenarios?
- What environmental benefits/drawbacks, market power issues, and financial risks are present in TEP scenarios?

Hirst and Kirby (2001) also identify needs for TEP in a deregulated environment. The key issues they identify include the following:

- Define and incorporate both reliability considerations and commerce considerations
- Include congestion cost considerations
- Include non-hardware alternatives such as altering generation flow paths and load mixes
- Develop planning assessment criteria for evaluating TEP scenarios

2.3 Transmission Planning with PCMs

Many electric entities, such as EROs and BAs, are attempting to address these needs in transmission planning studies. Transmission planning studies attempt to simulate future system operation of interconnections or regional areas, using any number of transmission expansion options that are developed based on committee-derived needs or from TEP models[6]. In some cases, these transmission expansion studies use a PCM to simulate the system, in order to address the system concerns outlined previously by ensuring that the system economics are accounted for (EnerNex, 2010) (Hamilton, et al., 2004) (WECC, 2009). For example, the WECC, through TEPPC, as discussed in Chapter 1, uses PROMOD for its planning studies. In further examples, large scale studies performed to determine the impacts and transmission needs needed to integrate large-scale additions of renewables, the Eastern Wind Integration and Transmission Study (EWITS) and the Rocky Mountain Area Transmission Study (RMATS) utilized PROMOD and ABB MarketSimulator, respectively, to evaluate transmission options. The EWITS (EnerNex, 2010) and the RMATS (Hamilton, et al., 2004) are reviewed in terms of transmission planning methods in the following paragraphs, in order to illustrate how a transmission planning study is conducted. The TEPPC

[6] Transmission planners use TEP models in order to evaluate the time of installation, location, and type of transmission lines that allow for optimal operation of a given system (Alguacil, Motto, & Conejo, 2003). The model may optimize on an economics base, a reliability base, or both. In general terms, this results in a mixed integer, nonlinear mathematical system of equations.

transmission planning method is detailed in Chapter 3, Section 3.2, as this is the planning process pertinent to this thesis.

With the expected increases in renewable energy penetration in the U.S. in the coming years, many planning entities conducted or are conducting transmission studies to determine what changes or additions need to be made to the transmission system to accommodate the influx. The RMATS was one of these, and was conducted to aid transmission planners in making transmission expansion decisions that included the projected increase in wind energy for the Rocky Mountain States area. The geographical area encompassed by this study included the states of Utah, Colorado, Idaho, Montana, and Wyoming. The goal of this study was to use PCM simulations of varying 2013 transmission configurations to determine the most cost-effective way to upgrade the transmission paths.

RMATS included a near-term 2008 base case of the WI, with the only new generation to come from those projects in the study area already under construction in 2003[7]. Four 2013 scenarios were then developed, with varying wind and other generation mixes based on the 2013 load and generation projections in the study area. Transmission overlays[8] for each scenario were developed using Work Group recommendations developed from utility integrated resource plans (IRPs). Each scenario was simulated in the PCM ABB MarketSimulator, both with the developed transmission overlay, and without to determine the congestion costs and operating costs associated with each scenario. The analyses of these results were then used to recommend transmission upgrades to transmission planners in the WI.

The Eastern Wind Integration and Transmission Study (EWITS) had the objective of determining the operational impact that an increased wind power penetration (20 – 30%) level would have on the EI of the U.S. This study developed four wind generation scenarios to use

[7] A high-wind 2008 case, with 2250 MW installed wind capacity as compared to the 508 of the standard base case, was also used to account for the possibility of more wind being installed.

[8] A transmission overlay, or topology, consists of the physical configuration, line types, and line capacities of transmission lines in the area in question.

in 2024 PCM system simulations, as well as a base case scenario consisting of approximately 6% (of the total power generation) wind. In order to conduct the integration study, three major tasks were undertaken: develop wind plant output data, analyze transmission requirements, and finally, analyze the wind integration results. Wind generation data pursuant to each scenario was determined from the Eastern Wind Data Study that developed wind generation forecasts from models utilizing three historical wind data years (2004, 2005, 2006). A detailed generation expansion analysis was performed to simulate the amount of conventional generation that would be available in 2024. Study assumptions for 2024 conditions were developed, including loads, fuel costs, regulations and policies, construction costs, etc. In particular, 2004-2006 FERC data was used to model the demand and energy, as well as 2006 power flow data. This data was used in initial PCM simulations in order to determine what transmission expansion would be needed for the wind integration analysis. First, each wind scenario was input in a PCM simulation, with the existing transmission network (constrained). Next, each wind scenario was inputted in a "copper sheet" PCM simulation in which all transmission constraints were removed (no congestion). Results from the constrained and copper sheet comparisons were used to develop a transmission overlay (topography) for each wind scenario to use in the final wind integration analysis, as well as to estimate the costs of congestion and transmission expansion. Transmission overlay topology developed using an economics-based TEP (see footnote 3) with the system inputs derived from the constrained and copper sheet PCM simulations. The overlays consisted of different configurations of 800-kilovolt (kV) high-voltage direct current (HVDC) and extra-high voltage (EHV) AC lines designed to handle the wind configurations in each scenario.

Both of these studies use PCMs to simulate the hourly operation of a system in order to compare transmission scenarios. In this way, the most cost-effective method for expanding transmission may be evaluated. There are drawbacks, however, based on the PCM operation. First, as mentioned previously, many PCMs do not cost-optimize the hydrogeneration (this includes both ABB MarketSimulator and PROMOD). This may have significant impacts on the simulation results, and the transmission expansion decisions, accordingly. Additionally, the

LMP-based modeling must assume a perfectly competitive market, with no consideration for additional restrictions/constraints in the transfer of power. This may result in transfer capability errors, generally overestimations (Hamilton, et al., 2004), also causing potential effects on transmission decisions made using PCM simulation results.

2.4 Hydrogeneration Modeling and Hydrothermal Scheduling

2.4.1 Hydrogeneration Modeling

In recent years, much research has been ongoing into methods that more accurately forecast hydrogeneration on a plant by plant basis. In addition, there are numerous methodologies that attempt to schedule the hydrogeneration dispatch with that of other generators in a power system within a production cost simulation, or hydrothermal scheduling. First, as touched on in Chapter 1, there is the simple method of using historical hydrogeneration from a representative year to model hydrogeneration. This modeling method is discussed in more detail in Chapter 3. Next, there are load following methods such as peak shaving (PS), which allocates the production of hydro power to the peak load periods, subject to the plant's operating constraints. Traditionally, PS models do not consider hydraulic inputs such as water balance and the travel time encountered with cascaded hydro plants. Simopoulos et al. (2007) developed a PS method using an aggregated hydro plant model, considering each individual plant as a hydro unit. Two steps were applied to solving the PS hydrogeneration; the first step was a traditional PS method that was iterated over all the individual plants, or units. The second step adjusted the "unit" hydrogeneration to optimize it within the hydraulic conditions. This second step used a quadratic programming optimization method which minimized the sum of the deviations of the PS-generated hydrogeneration from the optimum generation under hydraulic constraints. The authors then solved the system hydrothermal generation using a simulated annealing (SA) algorithm, with the new PS method optimized hydrogeneration as input. The enhanced PS method/SA system algorithm was tested on a

modified version of the Greek power system; these tests achieved effective results in a reasonable computing time (Simopoulos, Kavatza, & Vournas, 2007).

In addition, hydrogeneration modeling packages using dynamic programming (DP) such as RiverWare are commercially available, that incorporate all of the complexities of a river system. Riverware is object-based software for modeling the characteristics of a river basin (Zagona & Magee, 1999). In constructing a model, data on many "objects" are inputted and linked together. Each object has associated "slots" of input and output, and a method for solution of the unknown slots within the framework of the connected objects. Riverware may be run as a simulation or optimization. All slot solutions feed into the other objects and affect their slot solution. There are three objects that contribute to the hydropower calculation, which has four selectable methods of solution. Riverware iterates and solves the system, using linear programming (LP). The advantage of determining hydrogeneration in a Riverware simulation is that it develops the forecast within the framework of the river basin, which includes hydrological data and forecasting. More recent modeling has focused on the use of alternate methods such as neural networks (Gunasekara, Udawatt, & Witharana, 2006).

2.4.2 Hydrothermal Scheduling with Production Cost Modeling

PS modeling is widely used in production cost models, and a study by Wu et al. (1989) reviews the accuracy of these in comparison to benchmark hydrogeneration calculations performed with a Coordination-Equation Method (CEM). PS dispatches hydrogeneration during peak loading, thus "shaving" off the peak of the load. The emergence of numerous mathematical models gave rise to the question of whether PS was still a valid method for hydrogeneration modeling, and to investigate its accuracy. In comparing the CEM and PS, the authors found that the differences in accuracy were negligible. The PSM was always more computationally efficient and consistent than the CEM (Wu, Lee, & Hill, 1989).

There are many new emerging methods that more effectively integrate hydro with thermal in a production cost optimization schematic (Diniz & Maceira, 2008) (Simopoulos, Kavatza, & Vournas, 2007) (Borges & Pinto, 2008), the so-called hydrothermal scheduling problem (HS). Some methods for modeling HS include LP (Shawwash, Siu, & Russell, 2000) (Diniz & Maceira, 2008) (Chang, Aganagic, Waight, Medina, Reeves, & Christoforidis, 2001) and DP. In short term scheduling (STHS) the LP approach is suitable, and may be solved using a number of solution methods. For example, Chang et al. (2001) used mixed integer linear programming (MILP). The short term hydro scheduling problem is described as discrete, non-linear, and non-convex. The advantage the authors felt that using this method provided over others such as DP, decomposition, network flow programming, or non linear programming (NLP), was that the hydro system constraints could be added, and the nonlinearities added with piecewise linear approximations. Two test case hydro systems were solved using the MILP method within the CPLEX solver, and a branch and bound algorithm was used to optimize the solution. The authors obtained accurate solutions in an acceptable computational time. Diniz and Maceira (2008) solve the STHS problem using piecewise linear approximation (PLA). The model presented is a four-dimensional piecewise linear model that considers storage, turbine outflow, and spillage in a single function. The model was then applied to the day-ahead network constrained dispatch of a large system of mixed generators. A hydrogeneration simulation of the Brazilian electrical system was conducted using the model and results of this simulation indicated that the model was accurate, with low CPU times.

Dynamic programming methods are more suitable for the long term HS (LTHS); these take into account various hydro and thermal system constraints and come up with a series of non-linear equations to describe the system (Zambelli, Siqueira, Cicogna, & Soares, 2006). An example of the system of equations that make up the LTHS problem is presented in the Appendix, to provide an idea of the types of variables and constraints that are included. The resulting mathematical model can then either be deterministic or stochastic, in which one or more of the model variables (such as inflow or load) are determined either by past values (Zambelli, Siqueira, Cicogna, & Soares, 2006) (Neto, Cotia, Pereira, & Kelman, 1985) or by a

probabilistic method such as probability distribution or auto-regressive methods (Siqueira, Zambelli, Cicogna, Andrade, & Soares, 2006) (Gonzalez, 2002). In Zambelli et al. (2006), models were developed to solve hydrothermal scheduling with the input of river inflow forecasts, which is often not considered in production cost models. The performance of two deterministic models and two stochastic models were then compared. The deterministic models include a DP method for average inflows and a NLP method based on historical inflow. One stochastic, DP model uses an independent probability distribution function for inflow while the other stochastic DP model uses periodical autoregressive inflow determination. These models were tested on a case study system in order to compare results. The authors concluded that the deterministic models performed similarly, particularly for operational cost optimization. The second stochastic model listed above resulted in higher generation; however the first stochastic model better optimized operational cost. The deterministic models were more effective overall for the case study in question. There are a few commercially available PCMs that include DP hydrogeneration (GTMax and GridView).

2.5 Wind Integration

As described in Chapter 1, the integration of wind power to an electric system poses many challenges. First, there is the issue of its price-taking status. When wind resource is available, any generation derived from this must be used. This characteristic translates to an increase in on/off cycles for other generators in the system, putting an added burden on the system in terms of ancillary needs. As a result, system operational costs increase with higher levels of wind penetration. Transmission studies need to accurately simulate the wind in a future simulation scenario, and to be able to show the effects of increased wind generation on a future system in terms of transmission and system costs.

Second, the resource availability is variable, and is difficult to predict in long-term scenarios. Therefore, in terms of long term transmission studies, accurate representation of system flexibility is critical in a future system simulation. System flexibility can be defined as the ability

of the system to respond quickly and cost-effectively to unexpected load changes. As is the focus of this thesis, this flexibility may come from the hydro system, particularly in areas where hydropower provides a large portion of the regional system power. This section reviews literature on wind power integration to provide a background for its associated system complexities.

Some important wind integration issues at the forefront include interconnection, operating impacts, transmission planning and market issues, and finally accommodating large wind penetrations (Smith, Milligan, DeMeo, & Parsons, 2007). Operating cost increases of 10% or less of the wholesale value of wind resulted from integrations of up to 20% wind generation. The costs for maintaining the balance between the load and the total power generated by all power plants in the system are ancillary services costs. These costs increase when conventional power plants deviate from their optimum operation within the system due to variations in load from actual and that predicted in a unit dispatch. Operating costs may be discussed by operational time frames. First is the unit-commitment time frame (1 day to 1 week, 1 hr. time increments), in which the start and stop of units is determined within a cost based algorithm. Wind challenges this by the presence of imperfect wind forecasts. In the load-following time frame (1 hr. with 5-10 min. increments), there must be adequate reserve capacity to follow load fluctuations; wind is variable within this time frame, which adds to the reserve capacity needed. Lastly, in the regulation time frame (1 min.-1 hr. with 1-5 s increments), the load quality is maintained, and there must be sufficient regulating capacity available from on-duty regulating units.

System costs due to integration increase from regulation to unit commitment. This is demonstrated in Table 2.1, which includes a summary of the operational time frame costs of integration obtained from several wind integration studies.

Table 2.1: Timeframe wind integration costs from selected wind integration studies (Georgilakis, 2008) (Acker T. , Arizona Public Service Wind Integration Cost Impact Study, 2007).

Study	Wind penetration (%)	$/MWh			
		Regulation	Load following	Unit commitment	Total
UWIG/Xcel	3.5	0	0.41	1.44	1.85
CA RPS	4	0.45	Na	Na	Na
We Energies I	4	1.12	0.09	0.69	1.90
Great River I	4.3	Na	Na	Na	3.19
APS	5.9	0.42	1.88	0.95	3.25
BPA	7	0.19	0.28	1.00–1.80	1.47–2.27
PSCO/XCEL	10	0.2	Na	2.26	3.72
APS	14.8	0.37	2.65	1.06	4.08
PSCO/XCEL	15	0.20	Na	3.32	4.97
MNDOC/XCEL	15	0.23	Na	4.37	4.60
Great River II	16.6	Na	Na	Na	4.53
PacificCorp	20	0	2.50	3.00	5.50
We Energies II	29	1.02	0.15	1.75	2.92
MN/MNPUC	30	Na	Na	Na	4.41

There appear to be opportunities for reducing these costs; these can be policy, technology, or planning driven solutions. Wind plant interconnection has improved in the area of grid stability. Operational impacts at all timeframes may be able to be reduced by a combination of better data sets and more accurate wind modeling in order to address the reliability of the wind resource. As wind penetrations increase, additional transmission will be needed. Transmission planning is key for the large-scale integration of wind power. In the U.S., most of the regions with high wind resources are located far from population centers; therefore transmission lines are not sufficient to transfer large amounts of wind generation (GE Energy, 2010). Additionally, there exists a lack of incentive for entities such as generators or transmission line

owners to fund expansion; therefore, the policies related to system transmission expansion need restructuring, so that all power participants share in the costs (Georgilakis, 2008).

Other mitigation methods may include the use of large balancing areas and dynamic system scheduling. In order to keep increasing wind penetration levels, a thorough understanding of the wind resource and the grid are needed, including accurate wind plant data and modeling and system modeling (Smith, Milligan, DeMeo, & Parsons, 2007). Since forecast accuracy decreases with increasing time and with site complexity, combining forecasts into ensembles may improve the forecasts, so that more accurate generation can be planned by the grid (Georgilakis, 2008).

As discussed in Section 2.3, RMATS and EWITS studies were conducted to determine the system costs and the system transmission needs for increased levels of wind power penetration. In the EWITS study (see Section 2.3 for the study procedure), wind integration costs consist of incremental operational costs that are attributed to the variability and uncertainty of wind generation. In a PCM simulation, the wind generation forecast is used in the optimization of unit dispatch, and also is used to adjust the operating reserves needed. Therefore, any increased operating costs determined in the PCM simulation will take into account both of these integration effects. In order to determine the difference in operating costs incurred from wind, a no-wind-uncertainty scenario was run for comparison. The wind generation forecasts in these runs were replaced by "ideal" wind energy, in which the uncertainty was removed. Additionally, there was a case in which only the day-ahead forecast error was used in the unit dispatch, but not the reserve requirements (the "intermediate" case). This separates the operational cost differences into regulation and reserve costs. Table 2.2 shows the results of the analysis for all four wind penetration scenarios, using the 2004 load and wind profiles, where the day-ahead forecast error case gives the regulation costs, and the variable reserve case gives the reserve costs.

Table 2.2: Integration costs ($/MWh of wind energy) (EnerNex, 2010)

Scenario	Description	Day-Ahead Forecast Error (regulation cost) ($/ MWh)	Variable Reserve (reserve cost) ($/MWh)	Total Integration Cost ($/MWh)
1	**20% penetration, High Capacity Factor, Onshore**	2.26	5.74	8.00
2	**20% penetration, Hybrid with Offshore**	2.61	4.59	7.21
3	**20% penetration, Local with Aggressive Offshore**	2.84	2.93	5.77
4	**30% penetration, Aggressive On- and Offshore**	2.51	4.56	7.07

In all cases, the reserve integration costs are greater than those of the regulation, confirming the results found in other studies (Table 1.1).

Finally, the total integration cost is calculated as the difference between the operational cost of the ideal wind scenario and the wind penetration scenario; Figure 2.3 shows these results for all three profile years (refer to Section 2.3).

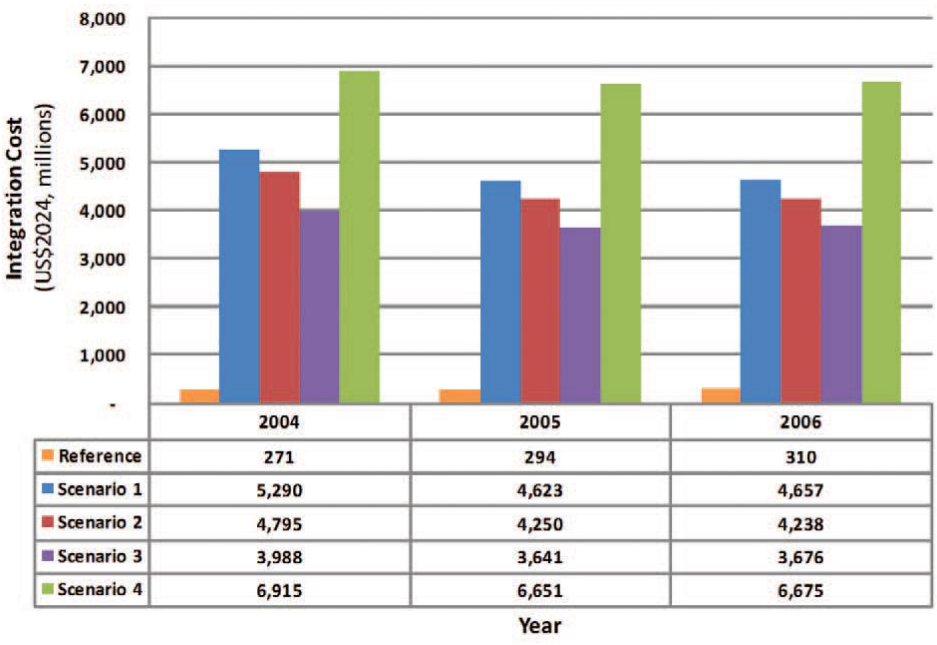

Figure 2.3: EWITS total wind integration costs (EnerNex, 2010)

The EWITS study then used these results to make some general conclusions about integrating up to 30% wind penetration, intended to aid transmission planners in expansion decisions.

3 MODELING AND ANALYSIS

The goal of a long-term PCM system simulation is to provide a realistic picture of the system operation for one year sometime in the future, so that future transmission issues and needs may be determined. The basic outline for a PCM-simulated transmission study is to develop several different system transmission scenarios, and perform these along with a base case. These scenarios may vary with generation configurations[9], load, transmission, or regional grouping configurations, to name just a few. The results of these simulations may then be compared to each other in terms of (for example) operating costs, transmission congestion, market pricing, or generation levels. Since a PCM simulates system operation within the confines of transmission, operation and economic constraints, the output analysis should be considered based on results relating to these. Two important questions to ask when performing a long-term transmission study using a PCM are:

- What constitutes a realistic system simulation?
- How is this verified?

These are the questions that the analyses presented in this chapter will attempt to answer, expressly with regards to hydrogeneration model input.

In this chapter, Section 3.1 specifically discusses PROMOD operation, and how TEPPC utilizes it for transmission studies. The answers to the questions posed above, as interpreted with respect to hydrogeneration modeling, are presented in Section 3.2. The deficiencies encountered with hydro models used in PCMs are highlighted, making the case for more effective ones. Finally, in Sections 3.3 and 3.4, the hydrogeneration models developed by TEPPC are outlined as a solution to these deficiencies.

[9] This might include planned generators, additional renewables, planned transmission constraints due to policies, etc.

3.1 PROMOD SCUC/SCED Solution and TEPPC Use

In order to generate the SCUC and SCED, PROMOD uses an hourly chronological DCOPF dispatch algorithm, which integrates the cost optimized dispatch of generators with that of the transmission, similar to the method described in Section 2.1. The solution of this algorithm minimizes system cost while remaining within the system's operational, transmission, and security limits. Due to the confidential nature of the program, only the general process of PROMOD is described next, neglecting specific algorithms and solution methods.

PROMOD uses inputs that fully describe the generator, load demand, and transmission characteristics of the system. For each thermal generator in the system, characteristic inputs include:

- Ramp rates
- Operation and maintenance
- Fuel requirements/Fuel costs
- Capacity (minimum and maximum generation)
- Reserve ability
- Outage rates
- Heat rates

These represent the generation constraints. The load demand is produced by adjusting a representative chronological hourly load shape with peak and energy forecasts. Transmission data includes:

- System bus and line locations (linked with generators and load areas)
- Transmission capabilities
- Regulatory contingencies
- Line power flow model

Other data includes:

- Hourly chronological hydrogeneration profile (HCHP) for hydro units
- Hourly chronological (HC) renewable generation profiles

A first dispatch pass of the system, without unit constraints, is used to generate starting points for the bus energy prices, using a LP solution. Next, based on the energy prices derived from the first run, a mixed integer program (MIP) optimizes the output of each generator to maximize profit. This results in a profit-optimized unit commitment. A second dispatch pass is then performed, including all unit constraints, generating another set of bus energy prices. The MIP commitment step is then re-optimized, reflecting the added constraints. The final dispatch uses the commitment schedule from the previous MIP solution, and performs an LP solution of the full DCOPF, as outlined in the previous section. This results in the final SCUC/SCED, as well as the final LMP values at each bus (EnerNex, 2010). Significant outputs are:

- Hourly chronological generation for all generators
- Hourly chronological LMP for all buses
- Hourly chronological transmission flow for all lines; monthly transmission losses
- Hourly chronological production cost, fuel consumption, operational hours for all generators; monthly operation and maintenance (O&M) and fuel costs

TEPPC develops the forecast year (usually a ten-year ahead timeframe) PROMOD inputs to perform the PCM simulations for a transmission study. A study plan begins with a data test case, which has the full forecast load for the study year, the transmission network topology, and the committed generators that are anticipated to still be in service. The load forecast is generated from the load shape of a representative year and adjusted based on future load forecasts. A forecasted transmission topology and power flow, committed generator characteristics, as well as hydrogeneration and renewable generation forecasts for the study year, are then developed (WECC, 2009).

Next, multiple resource portfolios are added, which consist of a hypothetical set of additional resources, each representing a different generation development scenario with all the associated PROMOD inputs. These portfolios are simulated along with the data test case without adding any new transmission; in this way areas of congestion may be assessed. Finally,

expansion cases are added, with each case representing a different transmission expansion scenario. PCM simulations of the system using these expansion cases provide the necessary information to regional planners to develop new cost-based transmission expansion strategies, based on specific generator/transmission scenarios. The process hierarchy is shown in Figure 3.1.

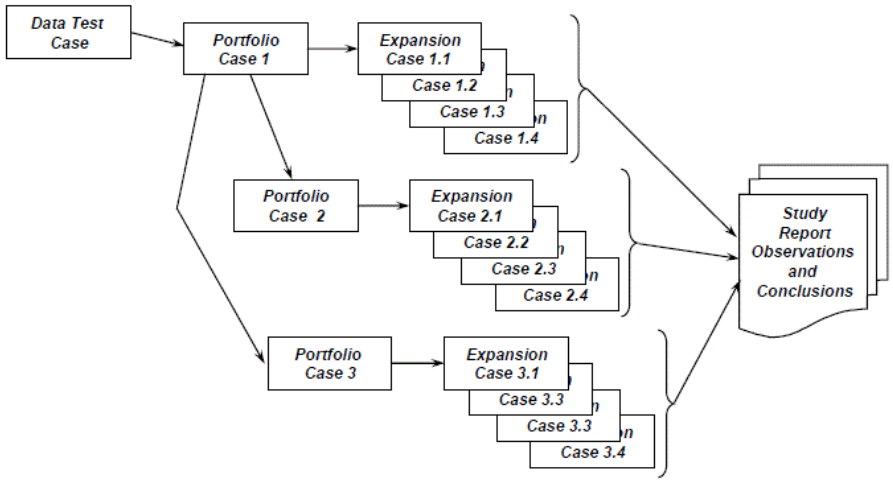

Figure 3.1: TEPCC transmission study process for PCM simulations (WECC, 2009)

In order to compare portfolio case simulations, TEPPC analyzes several sets of simulation results. First, the change in generation from one case to the next is examined to see how or if congestion in the transmission lines affects the generation. For example, if in one scenario, gas-fired generation increases, this could be due to congestion in the lines causing generation to move towards pipeline-transported gas energy. Second, transmission flow duration curves are compared between scenarios. When flow is congested, the line may be near or at its limit for longer periods of time. Flow duration curves may be compared with historical line flow curves; significant differences in the shape between simulated curves and historical curves may indicate that additional transmission capacity is warranted. Thirdly, LMP nodal values between scenarios may be compared.

3.2 PCM System Simulation Efficacy

This section will address the questions posed at the beginning of this chapter, with respect to the scope of this thesis. First and foremost, a PCM simulation is only as good, or realistic, as its inputs. In section 3.2.1, the hydrogeneration models used in producing the HCHP that are used as a simulation input are detailed as a response to this first question. Next, in section 3.2.2, the metrics and analyses used for judging the validity of a PCM simulation are discussed, again in the context of the issues pertinent to this thesis.

3.2.1 Hydrogeneration Modeling in TEPPC PCM System Simulations

As discussed in previous sections, inputs into a PCM generally include load forecast models, transmission network flow models, generation resources and reserves with operational characteristics and fuel prices, hydrogenation models, and renewable generation models. Figure 3.2 shows a conceptualized PCM flowchart with inputs and outputs.

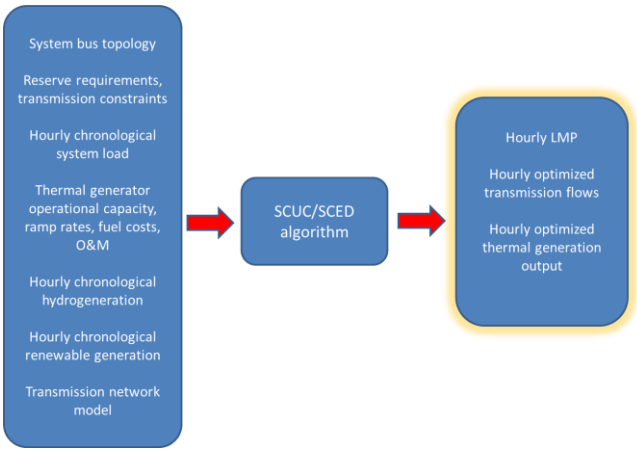

Figure 3.2: Generalized PCM schematic

For the resulting SCUC/SCED to realistically simulate the system in the future, the inputs must be as accurate as are feasible, given that the estimated future conditions determined by planners are, by definition, never a perfect representation. A future hourly chronological load is determined by adjusting hourly chronological historical load curves using load growth forecasts. It is assumed that for this type of load modeling, a more qualitative, rather than strictly quantitative result is desired. For actual, real-time dispatch scheduling, more sophisticated load models are employed in order to plan for the possibilities of discrete problematic load events (Hiskens, 2006). For a long-term system simulation, however, a qualitative load model will suffice, given that the planning assumptions are valid. The same is true for all the future input assumptions, such as fuel costs, and thermal plant O&M outage rates, where validity is qualitative rather than quantitative. For the hourly chronological generation inputs not optimized within the PCM algorithm, such as hydro and renewable energy generation, it is important that the model used to produce these inputs is as accurate as possible.

In terms of the hydrogeneration models used in long-term PCM transmission studies, some common modeling methods include HD and PS. HD modeling uses a representative year's HCHP, and alters it with a correction factor to produce the forecasted HCHP. The correction factor is system dependent; transmission study planners determine how the hourly shape needs to be modified. This may include temperature corrections, weather forecast corrections, etc. The HD forecast is input into the PCM, and is subtracted from the hourly load forecast. The resulting adjusted load is used in the thermal dispatch optimization algorithm. This method of hydrogeneration modeling is data intensive; an entire year of hourly plant generation is required (8760 data points). Additionally, the HCHP is hard-wired, that is, it cannot be adjusted in the model due to future load variations, since it is purely based on the hydrogeneration/load relationship present in the model year used. This presents problems in terms of accuracy; hydrogeneration/load anomalies present in the model year will be carried

forward to the forecast year, while the probability of future anomalies will not be accounted for. This deficiency can be seen in Figure 3.3, where the HD-modeled hydrogeneration of a hydro plant is plotted with the operating area load. There are several instances where the hydro shape deviates significantly from the load shape, indicating that the load pattern the generation was modeled with is different than that of the current load. In the red box, there appears to be a time shift difference, while in the red ellipse, a shape difference is present.

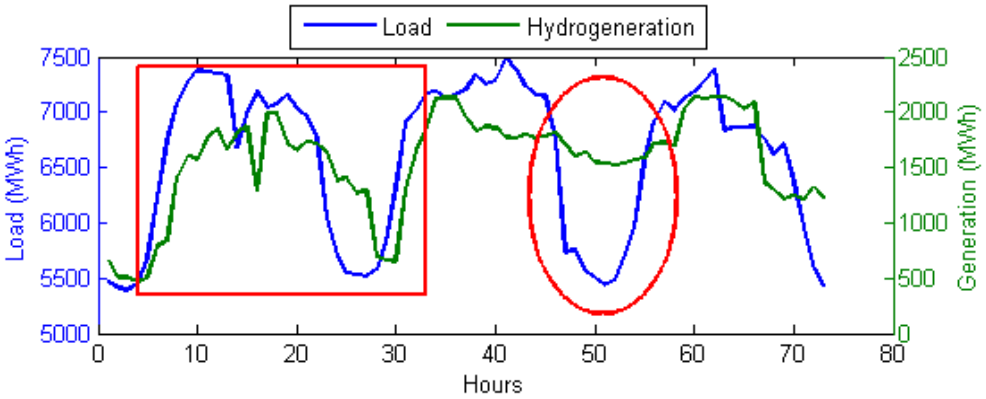

Figure 3.3: : HD-modeled hydrogeneration for John Day power plant in Washington, compared with the Bonneville Power Administration (BPA) load for the first 72 hours of July

Finally, the hydrogeneration is not cost or security optimized, therefore not dispatched as in a real-time situation, when these would be honored. A considerable drawback for modeling hydrogeneration with HD is that it prevents any available flexibility in a hydro plant to system changes such as renewable generation, system outages, market pricing, or transmission congestion from being utilized in the PCM. This is of particular importance when modeling future scenarios with significant penetrations of renewables, as hydrogeneration is sometimes an important factor in their integration, and because higher penetrations of renewables have a significant impact on system energy prices.

The PS method assumes hydro plants dispatch limited available energy during times of highest loads subject to minimum and maximum generation constraints. In this way, the resource-

limited hydrogeneration is dispatched to reduce the total operating cost of the thermal system (Simopoulos, Kavatza, & Vournas, 2007). The level to which the model is peak shaved depends upon the system make-up; in systems with a high hydro penetration, the peak shave level will be high, while the opposite is true for a low penetration system. A simple peak shave example follows, for descriptive purposes. Inputs for the model are maximum and minimum capacity of the hydro plant, hourly load values, and a peak shave level at which hydrogeneration should begin. The total hydrogeneration for a given time period, *T*, is determined by the following calculation:

$$\sum_0^T \min \left[C_{max}, \max \left(C_{min}, \overbrace{L_t - SL}^{\Delta L} \right) \right] \tag{3.1}$$

where C_{max} and C_{min} are the maximum and minimum hourly hydro plant capacities, L_t is the load for hour *t*, and *SL* is the shave level. When the load exceeds the shave level, if the difference between the load and the shave level, ΔL, is less than the difference between the maximum and minimum capacity, then $\Delta L$is the amount the plant will generate for that hour. This calculation is iterated until the optimum is reached. The following figure shows an example of a hypothetical weekly PS generation (Figure 3.4) for a given load profile. The plant minimum capacity is 100MW, the maximum is 400 MW, and the shave level is optimized at 885 MW.

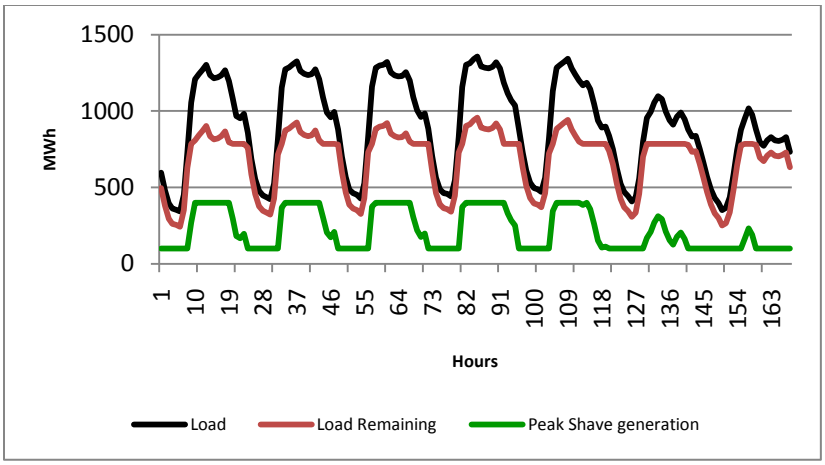

Figure 3.4: Hypothetical PS generation profile for a 7-day period

It can be seen from the blocky pattern of hydrogeneration distribution that the maximum capacity of the plant is dispatched during periods of peak load, and the minimum is dispatched during periods of lower demand. This gives the hydrogeneration more of a load following response, since it is modeled on the load being used in the simulation, rather than a representative HCHP, which in many cases is preferable to HD-modeled results. Figure 3.5 shows a similar plot to that of Figure 3.3, with the PS-modeled hydrogeneration for Brownlee power plant in Idaho for the first 72 hours of July compared with the Treasure Valley operating area load. The hydrogeneration shape closely follows that of the load, with the blocky pattern of switching from minimum to maximum generation.

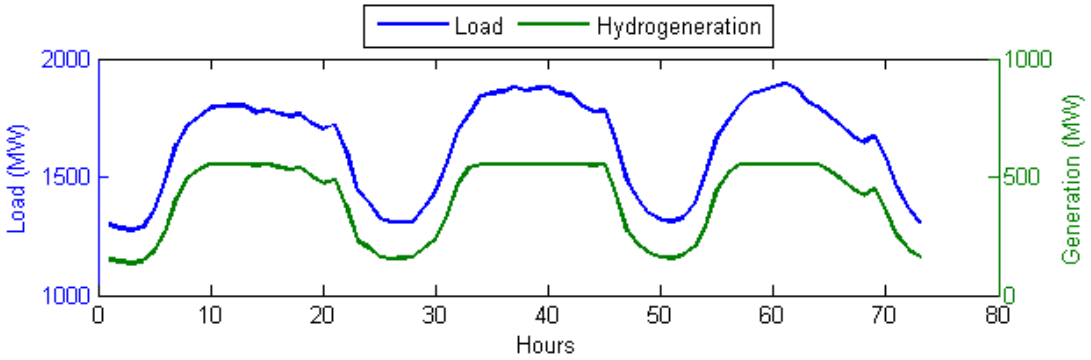

Figure 3.5: PS-modeled hydrogeneration for Brownlee power plant in Idaho, compared with the Avista (AVA) load for the first 72 hours of July

However, the PS hydrogeneration modeling method does not account for the plant's ability to adjust its dispatch to energy price variations. It also has some of the same disadvantages of HD, since it is again hardwired into the PCM model; therefore it is not cost or security optimized.

Many hydrogeneration plants have flexibility, or the ability to follow load. This ability to follow load allows the hydrogeneration to respond to unexpected changes in demand, as well as system factors such as renewable energy inputs and transmission constraints, which change the market energy prices. In a power system, this translates to more efficient operation in both operational cost and transmission usage. As discussed in Section 2.3, there have been many advances in models that accurately represent the hydrogeneration in hydropower systems. While these models often take into consideration many hydrogeneration constraints such as those encountered with environmental conditions, and those of the system such as transmission, pricing, and regulation, they are also extremely computationally time-intensive, and require large data sets and modeling manpower.

In order to produce effective studies of long-term transmission expansion planning forecasts, TEPCC requires a hydrogeneration method that uses minimal data and minimal modeling manpower, but satisfactorily represents a hydro plant's flexibility. As discussed in Chapter 1, this is particularly important in regions where hydrogeneration provides a significant portion of the total energy production. HD and PS were not providing TEPPC with the level of efficacy needed for hydrogeneration production-rich regions such as the Pacific Northwest. Therefore, two new modeling methods were developed in order to improve the HCHP modeling, with the ultimate goal of more realistic long-term PCM simulation results. These two methods are detailed in Sections 3.3 and 3.4 of this chapter.

3.2.2 PCM Simulation Metrics and Analyses

The outputs of a PCM system simulation vary based on operation, but in general include hourly:

- SCUC and SCUD for all generators
- Generator production cost
- Transmission flows (path and line)
- LMP at designated buses

From these outputs, analyses may be conducted to determine future system operating costs, generation distributions, transmission congestion, and market trends. As posed previously, how is the credibility of a long-term PCM simulation verified? With nothing to compare to, the outputs of the PCM simulation must be analyzed on a relative basis. The specific PCM outputs used in this thesis are:

- Model derived hydrogeneration
- Transmission flows on study-significant lines or paths
- LMP for study-significant buses
- Significant area loads

Analysis metrics were derived from these outputs for determining the accuracy of the case study simulations. First, the transmission flows for lines or paths may be examined. Duration curves may be plotted and compared with historical duration curves on that line or path. If the shape is similar, then the simulation is more likely producing accurate results[10]. Of course, this comes with the caveat that the basic patterns of system operation remain the same. For this reason, it is important to run a base case in long-term simulation studies, in which the only

[10] The flow magnitude may be higher depending on the path capacity, since demand generally increases in future scenarios.

change to the system is the load demand (WECC, 2009). When new transmission or operation scenarios are introduced, the duration curve may change shape significantly from the historic. Transmission flows are also important in comparing simulation scenarios, in that the congestion levels may be analyzed and compared. Figure 3.6 shows the duration curves for three different PCM scenarios, compared with historical duration curves. The PCM scenario shapes closely follow those of the historical, indicating that the simulation is reasonably representing system operation. The magnitude of the flow level is higher, due to the 10 year forecast time frame (see Footnote 2).

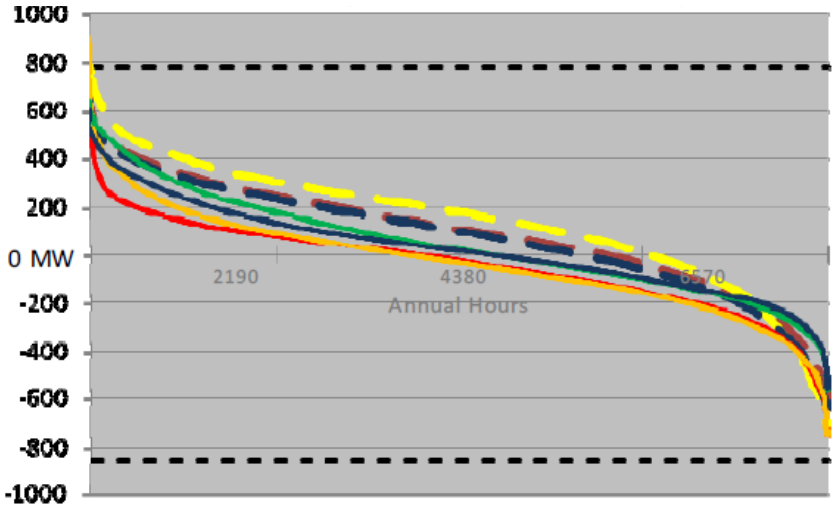

Figure 3.6: Yearly path flow duration for three PCM scenario flows (dashed lines) and three historical flows (solid lines). The dashed black line indicates the total transfer capability (TTC) of the path (WECC, 2009)

Since the main objective of a transmission planning study is to determine where and when in the forecast timeframe congestion may occur, it is important to define some transmission congestion metrics. In this way, scenarios may be compared and contrasted in terms of relative congestion levels. Each transmission path[11] in the WI has a total transfer capability (TTC) that defines the MW capacity limitation of power that it can transmit. The operational

[11] A path is a cut plane of transmission lines that serve a particular region in the WI operating area.

transfer capability (OTC) is the MW capacity based on the changing operating conditions of the system. Transmission paths are designed to operate at 100% of their OTC, which may or may not be the TTC at any one time (WECC, 2009). For the case study performed in this thesis, the OTC data was unavailable; therefore the TTC was used as the line operational limits. The congestion metrics used to compare transmission congestion in this study are T75, T90, and T99. These are defined as the time the transmission on a path is at 75%, 90%, or 99% of the TTC. The congestion metrics may then be calculated for a specific time period such as a week, a month, a season, or a year, and compared between scenarios. For the purposes of this study, a simulation scenario that is able to respond to path congestion by lowering generation would represent an accurate representation of a real-time system response. In a PCM simulation, as congestion goes up (line limits are reached), the energy price would be driven down and generation dispatch would be reduced, or routed to another line.

Next, LMP values are an important metric used to determine the efficacy of a system simulation. LMP values may be used to calculate various components of operating cost. One of these is the Load Cost (LC); the lower the load cost, the more reasonable the simulation is. For the purposes of this thesis, a LC metric is used:

$$LC_i(\$) = LMP_i\ (\$/MWh) \times Load_i\ (MWh) \tag{3.2}$$

where *i* is the time increment. The lower this value, the less it costs the system to produce the energy needed to balance the load. In comparing scenarios, it is useful to look at monthly, seasonal, and yearly load costs, since a more efficient scenario will for the most part have a lower load cost.

Another method to compare scenarios with respect to LMP is with standard deviation. The more fluctuations in LMP, the less efficiently the system is behaving. This is calculated as:

$$\sigma_{LMP} = \sqrt{\frac{1}{n}\sum_{i=1}^{n}(LMP_i - \overline{LMP})^2} \quad (3.3)$$

where σ_{LMP} is the total standard deviation of the entire data set, $\overline{LMP}$ is the mean LMP of the data set, and *n* is the total number of data points. This metric can be used as simulation verification, and is used in this thesis to compare the relative credibility of different scenarios.

Another simple, yet important, efficacy determination is how well the generation follows either the load or the price. Real-time system operation is fully dependent upon the load demand, and in turn, the energy price. In a simulation, if the hydrogeneration has a high correlation with the load, then it is operating as it would in a real-time situation, reacting to the energy demand. The same is true for energy price, since plants strive to produce power when price is high in order to maximize profits. A statistical correlation is:

$$CC = \frac{\sum_m \sum_n (A_{mn} - \bar{A})(B_{mn} - \bar{B})}{\sqrt{(\sum_m \sum_n (A_{mn} - \bar{A})^2)(\sum_m \sum_n (B_{mn} - \bar{B})^2)}} \quad (3.4)$$

where CC is the correlation coefficient, $\bar{A}$ is the mean of A (dataset 1) and $\bar{B}$ is the mean of B (dataset 2). This method is used in this thesis to compare PCM simulation scenarios.

3.3 Proportional Load Following Model and Evaluation Results

TEPCC has undertaken the task of developing methods that more accurately represent hydrogeneration for use in their long-term transmission studies. In order to accomplish this, TEPCC, in cooperation with Ventyx (the developer of PROMOD), has developed and tested the PLF model for hydrogeneration. This particular model is sensitive to the data and task constraints that TEPCC is under, namely limited access to specific hydrogeneration data and a need to recognize and utilize any inherent flexibility a hydro plant may have in a years-ahead

transmission study. The PLF approach to modeling hydrogeneration assumes that generation is proportional to load subject to minimum and maximum capacity and an energy limit. An additional variable, the proportionality constant (*K*), quantifies the ability of the plant to follow load, i.e. how flexible it is in ramping up or down. The *K* value describes hydraulic and fisheries/environmental constraints as one number, which characterizes the plant's ability to adjust to load. It only models transmission constraints and impacts of other generators on plant hydrogeneration - to the extent they limit historical plant flexibility. As a measure of the *K* value, plants without any operating flexibility have a *K* equal to zero, while plants with a high level of flexibility may have a *K* value as high as 5. The proportionality constant is found by regressing scaled hourly plant generation against scaled load:

$$\frac{G-\bar{G}}{\bar{G}} = K\frac{L-\bar{L}}{\bar{L}} \tag{3.5}$$

In some cases one *K* is suitable for all water conditions; in others it is not.

K factor calculations were performed on Grand Coulee Dam for 2009. The Bonneville Power Administration (BPA) 2009 scaled load was regressed with 2009 scaled Grand Coulee hydrogeneration. The *K* value for December was determined to be 2.42 (Figure 3.7), while that for August was 4.89 (Figure 3.8). From the regression, the correlation coefficient (R^2) value provides a measure of how well the plant generation correlates to the load demand. The R^2 value for December is 0.80, and for August it is 0.88, indicating that the plant generation correlates fairly well with the load. A plot of all monthly *K* values and correlation coefficients for 2009 is shown in Figure 3.9, providing illustration of the need for using month-specific *K* values in PLF-modeling scenarios in certain plants.

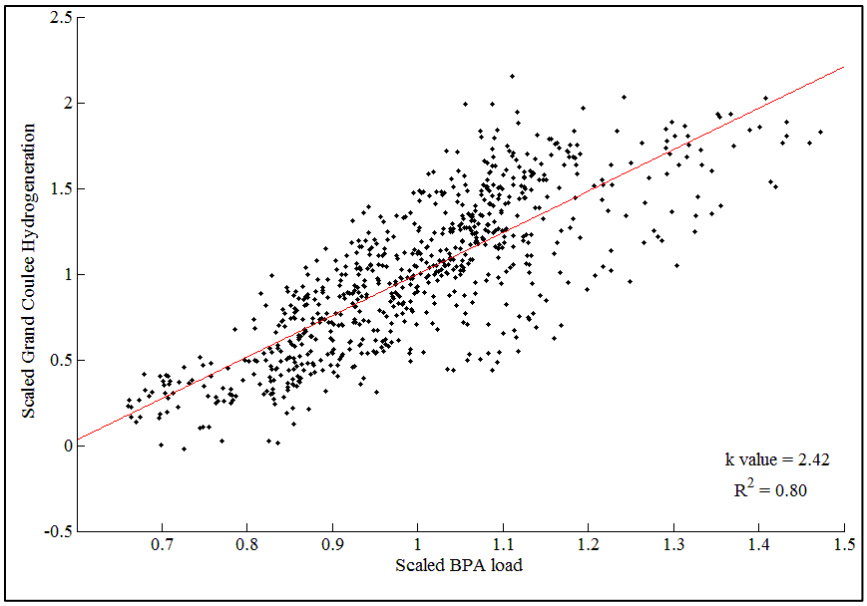

Figure 3.7: Regression between scaled hourly generation at Grand Coulee Dam and scaled load in the BPA control area during December 2009

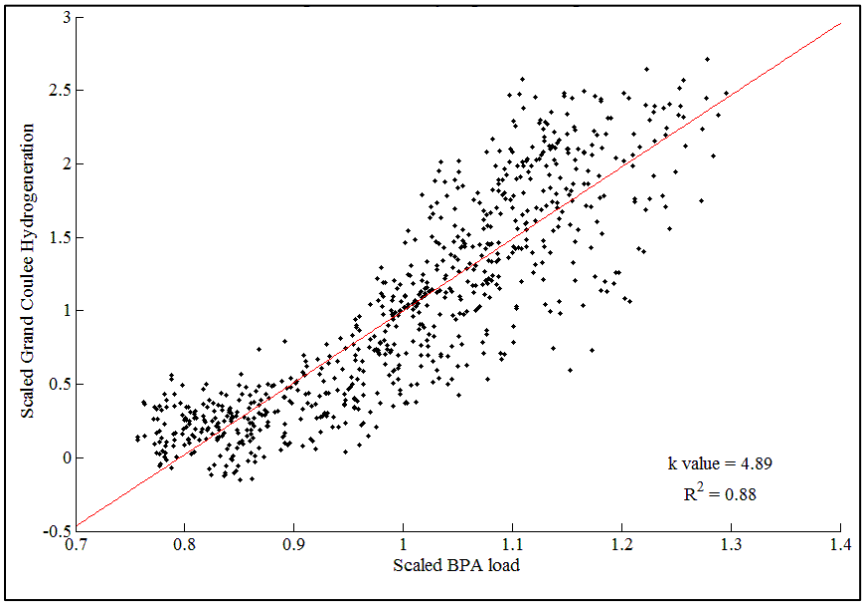

Figure 3.8: Regression between scaled hourly generation at Grand Coulee Dam and scaled load in the BPA control area during August 2009

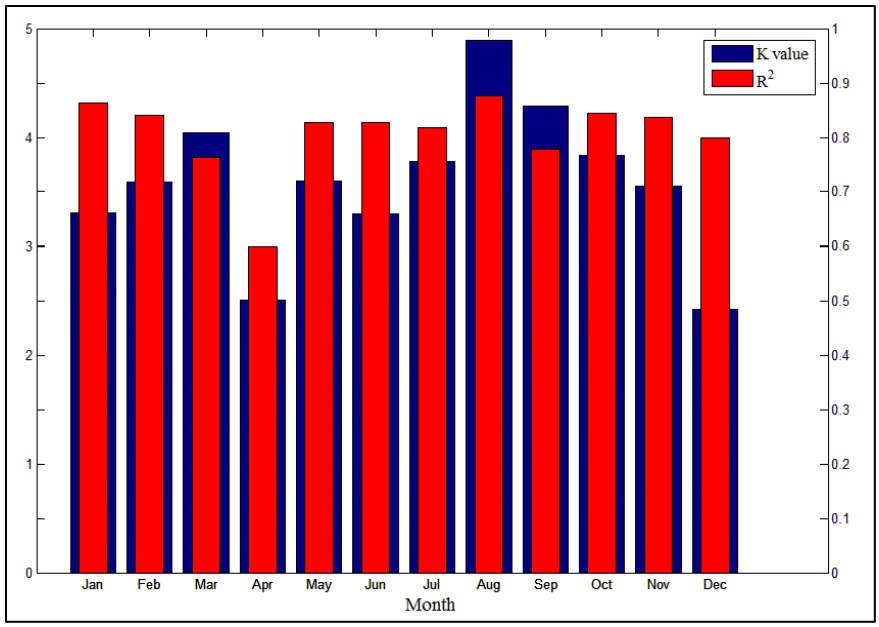

Figure 3.9: 2009 monthly K values and correlation coefficients for Grand Coulee Dam

In order to produce an hourly generation profile, the PLF model uses the algorithm:

$$G = \bar{G} + \frac{L-\bar{L}}{\bar{L}} K\bar{G} \tag{3.6}$$

where G is generation, L is load, K is the PLF constant, and over bars denote averages. The second term on the right hand side can be viewed as the plant flexibility, which modulates variability. It is a function of both average generation and the K value. This implies that in periods of high generation plant flexibility increases. To assess whether this is true one can investigate correlations between K and generation. As K values and loads increase the equation could yield a generation value greater than plant capacity. Similarly, large K and low generation could drive generation below a plant minimum or even negative. $\bar{G}$ is therefore replaced with G_0:

$$G = G_0 + \frac{L-\bar{L}}{\bar{L}} K G_0 \quad (3.7)$$

and is constrained by:

$$G_{min} < G_0 < G_{max} \quad (3.8)$$

Iterative adjustment of G_0 forces the average G to equal $\bar{G}$ within a convergence criterion. As average generation approaches plant capacity, plant variability decreases. In the extreme case of average generation equaling plant capacity, the plant runs at its capacity rating during all hours regardless of the K value. A root finding approach such as Newton's or bisection determines G_0. In Figure 3.10, the BPA load, Grand Coulee hydrogeneration, and PLF-modeled hydrogeneration for 3 days in four selected months are shown, using a K value and R^2 calculated as described above. It can be seen qualitatively in this figure that the higher the K value, the more closely the PLF-modeled hydrogeneration agrees with the actual. As a demonstration of the effect that R^2 has on the accuracy of the forecasted values, the top two plots compare December and April. These months have a similar K value, but a different R^2. The PLF-modeled hydrogeneration for December, with a R^2 of 0.8, follows load more closely than that of April, with a R^2 of 0.6. This difference is due to an increase in April hydrogeneration in response to increased water resource, rather than increased load. The quantification of the model effectiveness is assessed in an error analysis to follow.

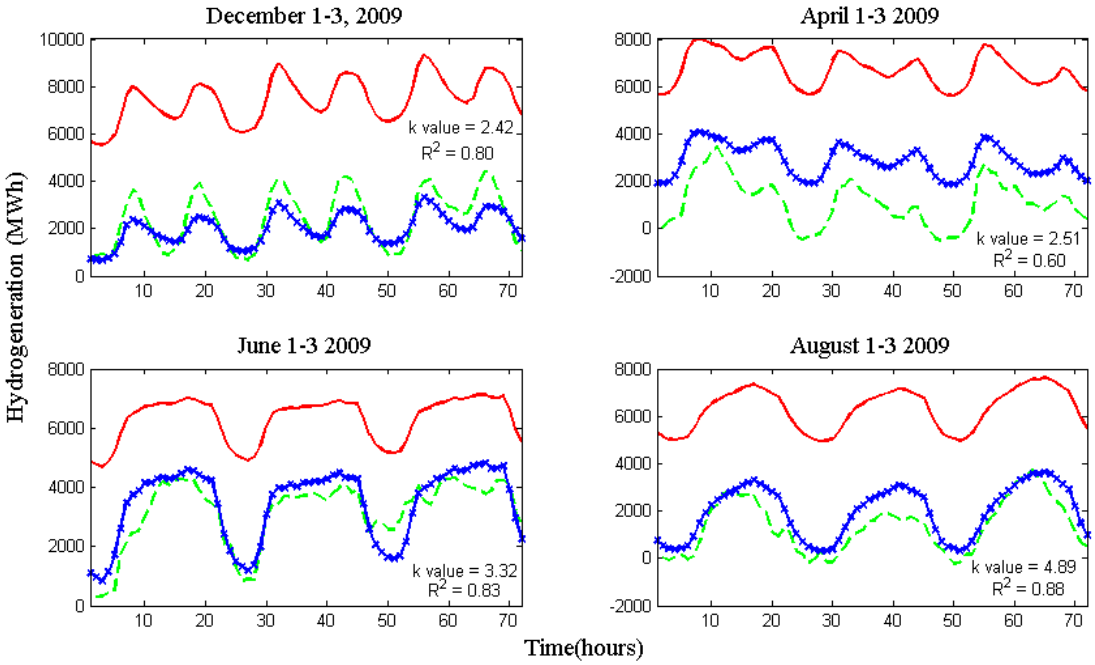

Figure 3.10: Comparison of 72-hour BPA load (red, solid), Grand Coulee hydrogeneration (green, dashed) and PLF-modeled Grand Coulee hydrogeneration (blue, x-marker) for four months in 2009

In order to quantify the effectiveness of the PLF model, a forecast error analysis was performed. Data for 2009 hourly hydrogeneration and hourly PLF-modeled hydrogeneration for Grand Coulee Dam were compared on a monthly basis using standard forecast error analyses as follows. First, the Forecast Error (FE) for each time step *k* was calculated as:

$$FE_k = F_k - A_k \tag{3.9}$$

where F is the forecast and A is the actual hydrogeneration value. The FE was divided by the nameplate capacity of the Grand Coulee power plant to normalize the value as a percent of capacity (NFE). Using these values, the Normalized Mean Absolute Error (N*MAE*) for each month was calculated as:

$$NMAE = \frac{1}{N}\sum_{k=1}^{N}|NFE_k| \tag{3.10}$$

where N is the number of time steps for the month. The monthly values for NMAE are shown in Figure 3.11.

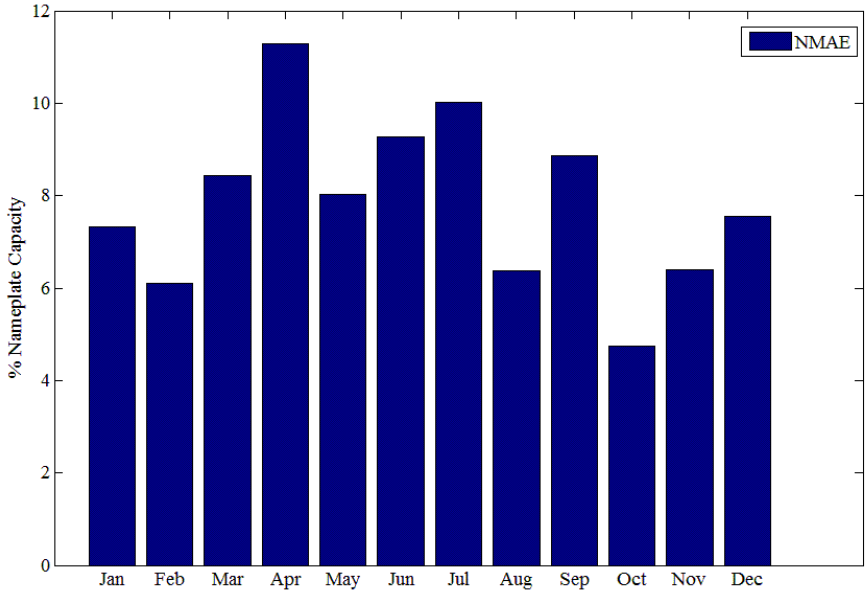

Figure 3.11: Normalized MAE for hourly PLF-modeled Grand Coulee Hydrogeneration, 2009

As discussed previously, although December and April had similar *K* values, the R^2 was quite different, resulting in a difference in model forecast accuracy. This can be seen quantitatively in Figure 3.11. April has a higher NMAE than December, indicating that the December PLF-modeled hydrogeneration is more accurate than April, verifying the qualitative results seen in Figure 3.10.

The use of PLF as a hydrogeneration model is advantageous only for those plants whose operation is governed by load. An example of this is seen in a comparison of three Northwestern dams. John Day, Chief Joseph, and Lookout Point dams were modeled for 2006 hydrogeneration using HD with 2002 data, and PLF using 2002 *K* values and plant characteristics. A correlation of the PLF-modeled results with the actual generation was

performed, with the results presented in Table 3.1. For John Day and Chief Joseph, PLF results in higher correlation values, with Chief Joseph having higher correlations, probably because it is less affected by fish operating constraints. Lookout Point has a variable operation that is less affected by load. Not surprisingly, historical data predicts its operation more accurately.

Table 3.1: Correlation coefficients of modeled hydrogeneration with 2006 actual hydrogeneration (Chisholm, Miller, & Davies, 2008)

Dam	2006 actual	2002 HD	2002 PLF
John Day	1.0	0.55	0.7
Chief Joseph	1.0	0.69	0.81
Lookout Point	1.0	0.37	0.30

In using PLF to model appropriate plants, TEPCC gains an advantage over historically derived generation profiles. First, the use of PLF reduces the data storage and processing time, since the hydrogeneration values needed include only the monthly plant minimum and maximum, monthly allowable energy, and monthly *K* constant, for a total of 48 numbers versus the 8760 needed for HD. Often, general knowledge of a plant's operation allows assignment of a *K* value, for cases in which hourly generation data are not available. This can often be assessed by obtaining minimal information from plant operators. For example, if the plant does not vary its generation over a 24 hour period, then the *K* value will be zero. In the case where plant generation routinely goes to zero at night, then *K* is equal to 4. If the plant generation sometimes, but not routinely, goes to zero, the *K* value is considered to be approximately 3.

Second, PLF calculated generation can be applied to forecasted loads, since the hydrogeneration shape is not coupled with the load, as in HD. Additionally, loads may be adjusted for non-dispatchable generation. By subtracting must run resources, such as wind and solar, from the load, the PLF model can generate a profile incorporating these resources. In this way, the flexibility of the hydro plant compensates for the must run resources. When a

PLF-modeled generation profile incorporating renewables is used as input in a production cost model, the resulting LMP pricing, in effect, accounts for the renewables. This method is tested in the 2019 case study presented in Chapter 4, and analyzed in Chapter 6.

Disadvantages in using the PLF model are that it doesn't take into account non-load operational constraints, and does not cost-optimize the hydrogeneration in the PCM's SCUC/SCED. Still, it can be a valuable tool for accounting for inherent hydro plant flexibility in long-term transmission studies. In addition, the PLF model can be a useful interim solution until more progress is made enhancing capabilities for modeling hydraulic constraints and interaction of hydro and non-hydro resources in PCMs.

3.4 HTC Method and Evaluation Results

PROMOD uses hydrogeneration profiles generated from HD, PS, or PLF to modify load curves used to produce the SCUC and SCED in PROMOD; therefore the hydrogeneration is not optimized within the system as is the thermal generation. An additional method available to TEPPC is HTC, a model within PROMOD that modifies the scheduling of hydro energy into the thermal commitment and dispatch algorithm as warranted by energy prices (LMP). As used by TEPPC, HTC adjusts hydrogeneration profiles created by PLF, dispatching a portion of the available resource based on price during the thermal unit dispatch.

Because HTC modifies the generation curve produced by PLF, it uses all the same monthly inputs with the addition of ramp rates and monthly "*p*" factors. The *p* factor represents the fraction (between 0 and 1) of a plant's dispatchable capacity that can adjust its output based on market price. One approach to calculating *p* comes from noting that PLF K values and their R^2 values provide a measure of plant flexibility. Flexibility can then be allocated between PLF and HTC. The range of plant generation, *A*, is estimated using the PLF equation:

$$A = \left[KG\frac{L_{max}-\bar{L}}{\bar{L}} - KG\frac{L_{min}-\bar{L}}{\bar{L}}\right] \quad (3.11)$$

Adjustments of a plant's flexibility designated to HTC can be made up to $4pC$ where C is the plant maximum capacity minus plant minimum generation and the four relates to the flexibility of moving up or down in each of two PROMOD SCUC/SCED iterations. Assuming PLF dispatches half of a plant's flexibility to follow the load and HTC dispatches the other half to react to market prices, an equation to obtain p can be derived:

$$4pC = \frac{A}{2} \rightarrow p = \frac{A}{8C} \quad (3.12)$$

It should be noted that because half of the plant's flexibility is now assumed by HTC, the calculated PLF K value should be halved when used in the PLF model. Table 3.2 displays the p factor calculation variables and the resulting p factor for three Northwestern hydro plants: John Day, Grand Coulee, and Chief Joseph.

Table 3.2: p factor calculation variables for three Northwestern power plants (TEPPC Hydromodeling Task Force, 2009)

	$(L_{max}-L_{min})L_{avg}$	R^2	K	G	C	A	p
John Day	0.57	0.32	1.27	1134	2480	1451	**0.07**
Chief Joseph	0.57	0.62	2.97	1162	2614	2498	**0.12**
Grand Coulee	0.57	0.65	3.9	2362	6765	6513	**0.12**

This is just one approach to calculating the p factor; other techniques may be used depending on the information available on a given hydro plant. Regardless of the techniques used, modeling experience has shown that p factors should not exceed approximately 0.11.

Once the *p* factors have been determined for specified hydro plants, the HTC modeling proceeds as follows. First, a PLF-modeled generation curve for a hydropower generator is created using the PLF input parameters. The PLF generation curve, maximum/minimum generator capacity, monthly energy, ramp rates, and monthly *p* factors are all then used as inputs into the HTC module linked to the SCUC/SCED algorithm. Based on these input parameters, PROMOD will re-dispatch a portion of the hydrogeneration determined by the PLF hydro schedule in concert with the thermal generators to optimize both the thermal and hydro generation. PROMOD then produces an optimized revised monthly generation time-series for each hydro plant for which HTC is applied.

A PROMOD simulation utilizing HTC results in not only an optimized hydro dispatch schedule, but also more accurate LMP valuations in the system. Figure 3.12 shows the dispatch of a hydro generator using HTC. The node price and the dispatch of the same generator using PLF is also shown. It can be seen that HTC generation increases over PLF when the price is high, and decreases below PLF when the price is low (black circles).

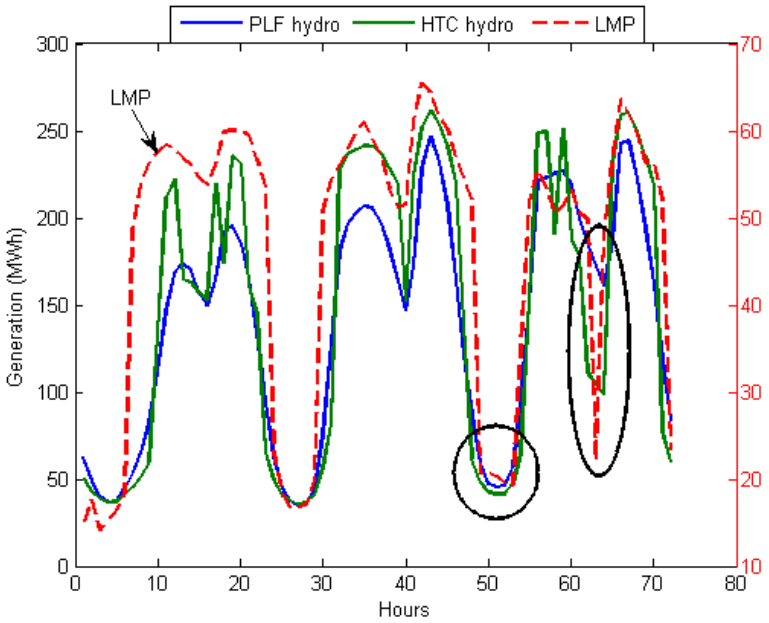

Figure 3.12: Hydro plant hourly dispatch schedule.

The utilization of HTC can result in lower and less variable LMP values at nodes. The northern region of British Columbia was simulated in PROMOD, utilizing HTC. Table 3.3 shows a comparison of LMP values and standard deviation, for PROMOD simulations using either PS hydro modeling or HTC. The use of HTC reduced the average LMP value as well as the standard deviation.

Table 3.3: Comparison of LMP values and standard deviations for the northern region of British Columbia (TEPPC Hydromodeling Task Force, 2009)

	Avg Daily Std. Dev	**Max Daily Std. Dev**	**Min Daily Std. Dev**	**Avg LMP**	**Max LMP**	**Min LMP**
Peak Shave	10.02	18.02	2.52	40.16	74.09	-1.96
HTC	8.99	17.06	2.05	40.00	72.24	0.99

With respect to wind power integration, the Chief Joseph 2009 hydrogeneration was modeled using PLF and simulated in PROMOD, with and without HTC. In both PROMOD runs, NWPP wind power was accounted for in the system load input. The results showed that the PLF-alone modeled hydro did not respond as effectively to the wind as did the HTC modified hydro profile (Figure 3.13). This visual result was confirmed numerically by correlating the wind generation with the hydrogeneration for both profiles. The results are shown in Table 3.4, along with values obtained from a similar analysis done with Grand Coulee power plant. A greater negative R^2 value was obtained for wind/HTC-modeled hydrogeneration correlations than that for PLF alone.

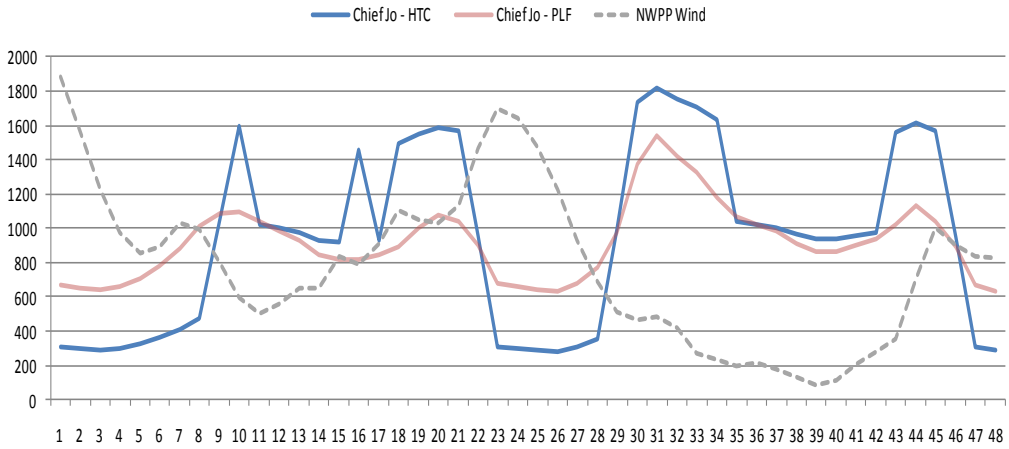

Figure 3.13: Chief Joseph hydrogeneration in comparison to NWPP wind generation for 48 hours in April, 2009 (TEPPC Hydromodeling Task Force, 2009)

Table 3.4: Comparison of wind/hydrogeneration correlation coefficients for PLF and HTC (TEPPC Hydromodeling Task Force, 2009)

Power Plant/Model Method	Wind/Hydrogeneration R^2
Chief Joseph/PLF only	-0.011
Chief Joseph/HTC	-0.209
Grand Coulee/PLF only	-0.090
Grand Coulee/HTC	-0.280

HTC does not work well with all hydro plants. For example, HTC would not be an appropriate modeling method if the majority of a plant's generation is determined by run of the river, environmental controls, or flood control.

TEPPC, having recognized the deficiencies of HD and PS for certain plants or regions, developed the two methods outlined in the previous sections. It was then important to use PLF and HTC on applicable hydro plants in a transmission simulation, and compare the outputs with an identical simulation, with hydro plant modeling performed with HD and PS. The next chapter discusses a 2019 PCM simulation performed in order to do just that.

4 2019 SIMULATION STUDY

This chapter outlines a WI simulation case study performed to demonstrate the effects that PLF and HTC modeling have on PCM simulation outputs, and to determine if the simulation efficacy is improved over those utilizing HD or PS. The 2019 transmission case study focused on optimizing the hydrogeneration modeling of the Pacific NW region of the WI. This region is characterized by high levels of hydro penetration, with the potential for high levels of wind penetration in the future.

4.1 Data Test Case and Simulation Scenarios

A data test case (DTC) was created for the entire WI system with system load, hydrogeneration, fuel costs and availability, thermo-generator characteristics, wind generation (using 2019 state RPSs), transmission power flow, etc. adjusted to 2019 levels. This DTC contained all of the inputs needed for a PROMOD simulation. A full description of the DTC development can be found in the TEPPC 2009 Study Program Results Report (WECC, 2010) with a brief summary in the Appendix of this document. Twelve plants in the NW were selected for hydrogeneration model variation; in each of three scenarios conducted using the 2019 DTC, the hydrogeneration modeling method in the DTC was altered, using traditional hydro-modeling methods, PLF, or PLF with HTC modification. The hydro plants were chosen by size, operational flexibility, geographical diversity, and operator diversity. In addition, all of these projects adjust their operation to meet electricity demand, so are suitable for modeling with PLF and HTC. Although there are approximately 200 hydroelectric projects in the northwestern United States, these 12 projects generated about 55 % of regional hydrogeneration in 2006. Some large projects, such as Bonneville Dam and Priest Rapids Dam, were not selected because fisheries constraints, not electricity demand, drive their operations; this makes them unsuitable for modeling by load following. Most are listed as run of river, in that they have limited storage capacity relative to their average daily flow. This is

characteristic of the Columbia River Basin which has less storage compared to its annual discharge volume than other large rivers in the US. While limited storage prevents them from distributing generation across months, most discharge into pools of downstream projects. Thus, they can regulate flows on a daily, and to some extent, weekly basis. Many can reduce discharge to zero during times of low load demand (graveyard hours) (Chisholm T. , 2010). The twelve plants are listed in Table 4.1, along with important details such as the plant nameplate capacity, the plant operator, the type of hydro plant (storage, run-of-river), the river it is located on, the balancing area it is contained in, and the hydrogeneration modeling method traditionally used by TEPPC. The geographic locations of the plants are depicted in Figure 4.1. The monthly *K* values and *p* factors used in the 2019 PCM simulations for each plant are listed in the Appendix.

Table 4.1: PNW hydro plants modeled in 2019 DTC scenarios

Plant	Nameplate Capacity MW	Operator	Type	Storage (thousand acre feet)	River	Balancing Area	Traditional Hydro-modeling Method
John Day	2160	USACOE – Portland District	Storage	534	Columbia	BPA	HD
The Dalles	1820	USACOE – Portland District	Run of River	50	Columbia	BPA	HD
Brownlee	585	Idaho Power	Storage	975	Snake	TVA	PS
Round Butte	247	Portland General Electric	Storage	535	Deschutes	PGN	HD
Chief Joseph	2456	USACOE – Seattle District	Run of River	201	Columbia	BPA	HD
Little Goose	810	USACOE – Walla Walla District	Run of River	50	Snake	BPA	HD
Boundary	1040	Seattle City Light	Run of River	26	Pend D'Oreille	SCL	HD
Wells	774	Douglas County PUD #1	Run of River	93	Columbia	DOPD	HD
Grand Coulee	6495	U. S. Bureau of Reclamation	Storage	5185	Columbia	BPA	HD
Rocky Reach	1279	Chelan County PUD #1	Run of River	37	Columbia	CHPD	HD

Plant	Nameplate Capacity MW	Operator	Type	Storage (thousand acre feet)	River	Balancing Area	Traditional Hydro-modeling Method
Noxon	466	Avista	Run of River	64	Clark Fork	AVA	PS
Lower Monumental	810	USACOE – Walla Walla District	Run of River	20	Snake	BPA	HD

Figure 4.1: Geographic distribution of PNW hydro plants. KEY: 1-Boundary, 2-Brownlee, 3-Chief Joseph, 4-Grand Coulee, 5-John Day, 6-Little Goose, 7-Lower Monumental, 8-Noxon, 9-Rocky Reach, 10-Round Butte, 11-The Dalles, 12-Wells

The three 2019 DTC PROMOD simulation scenarios are as follows. The first scenario (2019-HDPS) was a standard 2019 DTC, with all hydro modeling, including that of the selected PNW hydro plants, performed using HD or PS, dependent upon the hydro plant (see Table 4.1). The second scenario (2019-PLF) utilized the 2019 DTC, but modeled the NW hydro plants with PLF. The third scenario (2019-HTC) utilized the 2019 DTC, but modeled the NW plants using PLF, and then optimized generation of these plants with HTC.

In order to investigate the effectiveness that modeling with PLF and HTC has with the integration of renewable energy, an additional DTC was identified. In this case (2019LW), all

system inputs remained the same except that the predicted wind generation in the NW was decreased to that existing in 2010. The 2019 DTC contained 8,200 MW of wind capacity in the NW, while the 2010 had 2,600 MW. This 5,600 MW difference in wind capacity between the two is significant enough to differentiate between PCM simulation results (Pacini, 2010). The three hydromodeling scenarios described above were repeated with the 2019LW DTC (2019LW-HDPS, 2019LW-PLF, 2019LW-HTC). A listing of all of the scenarios, with identification labels, is presented in Table 4.2 for ease of reporting results.

Table 4.2: 2019 DTC PCM simulation scenario grid

DTC	Standard Hydro Modeling (PS or HD)	PLF-Modeling of NW Plants	PLF + HTC Modeling of NW Plants
2019	2019-HDPS	2019-PLF	2019-HTC
2019LW	2019LW-HDPS	2019LW-PLF	2019LW-HTC

4.2 PCM Output Overview

As mentioned in previous chapters, there are numerous outputs that may be obtained from a PCM simulation. For this thesis, the output data was restricted to selected hourly area loads, selected hourly area wind generation, selected hourly hydro plant generation, selected hourly bus LMP, and selected hourly path transmission flows.

As can be seen in Table 4.1, seven balancing authority (BA) areas[12] are involved, based on their containment of a selected hydro plant(s). These are:

- Bonneville Power Administration (BPA)
- Treasure Valley, part of Idaho Power (TVA)
- Portland General Electric (PGN)
- Seattle City and Light (SCL)
- Douglas County Public Utility District (DOPD)

[12] See Chapter 1 for WECC system description and the definition of a balancing authority.

- Chelan County Public Utility District (CHPD)
- Avista (AVA)

The geographic locations of these BAs are shown in Figure 4.2 (boxed in red). The 2019 hourly load and hourly wind generation for these specific areas are utilized in the analysis of the PCM results in Chapter 6. In four of these areas (BPA, PGN, AVA and TVA), hourly wind generation profiles were used in the data analysis. Only two of these, BPA and PGN, differed in the amount of wind generation from the 2019 DTC to the 2019LW DTC, as described in the previous section. This is due to the geographical location of planned 2019 wind plants. The wind generation in the AVA and TVA was the same for both DTCs.

Additionally, six transmission paths were chosen for which to analyze transmission flow data, shown in Figure 4.2, with its TTC, or the maximum flow the path can accommodate, listed in Table 4.3. These paths were chosen based on their level of importance in the NW. Lastly, twelve significant buses were chosen for which to analyze LMP, one for each hydro plant.

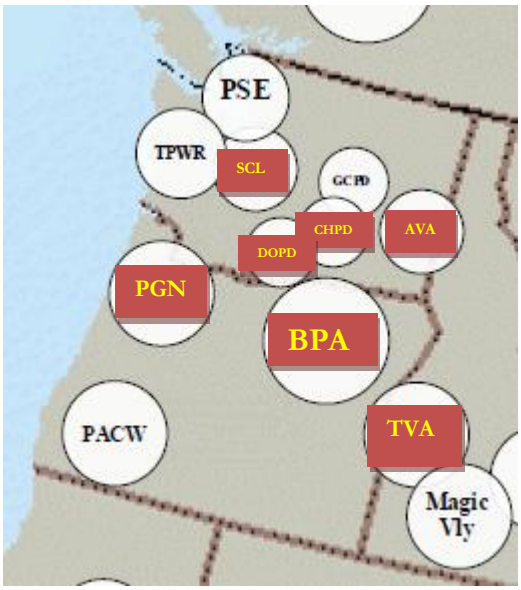

Figure 4.2: Balancing Authorities used in analysis of 2019 DTC scenario PCM simulation results

Table 4.3: Transmission paths used in analysis of 2019 DTC scenario PCM simulation results

Transmission Path	TTC (MW)	Abbreviation
California-Oregon Intertie	+ 4,800 /- 3,675	COI
Montana-Northwest	+ 2200 /- 1,350	MNW
North of John Day	± 8,400	NJD
Pacific DC Intertie	+ 3,100 /- 2,780	PDCI
West of Cascades-North	±10,500	WCN
West of Cascades-South	± 7,000	WCS

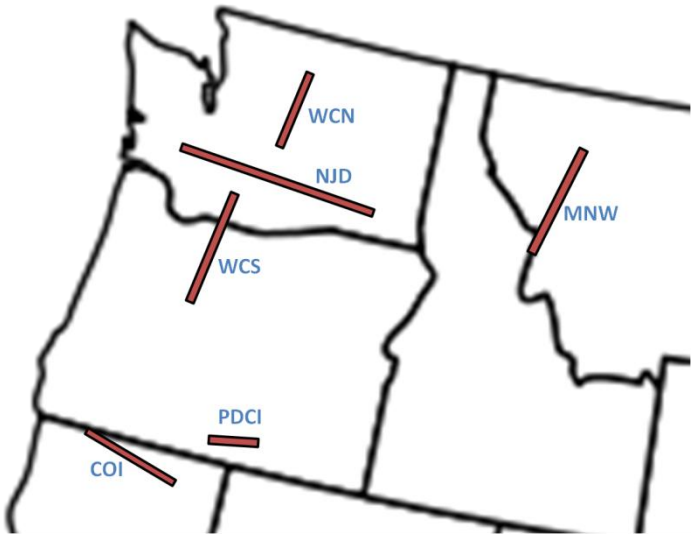

Figure 4.3: Geographic location of transmission paths used in analysis of 2019 DTC scenario PCM simulation results

The WECC defines seasons and load use hours, which will be used in reporting results in this thesis also. WECC system seasons are defined as follows:

- Winter: November – March
- Spring: April, May
- Summer: June – October

Heavy load hours in the WECC are defined as the hours 0600-2200 Monday through Saturday. Light load hours are defined as the hours 2200-0600 Monday through Saturday, and all hours on Sunday (WECC, 2009).

4.3 2019 Load and Wind Generation Overview

In this section, the area load and wind generation profiles used in the simulation scenarios are presented. The load for all areas was a 2019 load set derived for the TEPPC 2009 Study Program (WECC, 2010). The total yearly load in MW, by area, is presented in Figure 4.4. From this figure, it is obvious that the majority of the load demand is in the BPA, with subsequent demands in decreasing order: PGN, AVA, TVA, SCL, CHPD, and DOPD. The monthly mean load distribution for the year for the aggregated BAs, is shown in Figure 4.5. To provide a feel for the load variability within the seasons, the normalized standard deviation for each season was calculated as the standard deviation (Equation 3.19) of the data set (winter, spring, or summer) divided by the maximum load for that month, and multiplied by 100. This gives the standard deviation as a percentage of the load, so the relative area values can be compared. The normalized standard deviations of the seasonal loads for each BA are shown in Figure 4.6.

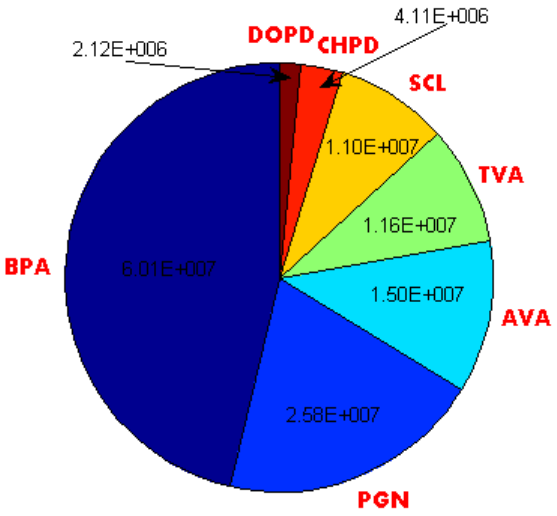

Figure 4.4: Yearly load demand for all BAs in MWh

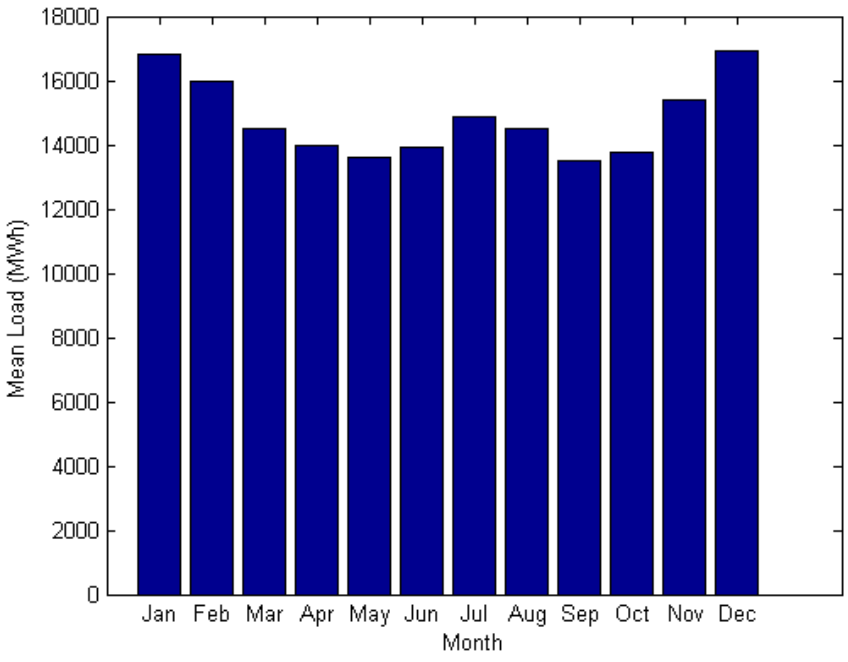

Figure 4.5: Monthly mean load distribution for aggregated BAs

Yearly load profiles are provided in the Appendix for further investigation. General trends are that 1) load variability is highest in the spring for all areas, and 2) that BPA, SCL, CHPD and DOPD have slightly higher summer variability than winter, while the opposite is true for PGN, AVA, and TVA.

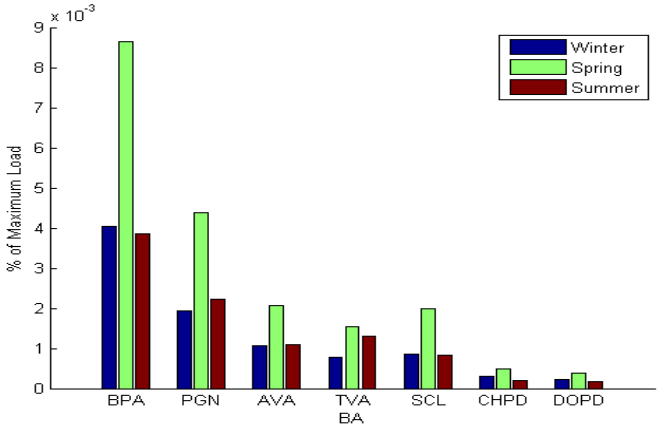

Figure 4.6: Seasonal normalized standard deviation of load for all BAs

The same sequence of data presentation is followed for the 2019 DTC and 2019LW DTC wind generation, where wind is produced in four of the areas (BPA, PGN, AVA, TVA). The yearly wind generation is shown in Figures 4.7 and 4.8, the seasonal wind generation distribution in Figure 4.9, and the seasonal normalized standard deviations in Figures 4.10 and 4.11. General trends for the wind data indicate that BPA by far has the largest amount of wind generation, followed by PGN, TVA, and AVA in descending total amounts. The spring season experienced the highest variability in wind generation, followed by summer, then winter. Again, yearly wind generation profiles are provided in the Appendix.

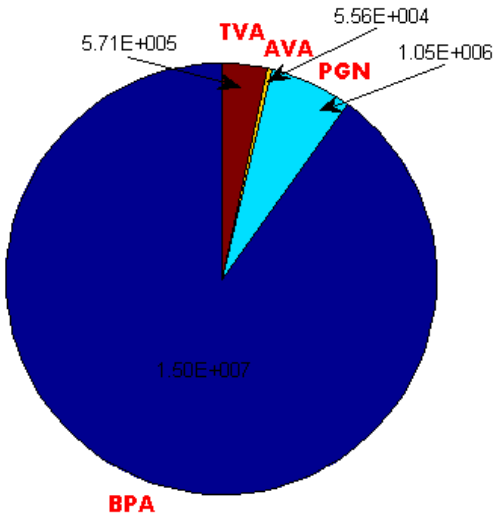

Figure 4.7: Yearly wind generation for all BAs in MWh, 2019 DTC

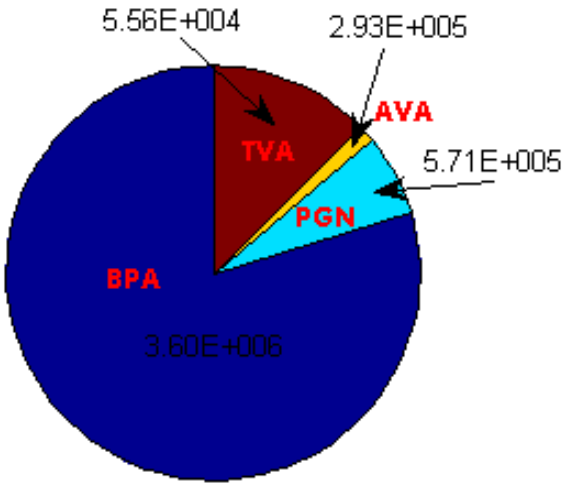

Figure 4.8: Yearly wind generation for all BAs in MWh, 2019LW DTC

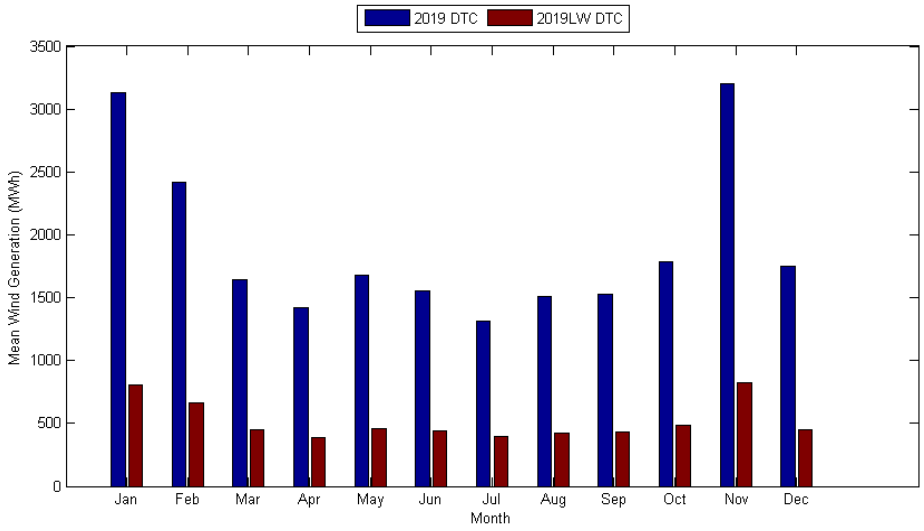

Figure 4.9: Average monthly wind generation for aggregated BAs, 2019 DTC and 2019LW DTC

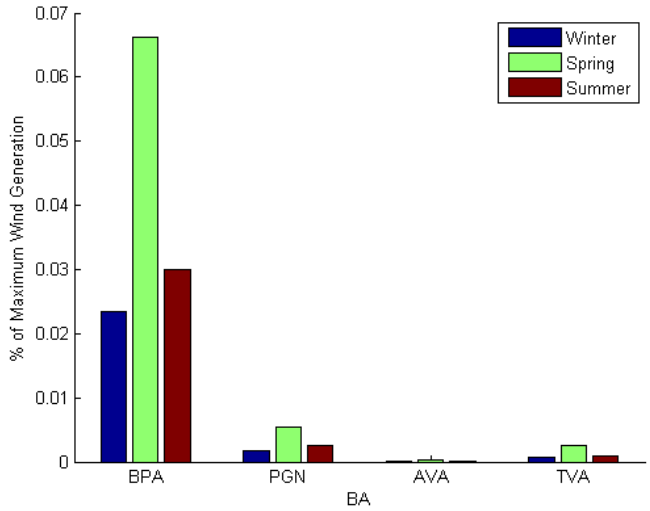

Figure 4.10: Seasonal normalized standard deviation of wind generation for all BAs, 2019 DTC

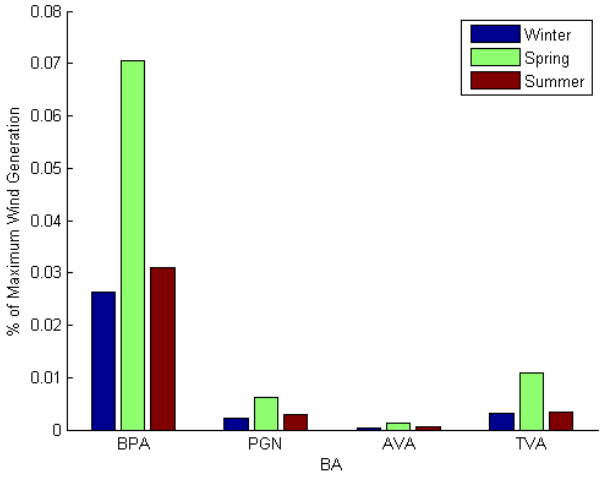

Figure 4.11: Seasonal normalized standard deviation of wind generation for all BAs, 2019LW DTC

4.4 Results Objectives

The overriding objectives for conducting this 2019 case study were:

1. Establish whether the PLF modeling method improves the load following response of hydrogeneration over that modeled with HD or PS

2. Determine if the HTC method improves the price following response of hydrogeneration over that modeled with PLF or HDPS

3. Determine if HTC modeling improves the hydrogeneration response to system events such as transmission congestion and renewable energy inputs over that of PLF

4. Demonstrate that TEPPC's utilization of PLF and HTC for hydrogeneration modeling in a PCM used for long-term transmission studies improves the veracity of the simulation results.

The next chapter discusses the results and analyses of the PCM modeling scenarios, in the context of these objectives.

5 IEEE Conference Proceedings Publication

Improving Hydrogeneration Representation in a Production Cost Model Used for Long-Term Transmission Studies in the Western Interconnection

C.M. Dennis, *Graduate Research Assistant*, R.C. Walish, *Graduate Research Assistant*, H.M. Pacini, *Planning Engineer*, T.A. Chisholm, *Hydraulic Engineer*, T.L. Acker, *Professor of Mechanical Engineering*

***Abstract*-- The Western Electricity Coordinating Council, recognizing the importance of interconnection-wide transmission planning, formed the Transmission Expansion Planning Policy Committee (TEPPC) in 2006. TEPPC is tasked with conducting regional transmission expansion planning studies involving system modeling; as well as performing analyses of future transmission congestion and operational impacts. TEPPC utilizes the production cost model (PCM) PROMOD IV© to model the Western Interconnection for these studies. In certain geographic regions, a high level of hydropower penetration necessitates careful consideration of hydrogeneration models used in the PCM to produce the most accurate system results. This work details the hydro modeling methods utilized by TEPPC for improving hourly hydrogeneration time series representations in transmission planning studies. The justification and benefits for using these methods are outlined in this paper, and the results of a 2019 transmission study are shown to illustrate of the advantages for employing these methods.**

***Index Terms*-- Hydroelectric generators, hydroelectric power generation, production cost model, hydrogeneration shape, power system modeling, proportional load following, hydrothermal co-optimization, WECC, system transmission studies, hydrogeneration model, transmission planning.**

INTRODUCTION

Hydropower penetration in the United States varies with respect to geographic region. Regions that have large rivers with steep gradients possess greater hydropower resource. Hydrogeneration differs from thermal generation in that it is not only limited by plant capacity, but also by water supply, and therefore energy availability. Hydrogeneration plants also have dispatchability constraints due to environmental or other operational factors (i.e. irrigation water deliveries, flood control, environmental release) that are sometimes unpredictable.

C. M. Dennis and R.C. Walish are candidates in the Master's of Science in Engineering program at Northern Arizona University in Flagstaff, AZ 86001 USA (email: cmd93@nau.edu, rcw32@nau.edu).

T. L. Acker is a Professor of Mechanical Engineering at Northern Arizona University in Flagstaff, AZ 86001 USA (email: Tom.Acker@nau.edu).

H. M. Pacini is a Staff Engineer with the Western Electricity Coordinating Council, Salt Lake City, UT 84103 USA. (email: hpacini@wecc.biz)

T. A. Chisholm is a Hydraulic Engineer with the Bonneville Power Administration Portland, OR 97208 USA (email: tachisholm@bpa.gov)

However, in many cases hydropower plants have significant generation flexibility arising from their particular operating regime; this may include reservoir storage, consistency of resource, and minimal environmental constraints.

Of primary concern to transmission planners is the incorporation of accurate hydrogeneration into models that are used for the long-term planning of transmission. By simulating the power system under different operating conditions, long-term transmission studies can investigate future transmission bottlenecks, line utilization, effects on locational marginal pricing (LMP), the adequacy of resources for future loads, and the economic impacts of transmission expansion. The Western Electricity Coordinating Council (WECC) performs such analyses in order to identify future transmission expansion needs for the Western Interconnection (WI). One method for analyzing future system transmission needs is to use production cost models (PCM) in order to simulate an economic system generation dispatch within the constraints of the system. Constraints present in the operating system include those of transmission (line capacities, transfer limits), generation (plant capacities and availabilities, ramp rates, operating costs), and security (power quality regulations, reserve regulations). Inputs to the system model then consist of a load model, generation model, and a transmission model. A PCM simulation produces a cost- and security-optimized unit commitment and dispatch schedule based on these inputs. Additional simulation outputs can include transmission utilization, LMP valuation, and system operational costs.

Representing the flexibility of a hydro plant in a PCM allows it to better respond to load variations and transmission constraints; therefore the generation can be cost-optimized, resulting in a more realistic system transmission. There are numerous methods available for modeling hydrogenation; these methods vary in data, computing, and manpower requirements. In general, the most accurate hydrogeneration models require large sets of data to account for multiple variables and multiple water availability scenarios, which leads to the need for extensive computing resources. However, transmission planners may have limited individual plant hydrogeneration data available to them due to proprietary issues, or may not have sufficient computing power or personnel to carry out detailed hydrogeneration modeling. In addition, the PCM is limited in its ability to model all relevant hydro plant characteristics and constraints. Modeling of hourly hydro output is often done outside the PCM, in which case the hydrogenation dispatch is not optimized within the constraints of the operating system, as is the thermal generation.

Transmission Planning at WECC

WECC is one of eight regional entities that have delegation agreements with the North American Electric Reliability Corporation (NERC). WECC's mission is to assure a reliable bulk electric power system in the WI. WECC, recognizing the need for a regional approach to transmission expansion planning, organized the Transmission Expansion Planning Policy Committee (TEPPC) to provide transmission expansion planning coordination and leadership across the WI. TEPPC works in close coordination with sub-regional planning groups, transmission operators, and others to perform regional economic transmission expansion planning studies in the WI.

One of TEPPC's primary responsibilities is to guide analyses and modeling for the WI's economic transmission expansion planning. As part of this responsibility, TEPPC develops an annual study program that details the transmission system expansion studies it will perform. Analyses and studies performed by TEPPC focus on plans with interconnection-wide implications and include a high-level assessment of transmission congestion and operational impacts. TEPPC is also responsible for the management of an economic transmission planning database that is made available to the public via the WECC website and serves as the starting point for congestion studies performed by TEPPC. In order to avoid confidentiality issues regarding data transparency, the TEPPC database includes information compiled from publicly available sources regarding loads, transmission, fuel prices, existing generation, and planned generation.

As of 2008, hydrogeneration made up approximately 54 percent of generation in the Northwest Power Pool (NWPP) operating area, as opposed to 29 percent of the generation in the entire WI [1]. It is essential that this level of hydrogeneration penetration is carefully modeled in order to effectively represent its impacts on future transmission simulations. TEPPC has limited access to hydrological data, individual plant characteristics and specific hourly generation data. Therefore, to fulfill its responsibilities with regard to regional transmission expansion planning, TEPPC models the WI using a commercial PCM, PROMOD IV©, which dispatches generation resources based on the variable cost of operation and within the operating constraints of the transmission system. Due to TEPPC and PCM limitations, methods are needed that effectively represent hydrogeneration in planning studies without requiring extensive, unit specific hydro data. TEPPC has endeavored to maximize long-term planning efficiency by developing or incorporating new hydro modeling methods that accomplish this objective.

TEPPC Hydrogeneration Modeling

Traditionally, TEPPC modeled hydrogeneration using historical generation data (HD) time series. This method assumes that future generation will be similar to past generation given similar loads. Historical generation patterns reflect constraints on the hydro power system in the year from which the data was taken. However, it does not reflect constraints that may be present in future operating conditions. If loads and generation are correlated, then generation must be updated whenever loads change. In addition, load or generation discrepancies in the data year are carried forward as predictions of future discrepancies. As discussed previously, one function of TEPPC is to carry out annual transmission expansion studies, and the forecast year is set based on the requests of TEPPC's stakeholders. This can be a 10- or 20-year forecast time frame; consequently, the lack of accuracy is an issue, particularly if the flexibility of certain hydro plants is not properly factored in.

Another common hydrogeneration model used in PCM packages is the peak shaving (PS) model. The PS model assumes plants dispatch limited energy during times of highest loads subject to minimum and maximum generation constraints. In this way, the resource-limited hydrogeneration is dispatched to reduce the total operating cost of the thermal system [2].

In recent years, research has been ongoing into modeling methods that more accurately forecast hydrogeneration, and therefore more effectively integrate it with thermal generation

and planning [2]-[4]. Some methods for modeling hydrogeneration include linear programming [5] and dynamic programming (DP). DP methods take into account various hydro and thermal system constraints and come up with a series of algorithms to describe the system [6]. These algorithms can be solved using mixed integer linear programming [7], Lagrangian relaxation [8], or neural networks [9], [10]. Hydrogeneration modeling packages using DP such as RiverWare are commercially available, and several of the production cost models include DP hydrogeneration (GTMax and GridView). While these models often take into consideration many hydrogeneration constraints such as those encountered with environmental conditions, and those of the system such as transmission, pricing, and regulation, they are also extremely computationally time-intensive, and require large data sets and modeling manpower.

In order to produce effective studies of long-term transmission expansion planning needs, TEPPC requires a hydrogeneration model that uses minimal data, minimal modeling manpower, but satisfactorily represents a hydro plant's flexibility. Two methods for better integrating hydrogeneration into a PCM-based transmission planning scenario have been tested. One of these, proportional load following (PLF), is a method for improving the modeling of hydrogeneration for plants whose operation is primarily governed by load variability. PLF modeling uses as inputs monthly plant minimum and maximum operating capacity, the allowable monthly energy, and an assigned proportionality constant ("K" value) determined by the plant's ability to follow load. This greatly reduces the hydro plant data requirements compared to HD, as will be discussed in a later section.

The second method is the hydrothermal co-optimization (HTC) model within PROMOD. HTC allows for a portion of the generation capacity of suitable hydro plants to be cost optimized within the system constraints as are the thermal generators. In this way, the flexible portion of the plant capacity is at the disposal of the system, and more accurate transmission simulation results can be obtained. Within PROMOD, HTC relies upon a PLF-modeled hydro shape and a "p" factor, which describes the fraction of a plant's capacity that is able to be cost-optimized within the full system constraints in the PCM. Both of these methods will be discussed in detail in the modeling section of this paper.

Following these method descriptions, results from a 2019 TEPPC simulation in the NWPP of WECC are presented as demonstration. Three scenarios were run in PROMOD, concentrating on twelve key plants in the NWPP of the WECC:

1. 2019 base case, standard hydrogeneration modeling on 12 key plants
2. 2019 base case, with the addition of PLF hydrogeneration modeling on 12 key plants
3. 2019 base case as above, with the generation of 12 key plants optimized using HTC

The results of these simulations, in terms of transmission utilization and LMP pricing, are discussed and compared. Finally, the advantages and disadvantages in utilizing HTC and PLF in PCM-based transmission planning are discussed.

MODELING

The following sections discuss TEPPC's use of PROMOD focusing on the aspects that are important to understanding the dispatch of resources in response to loads and operational

costs. Next, the hydrogeneration models TEPPC utilized prior to implementing the new models, HD and PS are briefly described, followed by sections describing the new methods (PLF and HTC) TEPPC has adopted for improving hydrogeneration representation in transmission studies along with the applicability, advantages, and disadvantages of each. Results from a 2019 transmission case study are used as demonstration of the advantages TEPPC gains in using these new modeling methods.

TEPPC's Use of PROMOD PCM

Production cost modeling equates total generation with the total load at each point in time, while minimizing operational costs within the constraints of the transmission system. In using PROMOD for transmission planning, TEPPC simulates the entire WI under varying conditions to identify future load, generation, or transmission issues that should be addressed before they arise. In looking at the transmission system as a whole, areas of congestion and bottlenecks can be identified. This aids system planners in decision-making for new or upgraded transmission lines. In addition, system configuration changes can be analyzed in advance to determine the economic impacts of such issues as increased renewables penetration, transmission line additions, decommissioning of plants, or fuel market fluctuations.

PROMOD encompasses sub-models for generation (i.e. the energy resource available within a given system), transmission, and load. The generator inputs needed vary based on the type of resource being used, but include operating capacities, heat rates, operation and maintenance (O&M) costs, fuel type and cost, forced outage rates, ramp rates, and minimum runtime and downtime. The transmission inputs include the buses and branches, generation to bus mapping, flowgates and contingencies, and line constraints. For the load input, annual peak and energy forecasts are applied to an hourly load shape and adjusted to produce the input demand shape. In addition, security operational requirements (spinning reserve, operational reserve), and tariffs are additional examples of possible inputs. PROMOD utilizes these inputs to generate a security constrained unit commitment and security constrained economic dispatch (SCUC, SCED).

PROMOD uses a direct current optimal power flow (DCOPF) analysis of the transmission system. A DCOPF is a linear approximation of the actual AC flow in the entire system, with the assumptions that there are small voltage angle differences between the lines, the line resistance is considered to be negligible, and that there is a flat voltage or all voltages magnitude are equal or close to unity. The optimized DCOPF of the system is incorporated with generation shift factors (GSF) to determine the LMP at each bus in the system being analyzed [13]. GSFs are a measure of what fraction of a generator's output goes through a particular line, or flowgate, in the transmission system, from the point of a reference bus.

Once the system generation has been optimized, the LMP pricing at each node is known, and these can be used to compare system scenarios in long-term studies. The scenarios TEPPC models in PROMOD each have varying load and resource assumptions based on both current and potential future energy policies. The TEPPC goal is to use the results produced by PROMOD to identify patterns in future regional transmission congestion, which

can then be used to inform decision-makers regarding future transmission expansion needs in the WI.

Historical Data and Peak Shave Hydrogeneration Model

The HD hydro modeling method uses historic generation values from the same year as the load shape being used. It requires one year of historical hourly loads to set the load shape, and any atypical hourly load patterns will be carried forward into the future year simulations. This presents a problem when there are anomalous load variations in a given year, and this year is used to model a future year's load profile. It is particularly troublesome when attempting to model hydrogeneration in the far future (i.e. 10 or 20 years ahead), as the system load profile, and therefore hydrogeneration profile, will most likely be significantly different. In addition, assessing the effects of transmission congestion using historical generation that may have itself been limited by congestion will underestimate potential future congestion.

Because the hydro generation is "hard-wired" into the PCM via use of a historical generation time-series, changes to the historical load shape require that the hydro generation profiles also be updated for those plants whose output changes based on changes in the load. Other correlations may exist between the load and hydro generation which will also require that the HD be updated or modified when the load shapes change. A considerable drawback for modeling hydrogeneration using HD is that it prevents any available flexibility in a hydro plant in response to system changes such as renewable generation, system outages, market pricing, or transmission congestion, from being utilized in the PCM.

The PS model essentially allocates hydrogeneration to peak load periods, and not to those periods when demand is low. Since hydrogeneration is resource limited, the PS model assures that the hydrogeneration will be dispatched during peak load periods, thereby reducing the thermal operating costs of the system. The magnitude of peak shaving that occurs depends upon the system make-up; in systems with a high hydro penetration, the peak shave level will be high, while the opposite is true for a low penetration system. The PS hydrogeneration model has some of the same disadvantages of HD, since it is also hard-wired into the PCM model. For both HD and PS, once the hydrogeneration shape is developed from the load profile, it is set and cannot change with system variations in PROMOD.

Proportional Load Following Model

TEPPC, in cooperation with Ventyx (the developer of PROMOD), has developed and tested a proportional load following model for hydrogeneration. This particular model is sensitive to the data and task constraints that TEPPC operates under, namely limited access to specific hydrogeneration data, limited modeling personnel, and a need to recognize and utilize any inherent flexibility a hydro plant may have in a years-ahead transmission study. The PLF approach to modeling hydrogeneration assumes that generation is proportional to load subject to minimum and maximum capacity and an energy limit. An additional variable, the proportionality constant (*K*), quantifies the ability of the plant to follow load, i.e. how flexible it is in ramping up or down. The *K* value describes hydraulic and fisheries/environmental constraints as one number, which characterizes the plant's ability to adjust to load. It only models transmission constraints and impacts of other generators on plant hydrogeneration - to

the extent they limit historical plant flexibility. As a measure of the *K* value, plants without any operating flexibility have a *K* equal to zero, while plants with a high level of flexibility may have a *K* value as high as 5. The proportionality constant is found by regressing scaled hourly plant generation against scaled load. In some cases one *K* is suitable for all water conditions; in others it is not.

Monthly *K* factor calculations were performed on Grand Coulee Dam for 2009. The Bonneville Power Administration (BPA) scaled load for 2009 was regressed with scaled Grand Coulee hydrogeneration for 2009. The *K* value for December was determined to be 2.42 (Fig. 1), while that for August was 4.89.

From the regression, the R^2 value for the correlation coefficient provides a measure of how well the plant generation correlates to the load demand. The R^2 value for December is 0.80, and for August it is 0.88, indicating that the plant generation correlates fairly well with the load. A plot of all monthly *K* values and correlation coefficients for 2009 is shown in Fig. 2, providing illustration of the need for using month-specific *K* values in PLF-modeling scenarios for certain plants.

In order to produce an hourly generation profile, the PLF model uses the algorithm:

$$G = \bar{G} + \frac{L-\bar{L}}{\bar{L}} K\bar{G}$$

where *G* is generation, *L* is load, *K* is the PLF constant, and over bars denote averages. The second term on the right hand side can be viewed as the plant flexibility, which modulates variability. It is a function of both average generation and the *K* value. This implies that in periods of high generation plant

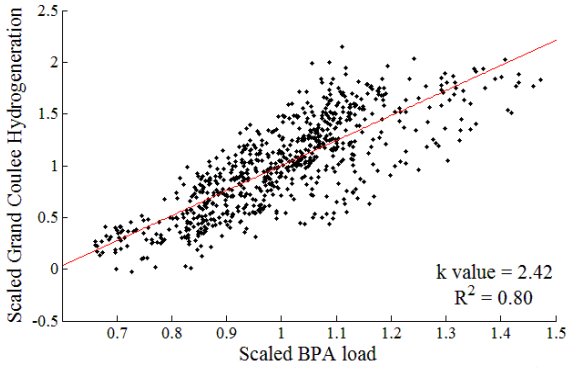

Figure 5.1: Regression between scaled hourly generation at Grand Coulee Dam and scaled load in the Bonneville Power Administration control area during December 2009

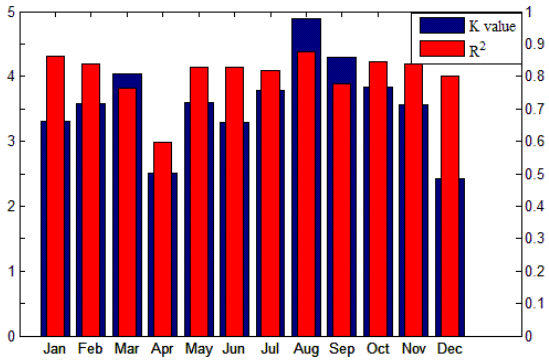

Figure 5.2: 2009 monthly K values and correlation coefficients for Grand Coulee Dam

flexibility increases. To assess whether this is true one can investigate correlations between *K* and generation. As *K* values and loads increase the equation could yield a generation value greater than plant capacity. Similarly, large *K* and low generation could drive generation below a plant minimum or even negative. *G* is therefore replaced with G_0:

$$G = G_0 + \frac{L-\bar{L}}{\bar{L}} K G_0$$

and is constrained by:

$$G_{min} < G_0 < G_{max}$$

Iterative adjustment of G_0 forces the average *G* to equal $\bar{G}$ within a convergence criterion. As average generation approaches plant capacity, plant variability decreases. In the extreme case of average generation equaling plant capacity, the plant runs at its capacity rating during all hours regardless of the *K* value. A root finding approach such as Newton's method determines G_0. In Fig. 3, the BPA load, actual Grand Coulee hydrogeneration, and PLF-modeled hydrogeneration for 3 days in four selected months are shown, with the *K* value used in the modeling and the R^2 calculated as described above.

It can be seen qualitatively in this figure that the higher the *K* value, the more flexible the plant is in responding to load variations. The top two plots compare December and April. These months have a similar *K* value, but a different R^2. The PLF-modeled hydrogeneration for December, with a R^2 of 0.8,

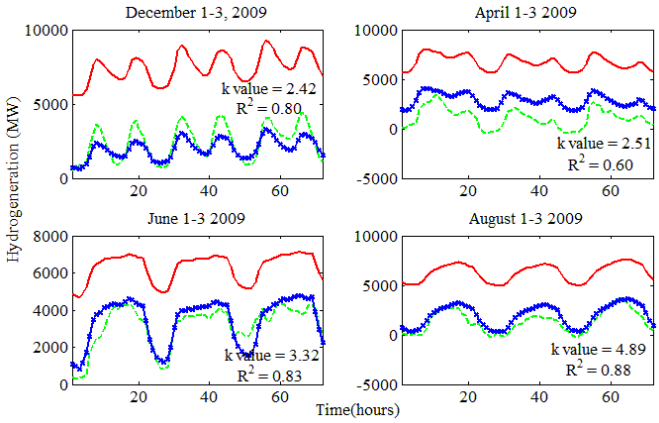

Figure 5.3: Comparison of 72-hour BPA load (red, solid), actual Grand Coulee hydrogeneration (green, dashed) and PLF-modeled Grand Coulee hydrogeneration (blue, x-marker) for four months in 2009

follows load more closely than that of April, with a R^2 of 0.6. This difference is due to an increase in April hydrogeneration in response to increased water resource, rather than increased load. The quantification of the model effectiveness is assessed in an error analysis to follow.

In order to quantify the effectiveness of the PLF model, a back-cast forecast error analysis was performed. Data for 2009 hourly hydrogeneration and hourly PLF-modeled hydrogeneration for Grand Coulee Dam was compared on a monthly basis using standard forecast error analyses as follows. First, the Forecast Error (FE) for each time step k was calculated as:

$$FE_k = F_k - A_k$$

where F is the forecast value and A is the actual value.
This value was divided by the nameplate capacity of the Grand Coulee power plant to normalize the value as a percent of capacity (NFE). Using these values, the Normalized Mean Absolute Error (NMAE) for each month was calculated as:

$$MAE = \frac{1}{N}\sum_{k=1}^{N}|NFE_k|$$

where N is the number of time steps for the month. The monthly values for NMAE are shown in Fig. 4.

As discussed previously, although December and April had similar K values, the R^2 values were quite different; resulting in a difference in model forecast accuracy. This can be seen quantitatively in Fig. 4. April has a higher NMAE than December, indicating that the

December PLF-modeled hydrogeneration is more accurate than April, verifying the qualitative results seen in Fig. 3.

The use of PLF as a hydrogeneration model is advantageous only for those plants whose operation is governed by load. An example of this is seen in a comparison of three Northwestern dams. John Day, Chief Joseph, and Lookout Point plants were modeled for 2006 hydrogeneration using HD with 2002 data, and PLF using 2002 *K* values and plant characteristics. A correlation of the PLF-modeled results with the actual generation was performed, with the results presented in Table 1.

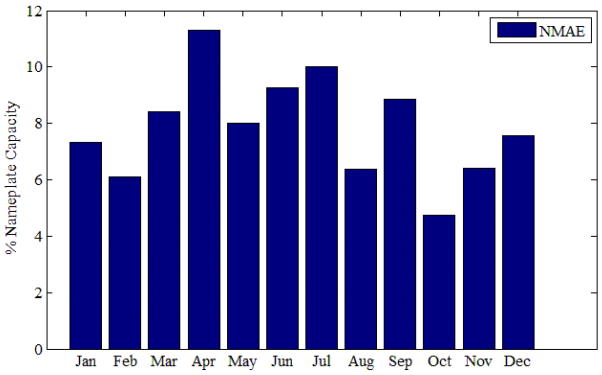

Figure 5.4: Normalized MAE for hourly PLF-modeled Grand Coulee Hydrogeneration, 2009

For John Day and Chief Joseph, PLF results in higher correlation values, with Chief Joseph having higher correlations, probably because it is less affected by fish operating constraints. Lookout Point has a variable operation that is less affected by load. Not surprisingly, historical data predicts its operation more accurately.

TABLE 5.1
CORRELATION COEFFICIENTS OF MODELED
HYDROGENERATION WITH 2006 ACTUAL HYDROGENERATION

Plant	2006 actual	2002 HD	2002 PLF
John Day	1.0	0.55	0.7
Chief Joseph	1.0	0.69	0.81
Lookout Point	1.0	0.37	0.30

In using PLF to model appropriate plants, TEPPC gains an advantage over historically derived generation profiles. The use of PLF reduces the data storage and processing time, since hydrogeneration values needed include only the monthly plant minimum and maximum, monthly allowable energy, and monthly *K* constant, for a total of 48 separate values versus the 8760 needed for HD. Often, general knowledge of a plant's operation allows assignment of a *K* value, for cases in which hourly generation data are not available. This can often be assessed

by obtaining minimal information from plant operators. For example, if the plant does not vary its generation over a 24 hour period, then the *K* value will be zero. Experience in the U.S. Pacific Northwest has shown that where plant generation routinely goes to zero at night, then *K* is approximately equal to 4. If the plant generation sometimes, but not routinely, goes to zero, the *K* value may be approximately 3.

Disadvantages in using the PLF model are that it doesn't take into account non-load related operational constraints, and does not cost-optimize the hydrogeneration in the PCM's unit dispatch step. Still, it can be a valuable tool for accounting for inherent hydro plant flexibility in long-term transmission studies. In addition, the PLF model can be a useful interim solution until more progress is made enhancing capabilities for modeling hydraulic constraints and interaction of hydro and non-hydro resources in PCMs.

Hydro Thermal Co-optimization Model

PROMOD uses hydrogeneration profiles generated from HD, PS, or PLF to modify load curves used to produce the SCUC and SCED in PROMOD; therefore the hydrogeneration is not optimized within the system as is the thermal generation. An additional method available to TEPPC is HTC, a model within PROMOD that modifies the scheduling of hydro energy into the thermal commitment and dispatch algorithm as warranted by energy prices (LMP). As used by TEPPC, HTC adjusts hydrogeneration profiles created by PLF, dispatching a portion of the available resource based on price during the thermal unit dispatch.

Because HTC modifies the generation curve produced by PLF, it uses all the same monthly inputs with the addition of ramp rates and monthly "*p*" factors. The *p* factor represents the fraction (between 0 and 1) of a plant's capacity that can adjust its output based on market price. For example, a *p* value of 0.2 implies 20% of a hydro-generator's dispatchable capacity may react to price. Adjustments of a plant's flexibility designated to HTC can be made up to $4pC$ where *C* is the plant maximum capacity minus plant minimum generation and the four relates to the flexibility of moving up or down in each of two iterations. One approach to calculating *p* comes from noting that PLF *K* values and their R^2 values provide a measure of plant flexibility. Flexibility can then be allocated between PLF and HTC. The range of plant generation, *A*, is estimated using the PLF equation:

$$A = \left[KG\frac{L_{max}-\bar{L}}{L} - KG\frac{L_{min}-\bar{L}}{L}\right]\frac{1}{\sqrt{R^2}} \quad (7)$$

where R^2 is obtained from the PLF regression analysis. Assuming PLF dispatches half of a plant's flexibility to follow the load and HTC dispatches the other half to react to market prices, an equation to obtain *p* can be derived.

$$4pC = \frac{A}{2} \rightarrow p = \frac{A}{8C}$$

It should be noted that because half of the plant's flexibility is now assumed by HTC, the calculated PLF *K* value should be halved. Table 2 displays the p factor calculation variables and

the resulting *p* factor for three hydro plants in the Pacific Northwest; John Day, Grand Coulee, and Chief Joseph.

This is just one approach to calculating the *p* factor, other techniques of calculating the *p* factor may be used depending on the information available on a given hydro plant. Regardless of the techniques used to calculate the *p* factor, modeling experience has shown that *p* factor values should not exceed approximately 0.1.

Once the p factors have been determined for specified hydro plants, the HTC modeling proceeds in PROMOD as follows. First, a PLF-modeled generation curve for a hydropower generator is created using the PLF input parameters. The PLF generation curve, maximum/minimum generator capacity, monthly energy, ramp rates, and monthly *p* factors are all then used as inputs into the HTC method. Based on these input parameters, PROMOD will re-dispatch a portion of the hydrogeneration determined by the PLF hydro schedule in concert with the thermal generators to optimize both the thermal and hydrogeneration. PROMOD then produces optimized revised monthly generation time-series for each hydro plant for which HTC is applied.

TABLE 5.2
P FACTOR CALCULATION PARAMETERS FOR THREE
NORTHWESTERN POWER PLANTS

Plant	$(L_{max}-L_{min})L_{avg}$	R^2	*K*	*G*	*C*	*A*	*p*
John Day	0.57	0.32	1.27	1134	2480	1451	**0.07**
Chief Joseph	0.57	0.62	2.97	1162	2614	2498	**0.12**
Grand Coulee	0.57	0.65	3.9	2362	6765	6513	**0.12**

2019 Simulation Modeling

The method analysis described herein focused on optimizing the hydrogeneration modeling of the NWPP region of the WI. This region is characterized by high levels of hydro penetration. Three test case scenarios were created for the entire WI system with system load, hydrogeneration, fuel costs and availability, thermal generator characteristics, wind generation, and transmission network configurations adjusted to 2019 levels. Twelve hydro plants in the NWPP were selected to test the PLF and HTC methods. The hydro plants were chosen by size, operational flexibility, geographical diversity, and operator diversity. In addition, the 12 projects selected routinely adjust their operation to meet electricity demand, and are therefore good candidates for PLF and HTC. Although there are approximately 200 hydroelectric projects in the northwestern United States, these 12 projects generated about 55 percent of WI hydrogeneration in 2006.

The three 2019 WI system PROMOD simulation scenarios are as follows. The first scenario (HDPS) is a standard 2019 TEPPC case; with hydro modeling of the selected 12 NW hydro plants performed using HD or PS, dependent upon the plant. PS was used for plants where hourly generation data was unavailable. In the second "PLF" scenario, the production time-

series for the 12 NWPP hydro plants were modified using PLF; all remaining plants were modeled as in the previous scenario. Within the third "HTC" scenario, the NWPP plants were modeled using PLF, which was then optimized using HTC in PROMOD. The scenarios are listed in Table 3 to facilitate presentation of results.

TABLE 5.3
2019 PROMOD SIMULATION SCENARIO GRID

Scenario	Standard Hydro Modeling (HD and PS)	PLF-Modeling of NW Plants	PLF + HTC Modeling of NW Plants
Scenario Abbreviation	HDPS	PLF	HTC

Transmission paths from which data were extracted for comparison were selected based on their connectivity to the selected hydro plants. One bus, or an average of significant buses, was selected for each plant in order to compare LMP values.

SIMULATION RESULTS AND DISCUSSION

Due to the significant size of the data set for the 2019 transmission simulations, only the Grand Coulee LMP data and the California-Oregon Intertie (COI) transmission path data is presented for brevity. The COI is a WECC path located between southern Oregon and northern California, and is often heavily loaded due to less expensive hydrogeneration making its way into load-heavy California. Grand Coulee Dam is located in central Washington and is a large producer of hydrogeneration (~6800 MW maximum capacity).

As a demonstration of increased responsiveness of PLF to load and HTC to LMP variations in the system, Fig. 5 shows the PROMOD simulated dispatch of Grand Coulee and the LMP price at a significant bus for the first week of April, 2019 for the three scenarios. The R^2 value between the generation and LMP price is shown in the lower right hand corner of each plot. It can be seen that the HDPS dispatch has the lowest correlation, improving significantly in the PLF simulation and even more so in the HTC dispatch.

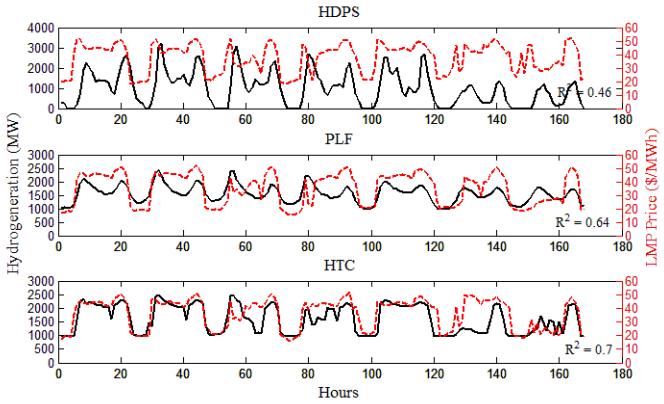

Figure 5.5: Hydrogeneration dispatch (black, solid) plotted against LMP bus price (red, dashed) for Grand Coulee in the first week of April, 2019. The R^2 between the two is shown in the lower right hand corner of each plot.

Select months were chosen for examining the impacts of PLF and HTC on transmission utilization. April is characterized by high hydro resource availability due to seasonal runoff and lower overall loads due to mild weather. It is expected that with higher LMP prices at buses (occurring at high loads), PROMOD-modeled transmission flows will increase, but must remain within transmission line constraints. Fig. 6 compares the April, 2019 hourly flow averages in all three scenarios for the COI path, as well as the average hourly BPA load. The BPA load is used simply as an example load shape; flows on the COI are affected by many other loads, especially those from California. Overall, the COI flow in the HDPS scenario is higher over the month, following patterns set in years before. Average flow in the PLF and HTC scenarios differ from that of HDPS significantly, due to the manner in which the modeling methods change the overall dispatch of the 12 NWPP plants. During the peak load period from 7 to 8 A.M., HTC re-dispatches from PLF in order to manage transmission restrictions. In the second peak at 8 P.M., the demand levels are lower and HTC can therefore increase dispatch (as compared to PLF) to respond to higher LMP prices. January is another interesting month to investigate since load is high, while the hydro resource is generally lower than in spring runoff, and therefore more expensive than in periods of higher resource availability.

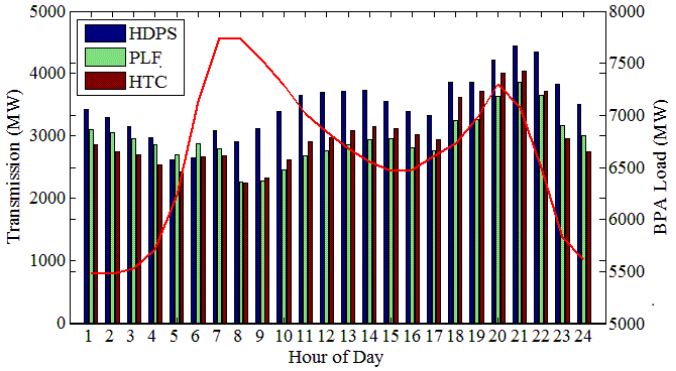

Figure 5.6: April 2019 hourly averaged COI path transmission overlaid with BPA Load (red line).

Fig. 7 compares the average hourly COI flow in January for all three scenarios against the average hourly BPA load. In this month, the transmission flow is similar to that of April, with HTC again re-dispatching from the PLF to better deal with transmission constraints, and increasing in the second peak when overall system line congestion is lower.

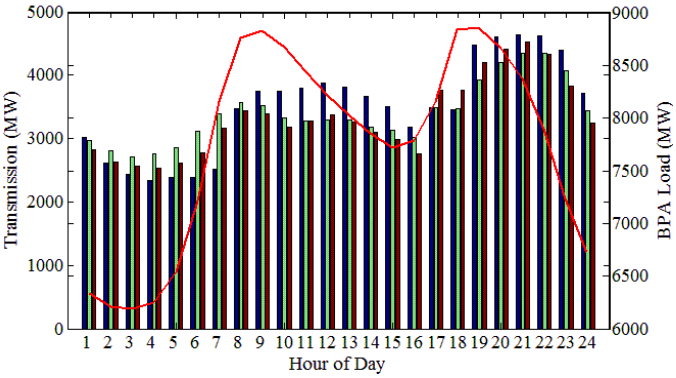

Figure 5.7. January 2019 hourly averaged COI path transmission overlaid with BPA Load (red line). Bars have the same designation as Fig. 6.

July, in contrast to January and April, experiences high load demand as well as high hydro resource. The average hourly transmission for July is shown in Fig. 8, and is quite different

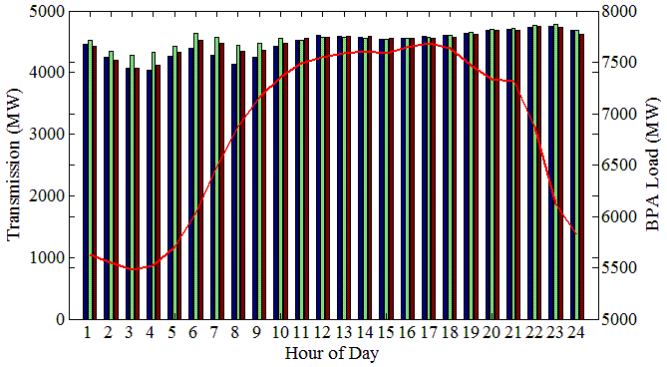

Figure. 5.8. July 2019 hourly averaged COI path transmission overlaid with BPA Load (red line). Bars have the same designation as Fig. 6.

than January and April. Since load demand in California and other areas is high, and the hydro resource in the NWPP is plentiful and less expensive than the thermal resources that are available, the average COI transmission flows are higher at all hours. In this case, the differences in transmission flows between the scenarios are small since the inexpensive and readily available hydro is being used to the maximum.

CONCLUSIONS AND FURTHER RESEARCH

The analysis of the efficacy of system-wide long-term transmission studies is difficult, in that there are numerous variables that must be estimated or assumed; and subsequently, actual transmission needs in 2019 won't be known for another 10 years. Regardless of these difficulties, future transmission plans benefit from modeling of the future system in order to best estimate the expected impacts and/or benefits of any proposed transmission/load/generation changes. TEPPC works to continue improving the results it obtains in transmission studies within both its limits and the limits of the PCM, by investigating the models that are available in, or can be incorporated into, PROMOD. These models can be tested with backcasts and other analyses. While this does not assure the accuracy of the forecasted transmission needs, it does provide some solid footing on which to base the soundness of the results. Further research is ongoing into the results obtained in the 2019 simulation case studies, including examining the effect of incorporating larger amounts of renewables, pursuant to the implementation of Renewable Portfolio Standards throughout the WI.

Based on the evaluations of PLF hydrogeneration modeling and HTC optimization of hydrogeneration dispatch conducted by TEPPC, it was determined that adopting these tools would be advantageous in future transmission studies. TEPPC systematically determined which plants in the WI were appropriate for PLF modeling and/or HTC. Applicable plants were assigned K values and/or p factors to enable their incorporation into the any future transmission studies. These methods are being used as an interim solution to the improvement of hydrogeneration representation in transmission studies using PCMs, until

dynamic hydrogeneration modeling becomes practical for use in TEPPC's transmission studies.

ACKNOWLEDGEMENT

The authors would like to acknowledge the support of Brad Harrison of Ventyx, an ABB Company, for reviewing the text.

REFERENCES

[2] Simopolous, D., Kavatza, S., & Vournas, C. "An enhanced peak shaving method for short term hydrothermal scheduling," *Energy Conversion and Management* 48 (2007): 3018–3024.

[3] Diniz, A.L., and M.E.P. Maceira. "A Four-Dimensional Model of Hydro Generationfor the Short-Term Hydrothermal Dispatch Problem Considering Head and Spillage Effects." *IEEE Transactions on Power Systems* 23, no. 3 (2008): 1298-1308.

[4] Borges, C.L.T., and R.J. Pinto. "Small Hydro Power Plants Energy Availability Modeling for Generation Reliability Evaluation." *IEEE Transactions on Power Systems* 23, no. 3 (2008): 1125-1135.

[5] Shawwash, Ziad K., Thomas K. Siu, and S. O. Denis Russell. "The B.C. Hydro Short Term Hydro Scheduling Optimization Model." *IEEE Transaction on Power Systems* 15, no. 3 (2000): 1125-1131.

[6] Siu, Thomas K., Garth A. Nash, and Ziad K. Shawwash. "A Practical, Hydro, Dynamic Unit Commitment and Loading Model." *IEEE Transactions on Power Systems* 16, no. 2 (2001): 301-306.

[7] Chang, Gary W., et al. "Experiences with Mixed Integer Linear Programming Based Approaches on Short-Term Hydro Scheduling." *IEEE Transaction on Power Systems* 16, no. 4 (2001): 743-749.

[8] Li, Chao-an, Eric Hsu, Alva Svoboda, Chung-Li Tseng, and Raymond Johnson. "Hydro Unit Commitment in Hydro-Thermal Optimization." *IEEE Transactions on Power Systems* 12, no. 2 (1997): 764-769.

[9] Gunesekara, C.G.S., Lanka Udwatta, and Sanjeewa Witharana. "Neural Network Based Optimum Model for Cascaded Hydro Power Generating System." *2nd International Conference on Information and Automation 2006 ICIA 2006 sustainable development through effective man-machine co-existence December 14-17, 2006, Galadari Hotel, Colombo, Sri Lanka.* 2006. 51-56.

[10] Kishor, Nand, Madhusudan Singh, and A.S. Raghuvanshi. "Particle Swarm Optimization based Neural-network Model fro Hydro power Plant Dynamics." *IEEE Congress on Evolutionary Computation (CEC 2007).* IEEE, 2007. 2725-2731.

[11] Wood, A.J., and B.F. Wollenberg. *Power Generation Operation and Control.* New York: Wiley, 1996.

6 SIMULATION RESULTS AND DISCUSSION

As discussed in Chapter 3, the efficacy of a long-term transmission study is often difficult to interpret, since there is no actual data with which to compare it. Therefore, a relative analysis method must be employed. In this chapter, Section 6.1 discusses the general efficacy of the simulation by presenting path transmission duration curves and LMP variability. Next, Section 6.2 details the results of the 2019 DTC scenarios (2019-HDPS, 2019-PLF, 2019-HTC), and compares them in terms of load following, price following, and system events such as congestion and renewable energy inputs. Section 6.3 further investigates the effects that renewable energy influx has by comparing the results of the 2019 DTC and the 2019LW DTC scenarios.

6.1 General Simulation Efficacy

In this section, the general efficacy of the simulation is assessed by comparing 2019 transmission path duration curves with those of averaged historical data. The historical path data was obtained from WECC, and included the years 2006, 2007, and 2008. All paths analyzed in this study (see Table 4.3) except for NJD had available historical data. In Figure 6.1, the yearly transmission duration curve for all three 2019 DTC scenarios for the WCN path is shown, and the results show that the path flow has a similar shape to that of the historical, with an increased magnitude, as would be expected for a 10 year ahead forecast. This indicates that the simulations are producing path flows that are comparable to that which would be expected in the future.

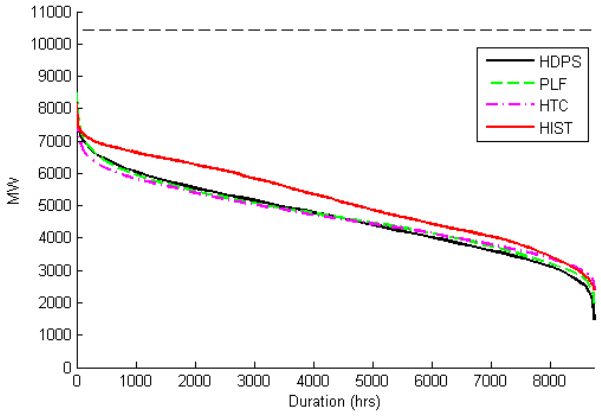

Figure 6.1: 2019 Transmission flow duration curves for all three 2019 DTC scenarios (HDPS, PLF, HTC) for the WCN, along with the historical (2006-2008) average. The black dashed line is the TTC

In contrast to the WCN path, the PCM scenarios for the PDCI path (Figure 6.2) show a departure in shape from that of the historical. Similar results were obtained in the TEPPC 2008 transmission study (WECC, 2009); this was attributed to the need for improving the modeling of DC lines. All other paths show a historical shape similarity, again indicating that the simulated transmission flow is viable. Transmission duration curves for the remaining paths are contained in the Appendix.

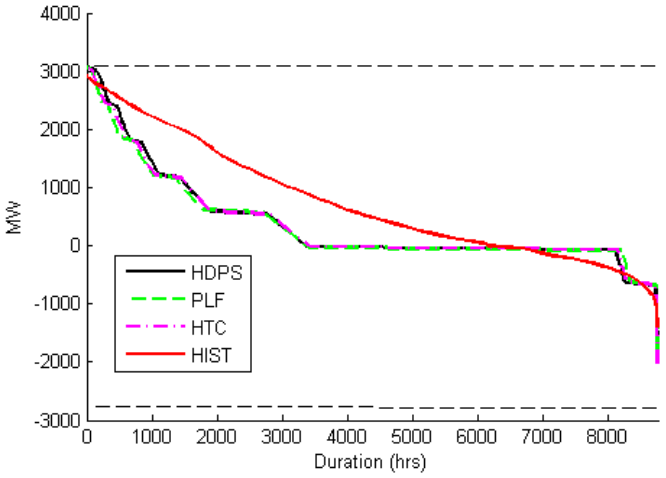

Figure 6.2: 2019 Transmission flow duration curves for all three 2019 DTC scenarios (HDPS, PLF, HTC) for the PDCI path, along with the historical (2006-2008) average. The black dashed line is the TTC

6.2 2019 DTC Scenario Comparisons

In this section, the three 2019 DTC scenario simulation results are presented and compared (2019-HDPS, 2019-PLF, 2019-HTC). The analyses used are those described in section 3.3.2. As stated in Chapter 3, since the future simulation results cannot be compared with any actual results to determine accuracy, the relative viability of the results can only be assessed. In section 6.2.1, the HDPS and PLF scenarios are compared in terms of load following representation. Section 6.2.2 contains the LMP analyses of the three scenarios, section 6.2.3 the congestion analyses, and section 6.2.4 the renewable event analyses.

6.2.1 PLF vs. HDPS Load Following

As a measure of the load-following ability of the generation in the 2019-HDPS and 2019-PLF scenarios, monthly correlations of plant generation to the corresponding BA load were

calculated as described in Section 3.2.2, and compared. Figure 6.2 shows the results for Grand Coulee power plant, which will be used as a representative plant for the BPA BA. In this figure, it can be seen that in all months, the PLF generation/load correlation is greater than that of the HDPS. This is confirmation of hydrogeneration modeling, in that the PLF-modeled hydrogeneration is derived from the forecasted load, while that of the HDPS (in the case of Grand Coulee, it is HD, as shown in Table 4.1) is derived from a representative load year.

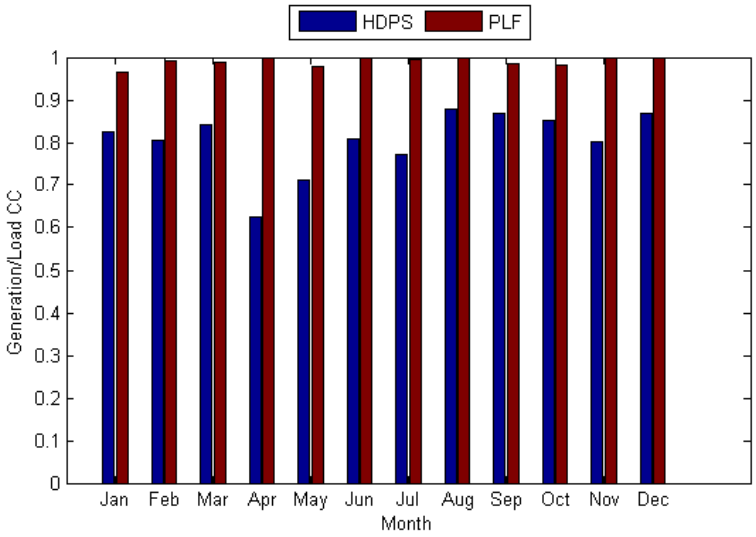

Figure 6.3: Monthly Grand Coulee power plant generation/ BPA load correlation

In the case of Noxon power plant (Figure 6.4), in which the generation is modeled using PS in the HDPS scenario, the same is true, with the highest plant generation/BA load correlation occurring in the PLF scenario. In this figure, it can be seen that the June correlation is low at 0.634, in comparison to the other months. In months where the month average generation is equal to the plant capacity, the PLF will model as a flat maximum generation; and therefore does not exhibit load following as it would normally. This behavior is illustrated in Figure 6.5, which shows the June Noxon hydrogeneration time series, along with the AVA area load.

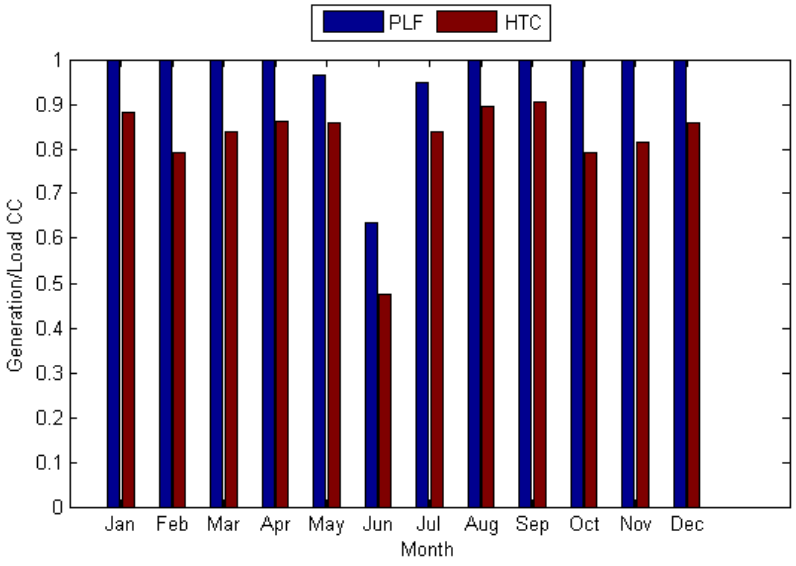

Figure 6.4: Monthly Noxon power plant generation/AVA area load correlation

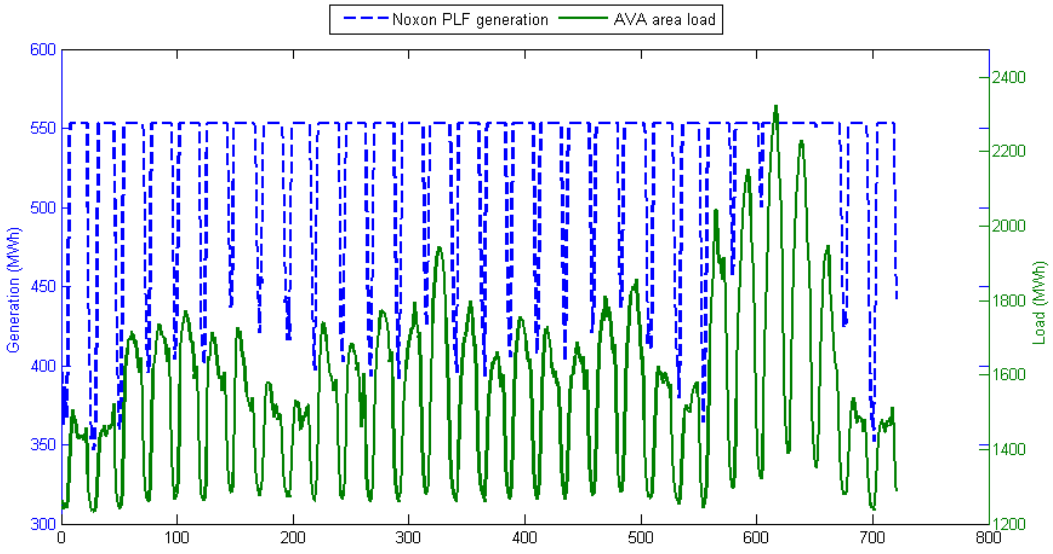

Figure 6.5: June PLF-modeled hydrogeneration for Noxon power plant compared with June AVA area load

To illustrate an extreme case, the Rocky Reach hydrogeneration/CHPD load monthly correlations are shown in Figure 6.6. In this instance, the HDPS-modeled hydrogeneration is poorly correlated to the load in all months, and in 3 of the 4 months it is actually negatively correlated. For the Rocky Reach plant, using PLF greatly increases the representation of the plant's ability to follow load, which will have positive effects on the simulation results. This concept is illustrated in Figure 6.7, which shows HDPS and PLF modeled hydrogeneration for Rocky Reach in the first 72 hours of February, a month with a negative HDPS generation/CHPD load correlation. The instances of anti-correlation between the HDPS generation and load can be clearly seen, as opposed to the PLF generation.

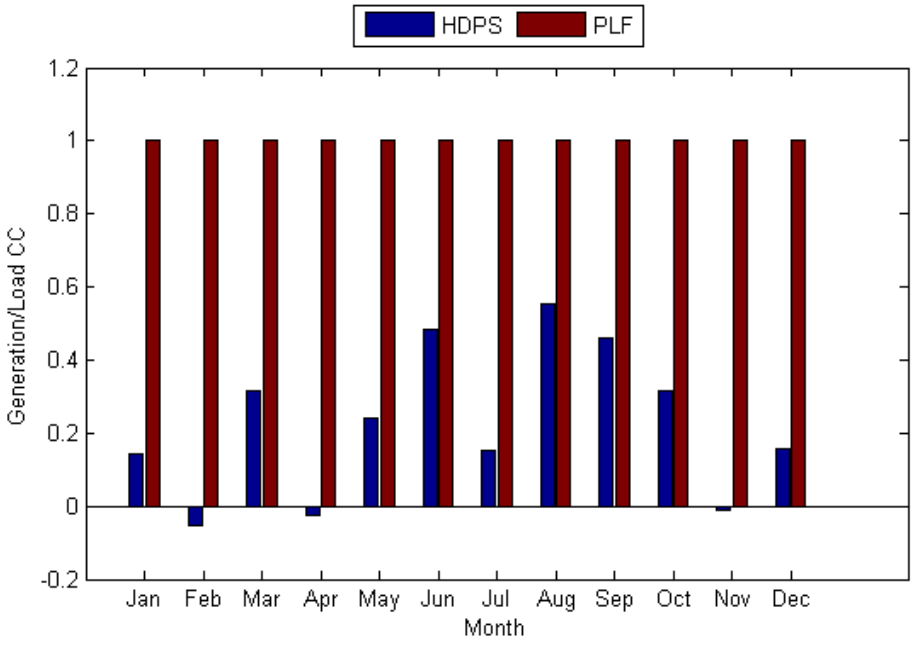

Figure 6.6: Monthly Rocky Reach power plant generation/CHPD area load correlation

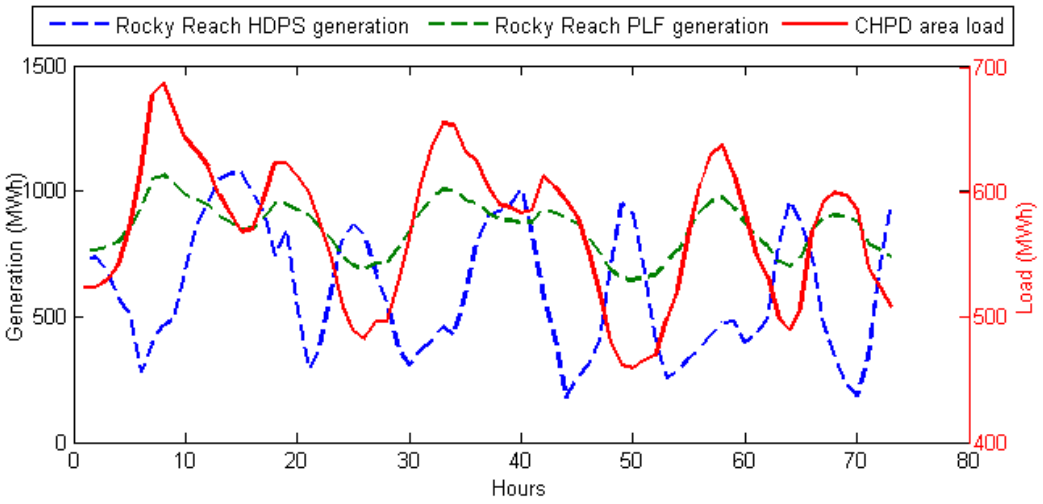

Figure 6.7: February 1-3 HDPS and PLF hydrogeneration for Rocky Reach power plant compared with CHPD area load

In order to determine the aggregate effect of modeling the hydrogeneration of several plants with PLF, the hourly hydrogeneration of all the study plants was summed in order to generate a combined hydrogeneration time series. Monthly correlations to the combined area load time series were then conducted. Figure 6.8 shows the results of this correlation. It can be seen in this figure that PLF-modeled hydrogeneration was better correlated to the load in all months compared to that of the HDPS-modeled hydrogeneration.

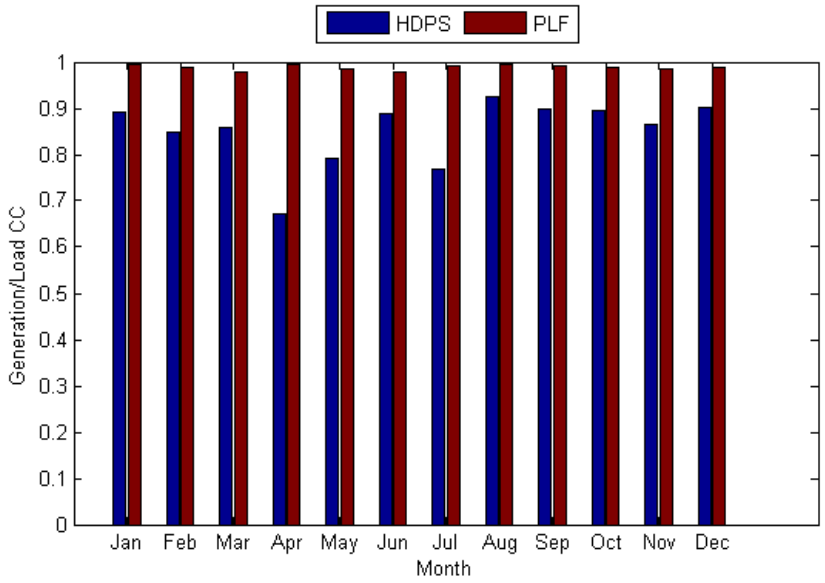

Figure 6.8: Monthly aggregated power plant generation/aggregated area load correlation

In long-term simulation studies (especially those with a 10-year + horizon), the load profile may be drastically different than the load on which a HD-modeled hydrogeneration time series is generated. Many hydrogeneration plants follow the load with hydrogeneration response; therefore it is important to capture this in a simulation. Based on the simulation results presented here, modeling the hydrogeneration of the study hydro plants with PLF improved their load following representation over that of HDPS.

6.2.2 Energy Price Response

A similar correlation analysis was conducted of the three 2019 DTC scenarios, this time correlating the plant hydrogeneration with the LMP at a significant bus. This gives an indication of how often the generation is high when the LMP is high, and vice versa. Therefore, it is an indication of the plant's hydrogeneration production response to system

energy price variations. A high correlation is indicative of a more realistic system operation simulation, as this is what occurs in "real time." For this analysis, the BPA plant hydrogeneration was aggregated into a "BPA hydrogeneration"; this was correlated to a BPA-area LMP average. Figure 6.9 shows the monthly aggregated generation/BPA LMP average correlations.

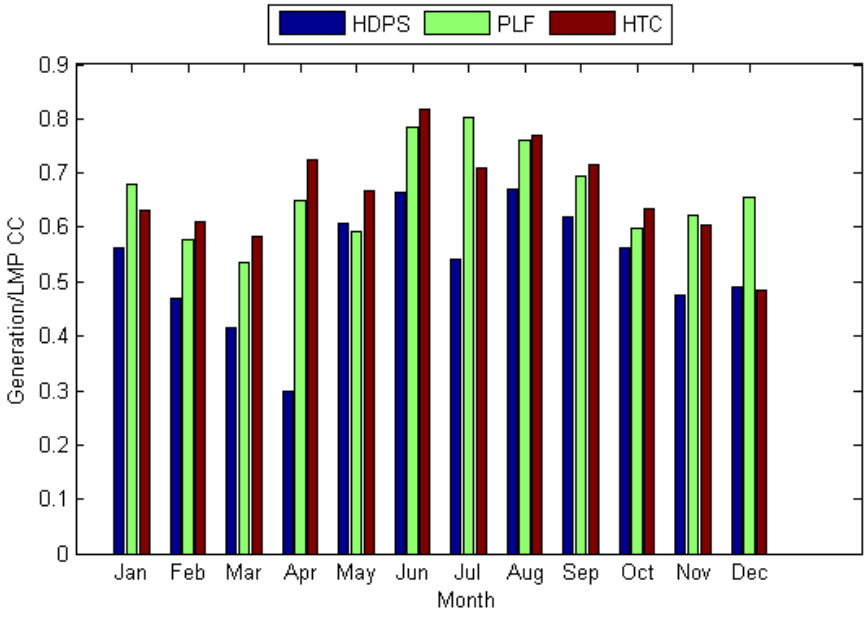

Figure 6.9: Monthly BPA hydrogeneration/averaged BPA LMP correlation

In all months but December, the HTC scenario hydrogeneration is more highly correlated to LMP than the HDPS scenario. This indicates that for the majority of months, the HTC scenario hydrogeneration is responding more effectively to price variations. Additionally, PLF-modeled hydrogeneration alone has a higher correlation to LMP than HDPS in 11 of the 12 months. This is due to the strong dependence of energy price on load. In general, when the load is high, the price will be high, barring the presence of system constraints such as transmission congestion or the additions of renewable generation. In comparing the PLF and

HTC scenarios, HTC has a higher correlation to LMP than PLF in eight of the twelve months. The months that the PLF scenario is higher (January, July, November, and December) are also the months in which the BPA load is highest (Figure 6.10). The months of January, November, and December are resource constrained, due to less resource availability in the winter. It is unclear what effect these conditions have on the scenario modeling, in other words, what the reasons for the higher correlations of PLF to LMP are in these months. Further investigations into plant operational details may reveal possible dispatch constraints as explanation.

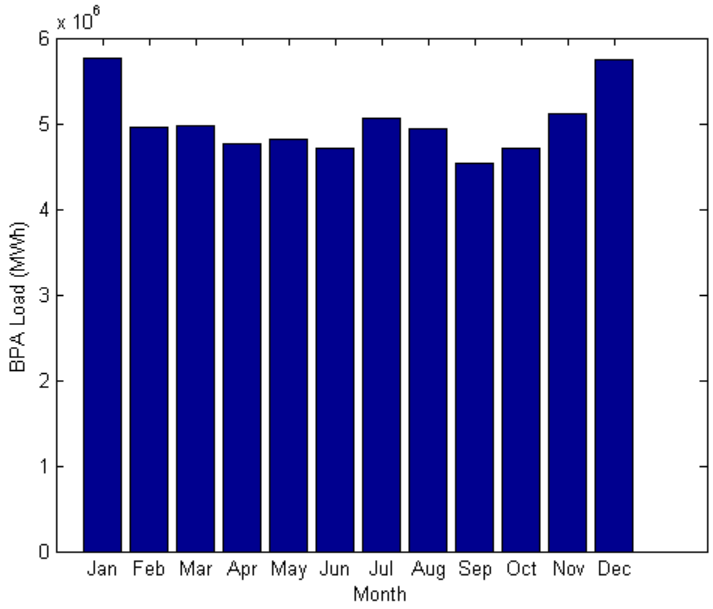

Figure 6.10: Monthly aggregated BPA load

Figure 6.11 depicts the generation/LMP correlations for the remaining NW plants, with varied results. For example, the HTC generation of Wells is more highly correlated with LMP than HDPS or PLF in all months but December. In contrast, the PLF generation of Round Butte is more highly correlated with LMP than HDPS or HTC in all months but June and August.

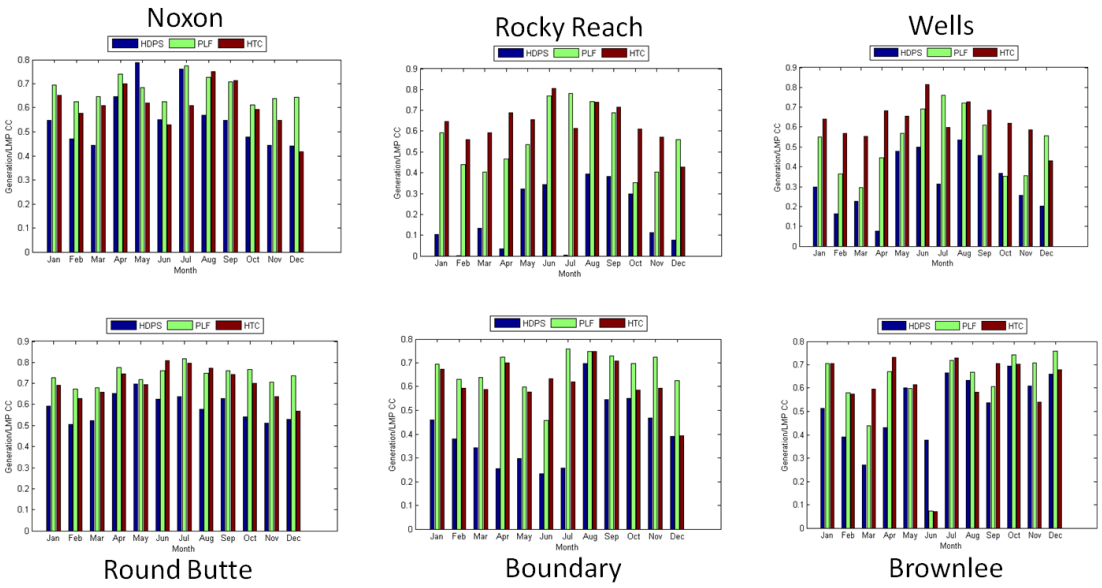

Figure 6.11: Monthly NW power plant generation/LMP correlation

These mixed results indicate that the relationship between plant generation and price is more complicated than that of generation and load. However, it is clear that in virtually every case, using either PLF or HTC modeled generation provides a more realistic response to price variations than that of HDPS modeling.

A specific example of the price responsiveness of the HTC scenario is illustrated in Figure 6.12. The hourly averaged 2019 DTC scenario dispatch for July at Grand Coulee power plant is shown, compared with the hourly averaged LMP. The inset shows the peak load hours; here it can be seen that the PLF dispatch is greater than the HDPS[13], theoretically due to its being modeled on the actual forecasted load. Next, it can be seen that as the LMP increases to its peak, the HTC generation re-dispatches above the PLF to take advantage of the higher energy prices. Then, as the price drops during the non-peak loading period, the HTC

[13] Grand Coulee plant is modeled with HD in the PROMOD 2019-HDPS simulation.

generation dispatches below that of the PLF. This represents a realistic response of generation to energy price.

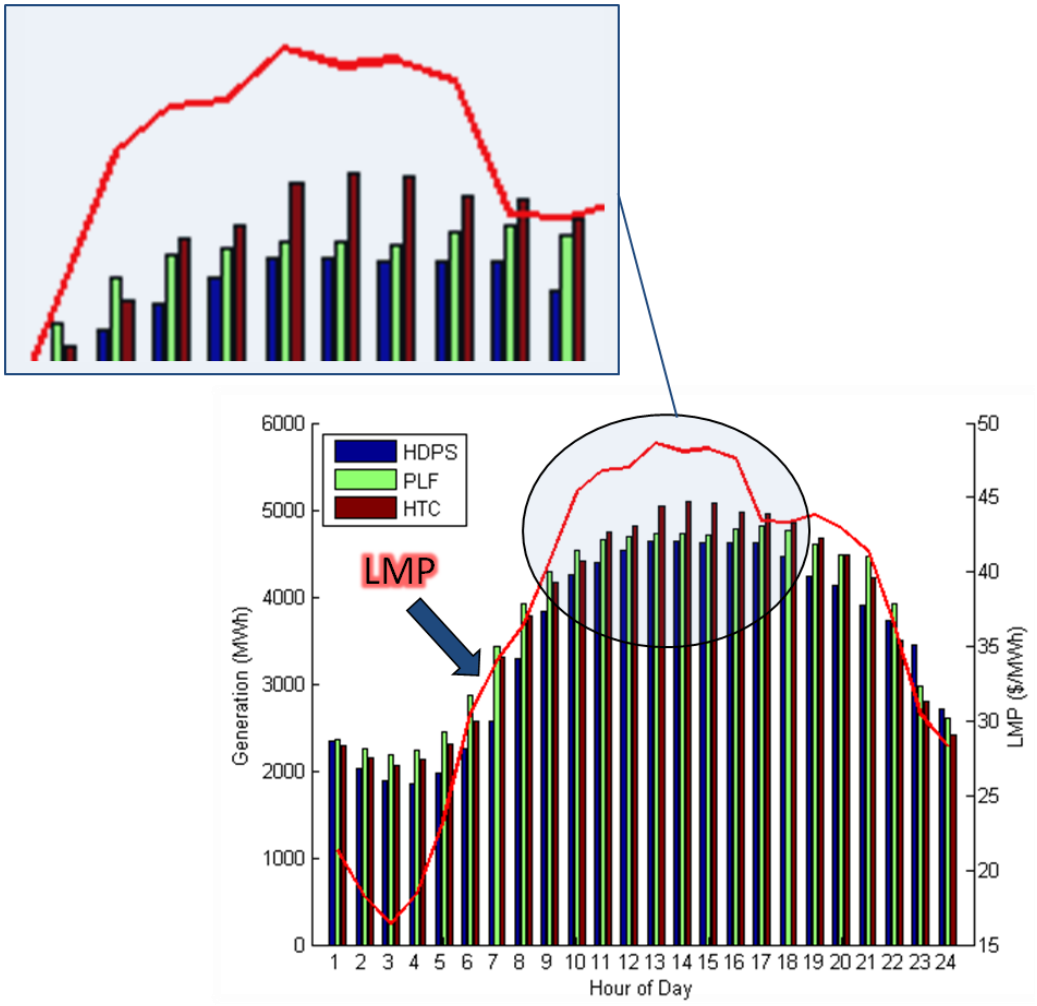

Figure 6.12: July hourly averaged generation for 2019 DTC scenarios compared with hourly average LMP

In continuing to investigate the LMPs for the three 2019 DTCs, another metric for comparing the viability of the scenarios is the LMP variability. As discussed in Section 3.2.2, the less

variation there is in the LMP, the more effectively the system is operating. Figure 6.13 demonstrates the yearly LMP variation for each plant, in all three scenarios.

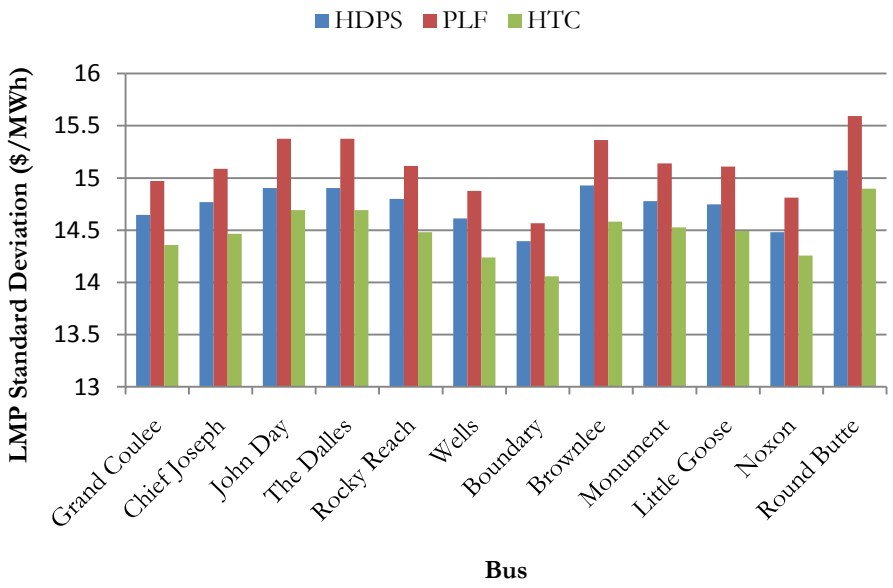

Figure 6.13: Yearly LMP standard deviation for all NW study buses
in the three 2019 DTC scenarios

The outcomes for each bus are consistently similar; the 2019-HTC scenario results in the lowest LMP variability in all plants, followed by the 2019-HDPS, and then finally the 2019-PLF. In parsing out the difference seen between the PLF and HTC scenarios, the results make sense in that the PLF generation is only responding to pre-determined load variations, and not to system operational variations. In a simulation, this causes the *system* to respond to the *hydrogeneration*, which will produce greater variation in the price. In the HTC scenario, the opposite is true, wherein the *hydrogeneration* responds to the *system*.

To look more closely at the LMP variation, the hourly LMP standard deviation for the entire year was calculated for the BPA bus averages; this is shown in Figure 6.14. The shaded box area represents the high load period, hours 0600 to 2200. It can be seen in this figure that the

HTC scenario nearly always has the lowest variability in this time frame, which is the most important in system operation.

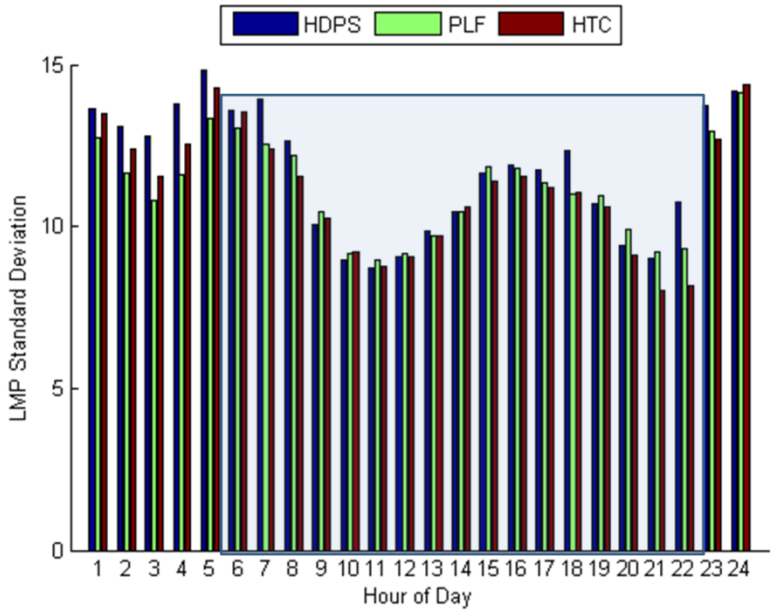

Figure 6.14: Hourly averaged standard deviation for the average BPA bus LMP (in $/MWh) for all three 2019 DTC scenarios

Load cost (Equation 3.2) is another LMP metric that may be used to differentiate scenario results. The LC represents the cost of the energy needed to meet the load, based on the LMP at a significant bus. Since a PCM simulation represents the cost-minimized system operation, a lower LC between simulation scenarios indicates that the factors present in the scenario result in lower system costs. In the 2019 case study, the only difference between the scenarios is the hydrogeneration modeling method. Therefore, looking at the LC differences between the HDPS, PLF, and HTC scenarios gives an indication of which scenario results in the lowest system costs. The yearly scenario LC for each BA in the case study was calculated; Figure 6.15 contains the BA breakouts for yearly LCs. In reviewing this figure, it is obvious that the HTC scenario results in the lowest LC for all areas except the DOPD and CHPD. This analysis

provides a significant indication that the 2019-HTC scenario system represents the most realistic, cost optimized system operation, as compared with the other two scenarios.

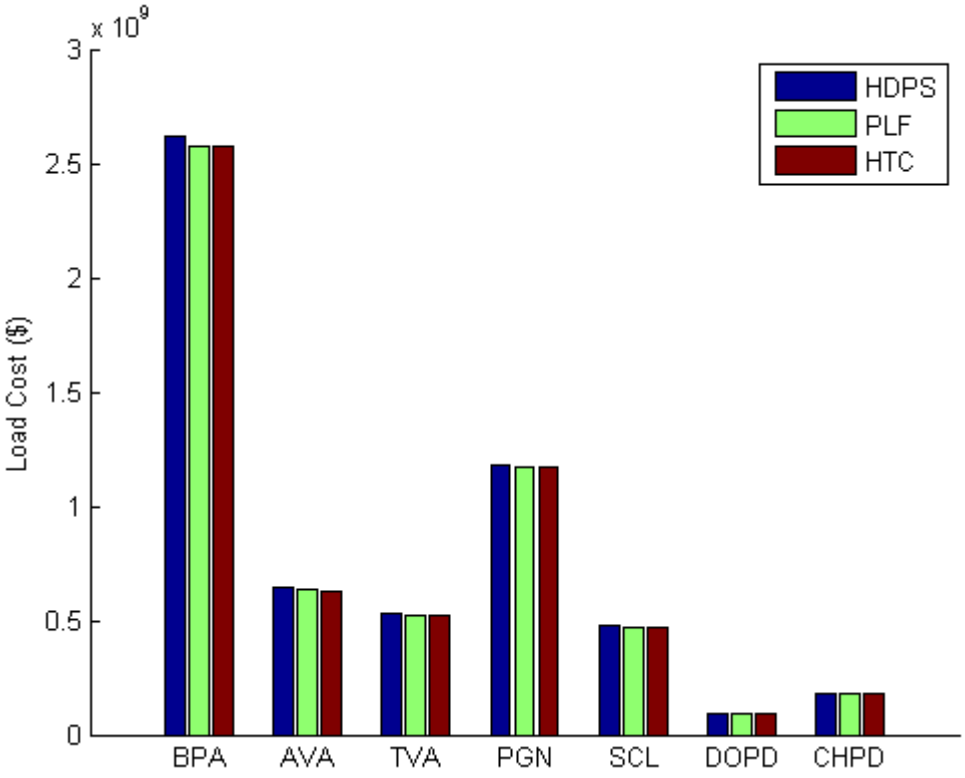

Figure 6.15: Yearly BA LCs for 2019 DTC scenarios

As detailed in Section 2.1, a PCM with LMP modeling optimizes the unit commitment and unit dispatch to meet the load of a modeled system by minimizing the operating costs of the system (incorporating the LMP), all while staying within the regulatory requirements, the transmission capacities, and generator operating characteristics. A generator will therefore respond to increases in load with an increase in generation, unless there is a constraint present (such as congestion, or low energy price), as it would in real-time. The HTC scenario exhibited this type of response more effectively than that of the PLF or HTC scenarios, which

have no capacity to respond specifically to price, since their dispatch is determined outside of the cost optimization algorithm in the PCM.

6.2.3 Transmission Congestion

In the next two sections, the relative veracity of the PLF and HTC scenarios are compared, with respect to system factors that affect the energy price. As stated in Chapter 4, the WECC year is defined by the winter, spring, and summer seasons. In the NW, the winter season sees high load demand, while the spring is characterized by increased resource. Summer also sees increased load demands, including those from other regions such as California. In the summer, less costly, readily available NW hydrogeneration is transmitted to other regional areas through paths such as the COI and PDCI. These two paths are historically congested (WECC, 2009). The increased transmission flow in the summer months can be seen in Figure 6.16, which shows the total transmission flow on all of the selected NW paths for the 2019 DTC scenarios for each month. Clearly, the transmission flows increase in the summer, particularly June and July, due to the demand not only from the NW but also from other regions.

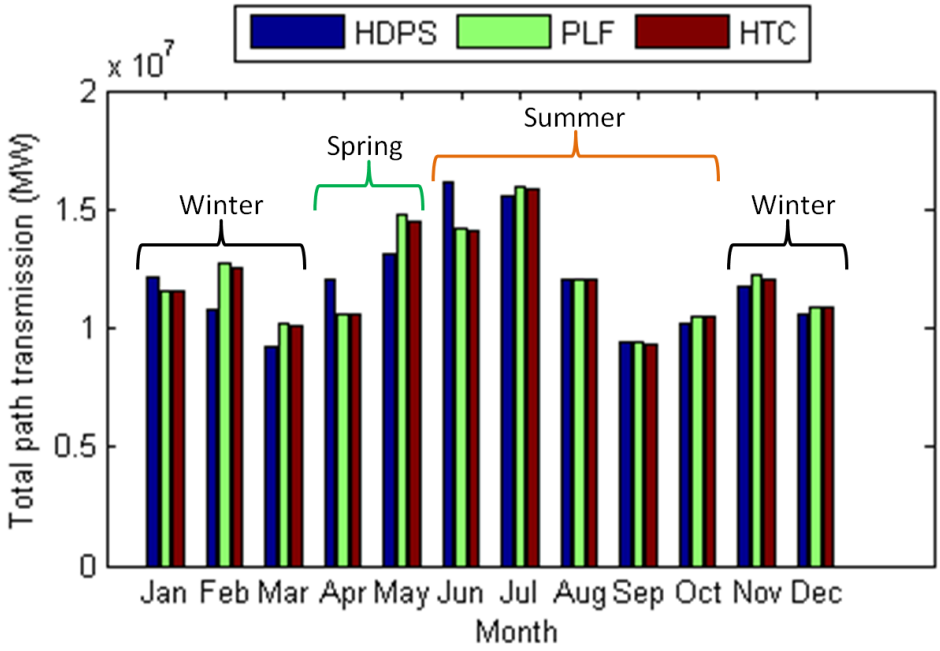

Figure 6.16: Monthly NW study path transmission for the 2019 DTC scenarios

One would expect, as a result of the load/transmission pattern seen in the summer, a higher occurrence of path congestion in these months. Seasonal path congestion metrics were calculated for the COI and PDCI paths for the summer months, as outlined in Section 3.2.2. For the purposes of this thesis, transmission at the T75 level represents heavy path load levels, at T90 extra heavy path load levels, and at T99 maximum load levels. Other lines in the NW study region do not experience congestion to the level that the COI and PDCI paths do, due to their line capacity. Figure 6.17 displays the congestion metrics for the COI path. At the T75 and T90 loading levels, the time percentage for the HTC and PLF scenarios are approximately the same. However at the T99 level, where energy price is most likely affected, the percentage of the HTC scenario is lower, indicating that the generation was reduced in response.

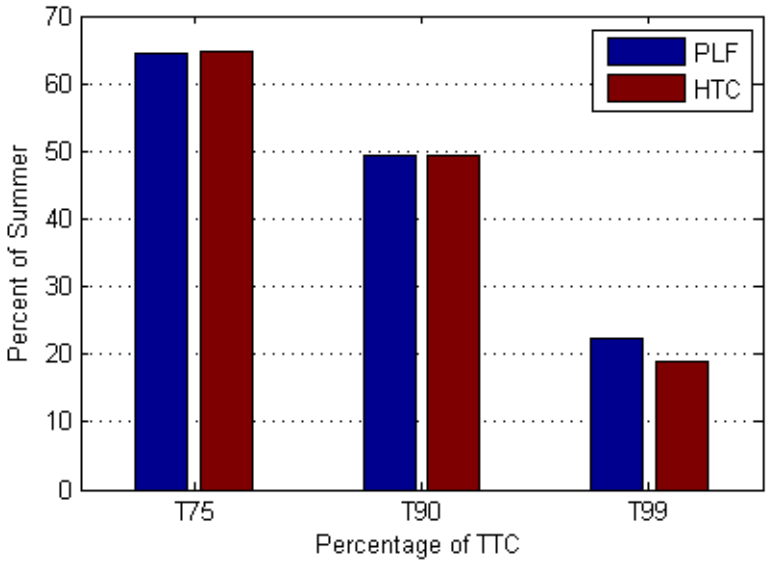

Figure 6.17: COI congestion metrics for 2019 DTC scenarios

The congestion metrics for another summer-congested path, the PDCI, is shown in Figure 6.18. The percentage of T99 levels is again reduced in the HTC scenario.

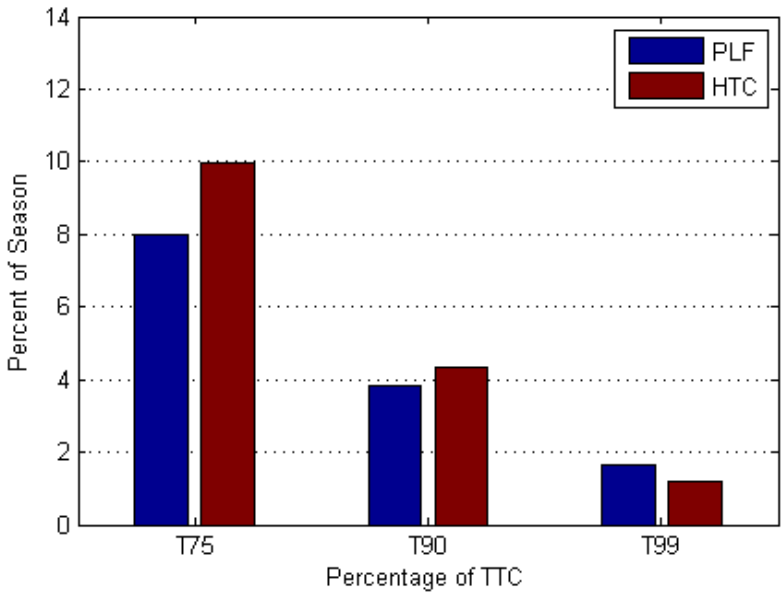

Figure 6.18: PDCI congestion metrics for 2019 DTC scenarios

As a further illustration, the hourly T99 instances in a 48-hour period in the third week in July for the COI were extracted, and compared with the hourly aggregated BPA plant generation for these instances. Figure 6.19 shows the results, so that the HTC response can be differentiated from that of PLF. From this figure, it can be seen that at maximum transmission flow levels, HTC hydrogeneration responds by re-dispatching below that of the PLF. The HTC scenario is reacting in a realistic fashion, since hydro production will decrease when congestion is present (Equation 2.3). Therefore, the percentage of T99 levels is lower due to this decreased production, which represents a more "real-time" system operation.

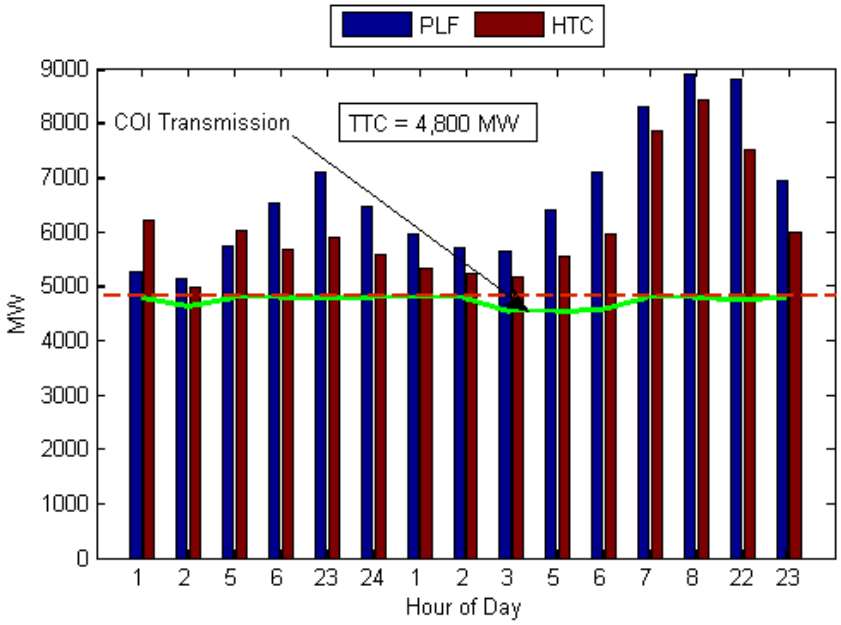

Figure 6.19: COI T99 transmission hours for a 48-hour period in the third week in July (green solid line), compared with the 2019 DTC scenario hydrogeneration dispatches from the same instances. The red dashed line represents the TTC of 4800 MW

6.2.4 Response to Renewables

An important aspect in conducting long term transmission studies is that of increased levels of renewable energy. As of 2009, twenty four states have an in-place, mandatory RPS; these contain requirements that a specified percentage or amount of power must come from renewable resources by a given date (U.S. Department of Energy, 2009). Transmission planners must incorporate these RPSs into the energy forecasts used in transmission studies, in order to properly plan for the generation mix. As discussed in Section 2.5, renewable energy presents particular issues for system operation; therefore it is important that a PCM used in long term transmission studies simulate these effects. In this case study, forecasted wind generation is inputted into PROMOD along with the forecasted load, where it is then subtracted as a must-run resource. The remaining load-net-wind is then used in the cost-

optimization algorithm. Therefore, when the wind generation increases, the load for the other generators in the system decreases, and vice versa. In addition, the addition of wind tends to drive energy prices down, as there is "technically" lower load to serve. Since wind is variable, these increases and decreases can be quite sudden, when considered in a planning time-frame. In order to examine the effects of these wind ramps on the hydrogeneration scenarios, the Grand Coulee hydro dispatch for the 2019 DTC scenarios is shown in Figure 6.20, along with the BPA wind generation. This figure shows the hours of 0600 to 1800 for a day in November, in the peak loading period of the day. November represents a month with increased levels of wind production in the BPA.

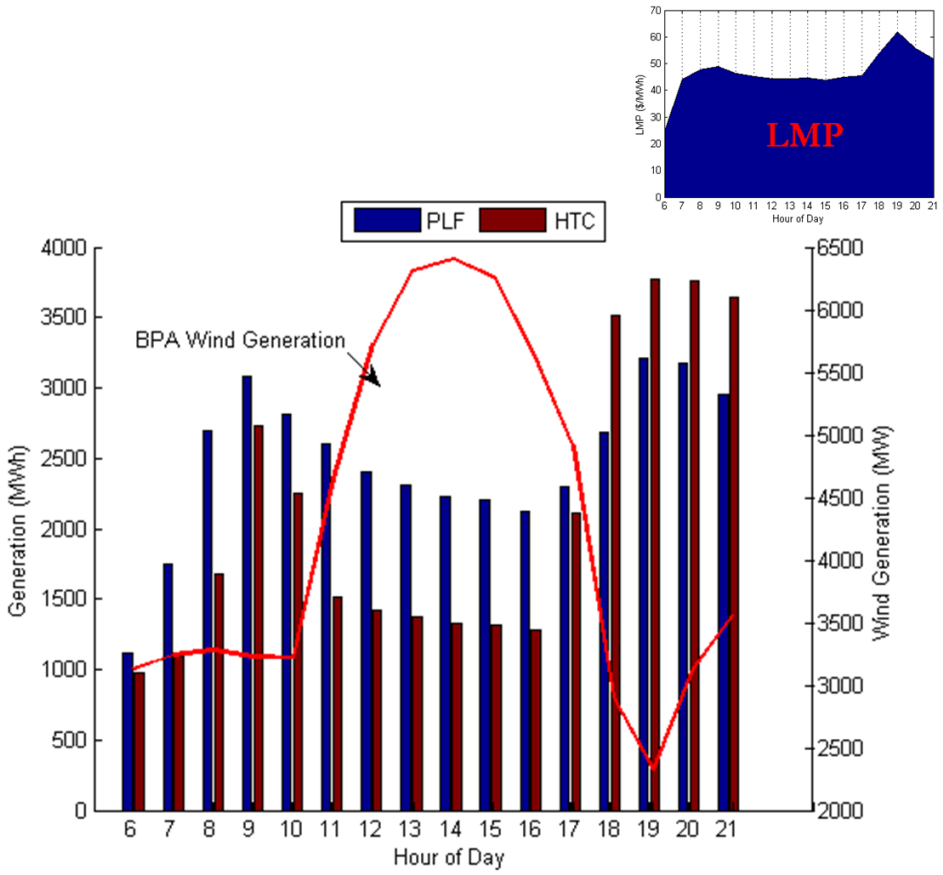

Figure 6.20: Grand Coulee 2019 DTC scenario hourly hydro dispatch compared to BPA wind generation, November 13

The HTC dispatch, which is already lower than the PLF due to lower energy prices in the early hours (hour 0600), begins ramping up in response to loading increases in the morning hours (hours 0700-0800), but then decreases in response to the wind increase ramp (hours 0900-1500). The HTC generation remains low during the wind event, and then re-dispatches above the PLF as the wind ramps down, to take advantage of peak energy prices (hours 1600-1800, see inset for LMP in Figure 6.20).

Recalling Figure 4.11, the NW wind is less variable in the winter months, such as November. It is important then to inspect a Spring wind event, namely on April 6, when there is significant variation in the wind generation throughout the day. Figure 6.21 shows the 2019 DTC scenario generation dispatches for the hours of 0600 to 2400, compared to the BPA wind generation. The sensitivity of the HTC response to the wind ramps can be seen, particularly in the later part of the day (hours 1400-2200), when HTC dispatches below that of PLF in response to wind increases, and increases dispatch as the wind ramps down. The HTC dispatch increases considerably over the PLF in the peak energy price period of approximately 1900-2200 (see inset, Figure 6.21). PLF follows a much smoother dispatch pattern, since it is not responding to the price differentials that result from the wind variations, rather just the load.

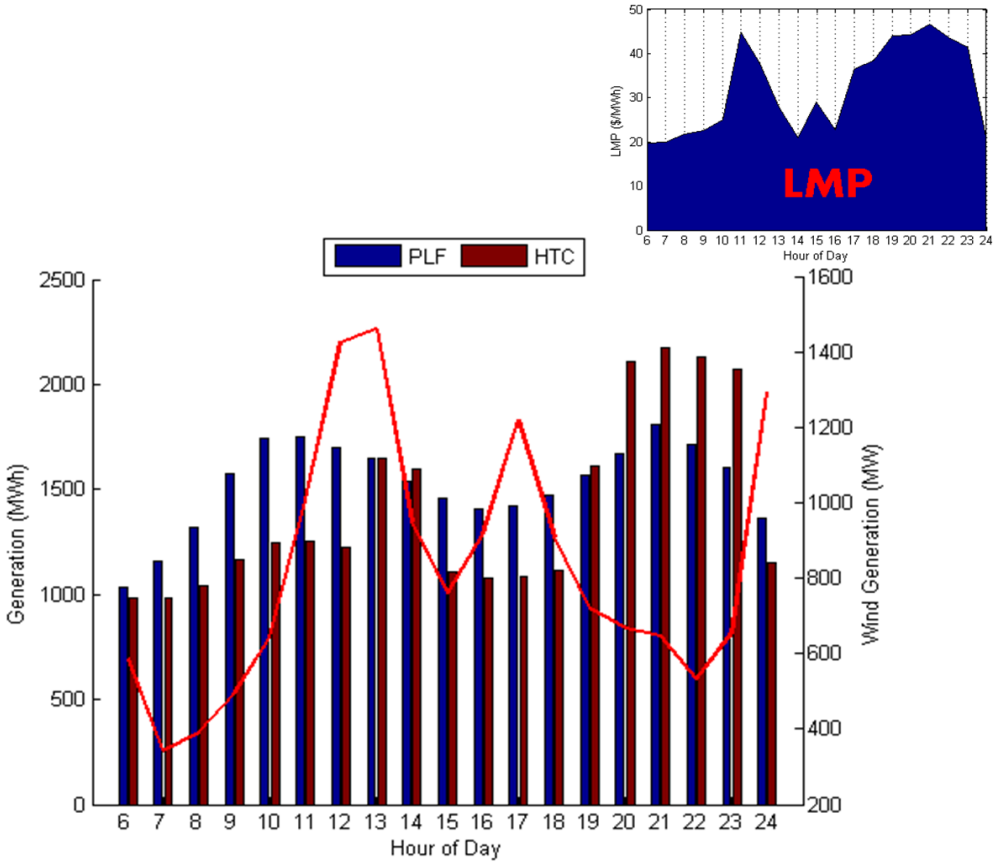

Figure 6.21: Grand Coulee 2019 DTC scenario hourly hydro dispatch compared to BPA wind generation, April 6

Theoretically, if wind generation is low, the hydro generation should increase, and vice versa. In order to evaluate this in the simulation, the hydrogeneration was correlated to the wind generation. Figure 6.22 shows the monthly aggregated BPA 2019 DTC scenario hydrogeneration/BPA wind generation correlations. In all months, the HTC generation is more strongly anti-correlated with that of the wind generation (in a weak sense, indicated by the small CCs), indicating that the HTC scenario is reacting more effectively to wind events. The Noxon generation/AVA wind generation correlation produced similar results (Figure 6.23).

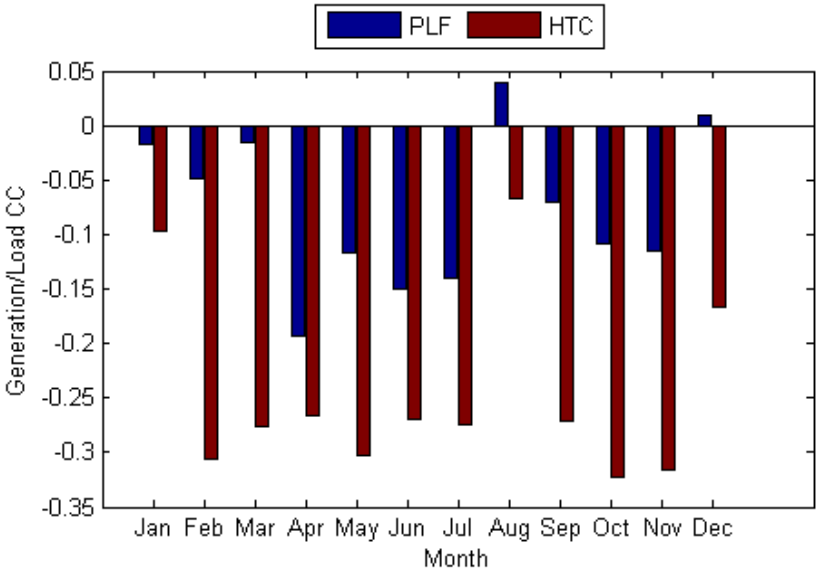

Figure 6.22: Monthly 2019 DTC scenario BPA aggregated generation/BPA wind generation correlation

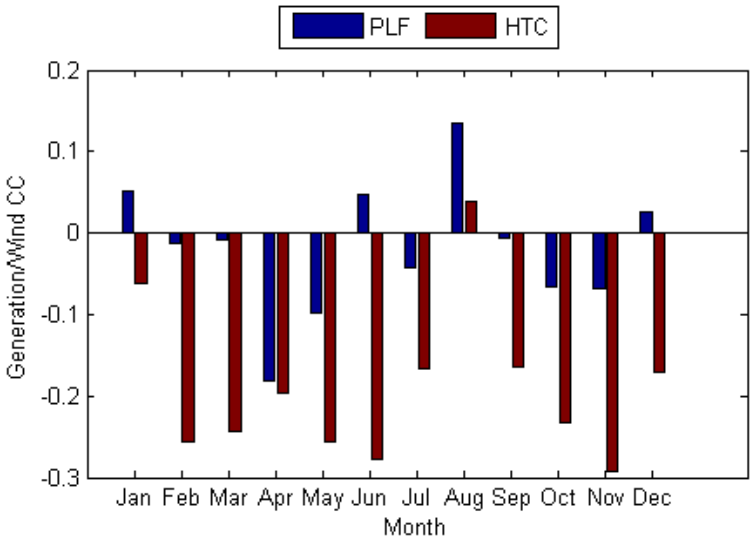

Figure 6.23: Monthly 2019 DTC scenario Noxon generation/AVA wind generation correlation

The same is not true for the Brownlee generation/TVA wind generation correlations, shown in Figure 6.24. In this case, the generation in both scenarios is somewhat positively correlated, though again weakly. The reason for this difference is unclear at this time; further investigation into specific plant operations may yield some explanation.

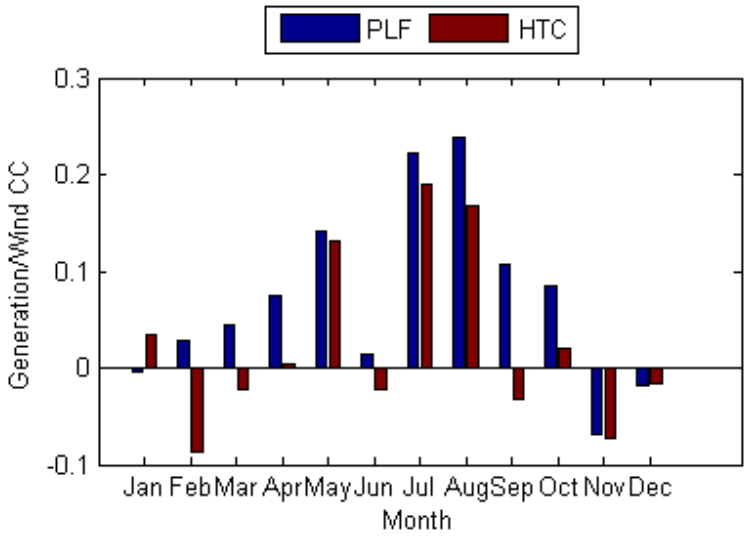

Figure 6.24: Monthly 2019 DTC scenario Brownlee generation/wind generation correlations for the TVA BA

The total NW hydrogeneration was correlated with the total NW area wind generation, with the same results as in Figure 6.22 (Figure 6.25).

Overall, the wind event analyses presented in this section point to the HTC scenario as the most responsive in a PROMOD simulation. Of course, the HTC hydro modeling is also responding to other system factors that affect price such as congestion, so the effect may not always be predictable, as seen in Figure 6.23. The effects of wind on a PROMOD system simulated are further investigated in the next section, in which the results of the 2019LW DTC are compared with those of the 2019 DTC.

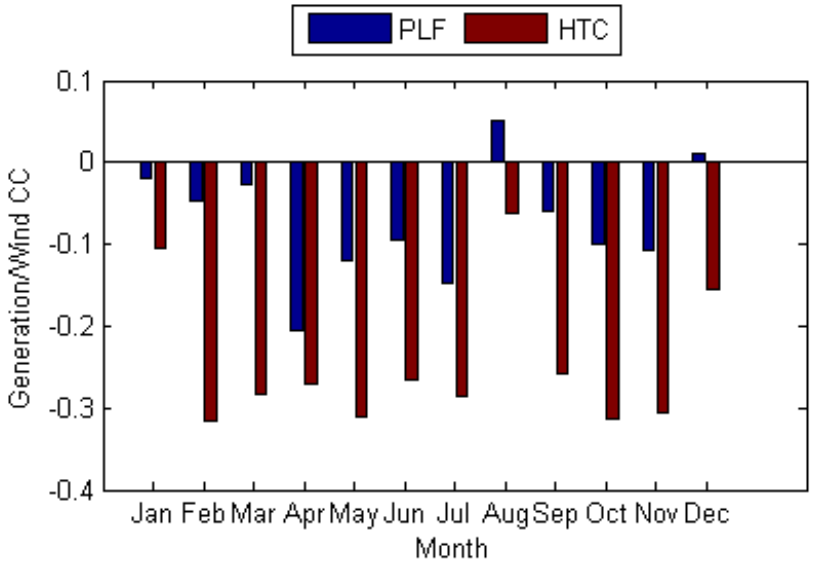

Figure 6.25: Monthly 2019 DTC scenario NW aggregated generation/NW wind generation correlation

6.3 2019 DTC vs. 2019LW DTC

The PCM simulation study conducted in this thesis included an additional DTC, the 2019LW, with HDPS, PLF, and HTC scenarios. As discussed in Chapter 4, this DTC included approximately 5600 MW less wind capacity than that of the 2019 DTC. Comparison of these two DTCs allows the wind effects to be parsed out. For this analysis, the aggregated NW plant generation, the averaged NW LMP, and the aggregated NW transmission are used, unless breakout data is necessary. As a reference, the wind generation in the 2019 DTC represented 12.9 percent of the load, and in the 2019LW DTC, 3.5 percent. Table 6.1 shows the summary of the total DTC NW wind generation for the case study year, as well as the NW load.

Table 6.1: Total NW wind generation comparison between DTCs, and percentage of total NW load

Year 2019	MWh	Percent of Load
Total forecasted NW load	1.30E+08	
Total 2019LW DTC NW wind generation	4.52E+06	3.5
Total 2019 DTC NW wind generation	1.67E+07	12.9

First, the effect on NW hydrogeneration may be examined. Figure 6.26 shows the total NW plant hydrogeneration for all three scenarios for the two DTCs. The HDPS scenario generation is the same for both DTCs, since it is based on the historical generation, and doesn't take into account the variations in wind generation. However, the PLF generation between the two DTCs is quite different, showing a greatly decreased amount of hydrogeneration in the 2019-PLF as compared to that with lesswind (2019LW-PLF). In the 2019LW-HTC, the hydrogeneration is reduced significantly from that of the PLF, presumably accounting for the response to lower energy prices. Interestingly, the difference between the 2019-PLF and 2019-HTC is not as drastic.

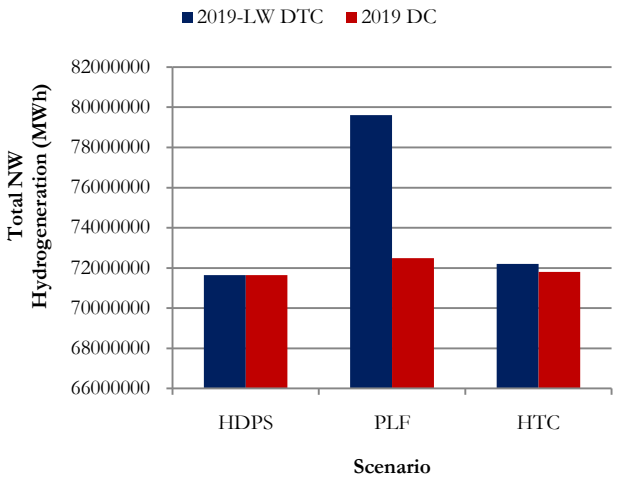

Figure 6.26: Total NW hydrogeneration for the two DTCs by scenario

Looking at the total energy price average for the DTCs, the LMPs are higher as would be expected in the 2019 DTC, since higher levels of wind generation drive the prices down by reducing the use of higher cost resources (Figure 6.27).

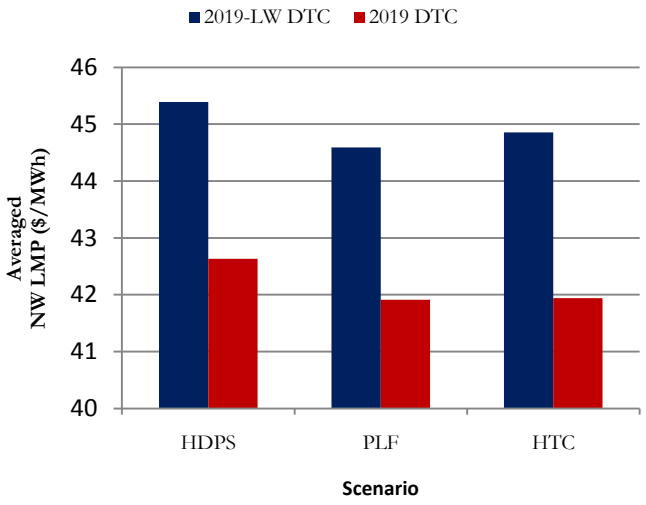

Figure 6.27: Average NW LMP for the two DTCs by scenario

Next, the average NW LMP variability is shown in Figure 6.28 for the 2019LW and the 2019 DTCs. According to this figure, the LMP variability increases with the higher levels of wind generation in the 2019 DTC. This confirms the idea that the energy price in a PCM is sensitive to price-takers such as wind and solar. As an illustration of this, refer to Figure 6.21, in which the daily LMP variability can be seen on a day with a variable influx of wind. Note also in Figure 6.28 that the HTC scenario in both cases had the lowest LMP variability of the scenarios, which again confirms that modeling the NW plants with HTC results in a more realistic representation of a future system.

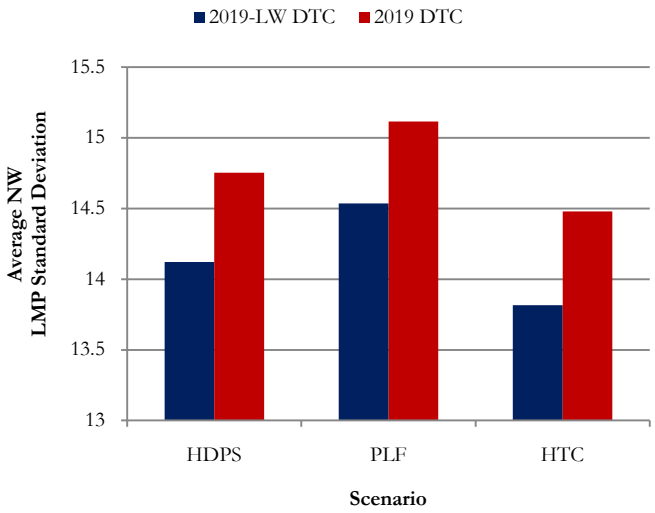

Figure 6.28: Average NW LMP standard deviation for the two DTCs by scenario

It is also of interest to compare the load costs of the 2019 and 2019LW DTCs. Figure 6.29 plots the difference (Δ) in yearly average LC between the 2019LW and 2019 DTC scenarios for each of the study BAs. Since the results have positive values, the 2019LW load costs are higher in all cases; this is a logical result in that the 2019 LMPs are lower due to the increased wind. The HTC scenario has a higher Δ in all BAs, indicating that the 2019-HTC scenario responds more to the decreased energy prices. The DTC total NW LC comparison is summarized in Figure 6.30. The lower load costs of the 2019 DTC caused by the higher wind penetration indicate how the LMP reductions affect the cost for serving the NW load.

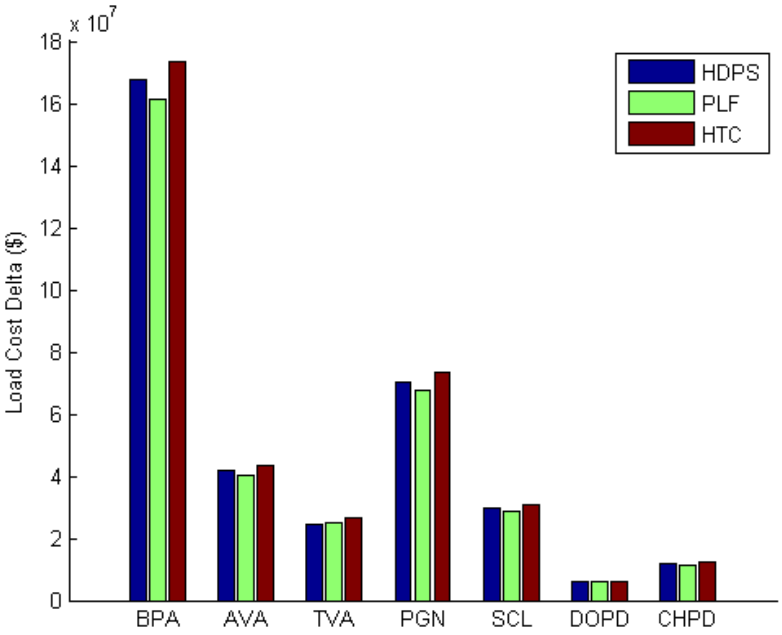

Figure 6.29: Load cost difference between the 2019LW and 2019 DTC scenarios by area

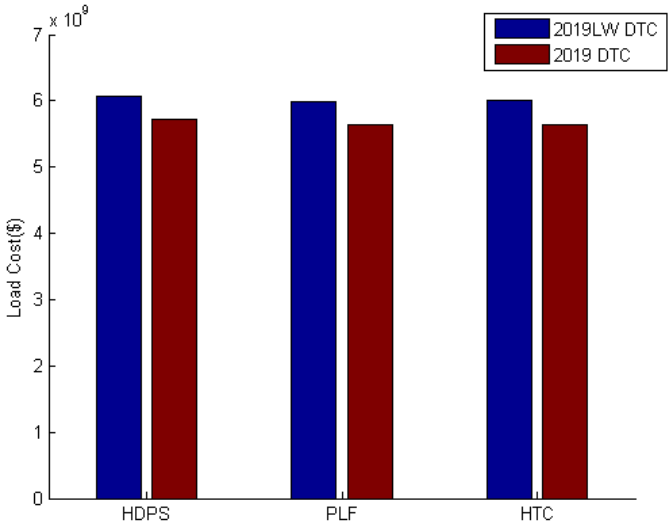

Figure 6.30: NW averaged LC for the 2019LW and 2019 DTC scenarios

Additional comparisons between the DTCs can be made by looking at the transmission and transmission congestion. One would expect that with higher wind generation levels, transmission congestion would increase. First, a comparison of yearly duration curves can be used to see where congestion differs between the DTC scenarios. Figure 6.31 shows the duration curves for all scenarios in both DTCs for the COI path. While the patterns are similar, the magnitudes are different. It is clear that the 2019 DTC scenarios encounter longer periods of high transmission flow, as compared to that of the 2019LW, as would be expected.

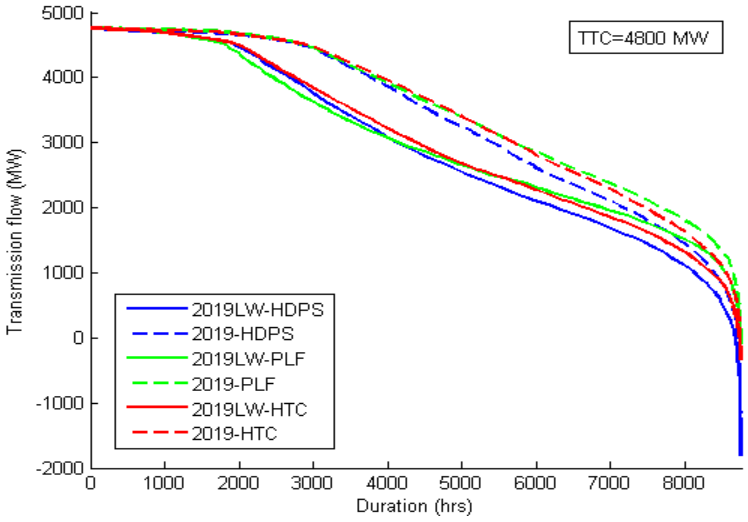

Figure 6.31: COI transmission duration curve for all scenarios in the 2019LW and 2019 DTCs

Similar results are seen in Figure 6.32, which shows the duration curves for the PDCI path, the other selected paths are unremarkable, and do not differ from the 2019 transmission duration curves shown in the Appendix.

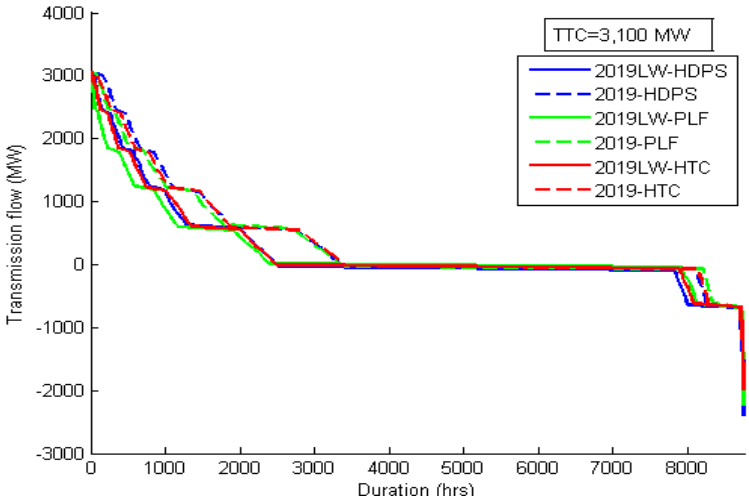

Figure 6.32: PDCI transmission duration curve for all scenarios in the 2019LW and 2019 DTCs

A comparison of the transmission metrics concentrated on the COI path, since this exhibits measurable T99 congestion, particularly in the summer. Table 6.2 shows the T99 percentages for the summer season for the COI, in both DTCs. The difference is obtained by subtracting the 2019LW T99 percentage from the 2019 T99 percentage. A positive value indicates that the T99 percentage is less in the 2019LW DTC than the 2019 DTC; the opposite is true for a negative value. The PLF and HTC results are predictable, in that the higher wind DTC has a greater T99 than that of the lower wind DTC. The HDPS difference, however, is negative, indicating that there is more congestion in the less wind DTC. This is not a feasible result, since congestion would possibly increase with a 9.4% increase in NW wind penetration (see Table 6.1)

Table 6.2: DTC T99 differences by scenario

Path	Scenario	2019LW DTC Summer T99	2019 DTC Summer T99	T99 Difference (%)
COI	HDPS	14.98	14.81	-0.16

Path	Scenario	2019LW DTC Summer T99	2019 DTC Summer T99	T99 Difference (%)
	PLF	14.84	22.28	7.43
	HTC	13.26	18.90	5.64

In concluding the analysis of the DTC comparison, the observation can be made that the results overall corroborated previous assumptions about the effects that increased wind penetration has on system operation. This is demonstrated in the duration curves and the LMP results, where in all scenarios the increased wind led to increased LMP variability, and lower LMP values. However, the scenario generation comparison revealed that the HDPS generation would not lead to accurate representation in the different DTCs, since it had no change between the scenarios. In addition, the results shown in Table 6.2 indicate an unrealistic response to summer congestion on the COI in the HDPS scenario.

7 CONCLUSIONS, IMPLICATIONS, AND FURTHER STUDIES

7.1 Summary and Conclusions with Thesis Objectives

In concluding the results of the hydrogeneration model analysis and the 2019 simulation study, the thesis objectives presented in Chapter 1 will be addressed.

1.) Evaluate current literature pertaining to transmission planning, PCMs, hydrogeneration modeling in PCMs, and wind integration, and 2.) Demonstrate the need for improving hydrogeneration modeling in PCMs used for transmission studies - First, the literature background introduced in Chapter 2 outlined the various transmission planning methods used in the power industry. These planning methods often involve the use of a PCM simulation for proposed transmission expansion plans, in order to capture the economics of the system operation as well as those of the physical and technical operation. A PCM simulation, while capturing the thermal dispatch of the system, may have limitations in dealing with hydrogeneration dispatch. The hydrogeneration modeling literature review revealed that there are numerous methods to accurately cost-optimize and capture the complexities present in the production of hydrogeneration, such as resource availability and operational constraints. However, these present problems in a system-wide PCM, since they often require large amounts of hydrological and generator-specific data. This is often not available to transmission planning entities. Additionally, the literature review demonstrated that there are challenges with integrating renewable energy, in particular wind energy, into the grid. Therefore, it becomes important in transmission planning to capture the effects of wind on a future system.

3.) Present two new hydrogeneration models and present a model error analysis on the novel modeling methods, and *4.) Demonstrate improvements in the representation of hydrogeneration due to the utilization of these modeling methods in a PCM-simulated transmission study* - Chapter 3, in presenting the traditional hydrogeneration models used in TEPPC PCM transmission studies, addressed the deficiencies

these pose to a realistic representation of hydrogeneration dispatch within the system as a whole. The main issues that the HD and PS modeling methods have are that:

1.) They do not adequately capture the ability of some plants to follow the load, that is, to adjust their dispatch in response to load variations. This results in a less than realistic simulation
2.) The dispatch is hard-wired into the PCM, and cannot be cost-optimized as is the thermal dispatch; therefore the ultimate simulation result is less than realistic
3.) The HD or PS modeled hydrogeneration does not reflect the effects of renewable energy

Based on these deficiencies, and on TEPPC's current inability to use more complex hydrogeneration methods, the PLF and HTC methods were presented as an interim solution to more accurately capture a hydro plant's ability to follow the load and to respond to system energy cost considerations in a long-term transmission PCM simulation. An initial analysis of these models revealed that the PLF method, in using the *K* value to capture the plant's ability to follow load variations, more effectively modeled the hydrogeneration of applicable plants. Also, in initial analyses, the HTC hydrogeneration modification method within PROMOD was able to capture the price-responsiveness of a portion of the hydrogeneration, described by the *p* factor.

The 2019 simulation study was designed to show the improvement of using PLF or HTC in a PCM simulation, and to determine the effects of increasing wind energy on these modeling methods. Evaluating the efficacy of a long-term simulation is difficult, in that there is no actual data with which to corroborate it. Subsequently, relative analysis methods must be employed to compare the relative efficacy of the simulations. The questions, as discussed in Chapter 3, which should be asked, are then:

1.) What constitutes a realistic system simulation?

2.) How is this verified?

To answer the first question, in the context of hydrogeneration, a realistic simulation is one in which the hydrogeneration dispatch behaves as it would in real-time, by responding effectively to variations in load and energy price. The energy price is affected by numerous system factors[14]; however, in this analysis, only the effects of congestion and wind energy were investigated. To answer the second question, then, the load following effectiveness of the scenarios was verified by correlating the hydrogeneration dispatches with the load, and comparing. Also, to verify the hydrogeneration response to energy prices, LMP analyses such as correlation with the generation, variability, and load costs were used to compare the scenarios.

The load following analysis for the 2019 DTC found that the PLF modeling method resulted in higher correlations between the hydrogeneration and dispatch than the HDPS method. This was true for both individual NW plants, and subsequently in the aggregated plant make-up. Load following is an important quality to capture in a PCM simulation, since the efficient operation of a power system relies on the ability of the generators to respond to load variations with increases or decreases in generation. In addition, energy price is highly correlated with load. Barring the presence of other factors, when the load is high, the energy price (thus the LMP) is high, and vice versa. In the absence of any actual hydrogeneration cost-optimization, the representations of hydrogeneration load following can therefore, in effect, provide some measure of energy price response. Therefore, the improvement in the generation/load correlations found in the PLF scenario represent a more realistic representation of the hydrogeneration in the future system.

In looking at the energy price response directly, the generation/bus LMP correlations for the 2019 DTC showed that the HTC scenario, for the most part, resulted in higher correlations in

[14] These factors are numerous, and can include fuel prices, reserves, generation make-up and characteristics, transmission losses, etc., as discussed in Section 2.1.

more cases than those of the HDPS and PLF. This is an expected result, since the HTC-modeled generation is cost-optimized within the PROMOD algorithm, therefore it should respond to system economic variations. However, the PLF scenario had a higher correlation than that of the HDPS in most cases, indicating that it provides an improvement over the HDPS scenario in energy price response. As discussed in the paragraph above, this is due to the complimentary relationship of load to energy price. Interestingly, in some monthly correlations, the PLF scenario had a higher generation/LMP correlation than that of the HTC. This indicates that the generation/energy price association is more complicated than that of the generation/load. A reasonable explanation for this occurrence is that the energy price has many more factors affecting it, and in a simulation involving an entire operating system, these factors can be numerous and difficult to parse out.

As discussed in Section 3.2.2, the LMP variability can provide an assessment of the simulation efficacy. A realistic system simulation should exhibit lower variability in energy price, since in real-time, optimal, efficient operation would result in smooth price transitions, barring any anomalous occurrences such as large outages or extreme load spikes. Comparing the bus LMP variability of the three scenarios, the HTC had lower overall variability in all examined buses than either the PLF or the HDPS scenarios. In addition, the PLF scenario had higher variability than either the HDPS or the HTC for all buses. This indicates that in a simulation with PLF modeling, the *price* is affected by the *hydrogeneration*, whereas in a simulation with HTC modeling, the *hydrogeneration* is affected by the *price*. This concept makes sense in the context that the HTC hydrogeneration is cost-optimized, and therefore redispatches above or below that of the PLF in response to energy price variations.

Next, in parsing out some factors that have an effect on the energy price, the transmission congestion levels of the 2019-PLF and -HTC scenarios were compared, since previous analyses indicated that these methods more effectively represented the hydrogeneration in the simulation than the HDPS. Only two paths out of the six selected for analysis experienced

significant congestion, these were the COI and PDCI. These paths experienced some amount of maximum load level congestion (T99) in the summer months, due to inexpensive, readily available hydro energy going to meet the high load demand from California. The HTC scenario simulation resulted in lower percentages of T99 congestion than the PLF on both the COI and the PDCI in the summer. This indicates that the HTC model responded to the lower energy prices that resulted from congestion, and dispatched lower generation accordingly.

5.) Discuss the effects of increasing wind integration in a PCM-simulated transmission study utilizing these methods - Wind affects the energy price at associated buses, since technically there is lower load to serve, reducing the price at the bus. In regards to response to renewables, the HTC scenario again responded more effectively to the influx of wind energy than that of PLF alone. This was shown in the HTC generation response to wind ramp events, in which the generation dispatch was reduced in the presence of wind generation, and increased when the wind event subsided. The PLF generation did not respond as effectively to the price sensitivities as did the HTC generation. Direct correlations of the wind generation/hydrogenation for the scenarios produced mixed results at some plants, but the overall aggregated response showed that the HTC scenario hydrogeneration was more highly anti-correlated to the wind generation. The wind event analyses provide some level of confidence that a simulation using HTC with applicable hydro plants results in a more realistic representation of the system as a whole.

Since increasing levels of renewable penetration are expected in the future due in place RPSs, it is important to ensure that changes in penetration levels are properly reflected in a PCM-simulated transmission study. Two different system wind penetration levels were tested, the 2019LW DTC with wind constituting 3.5 percent of the load, and the 2019 DTC with a 12.9 percentage. A results comparison of these DTCs indicated that both simulations were responding predictably to increased wind. However, the HTC scenario was again more reactive to energy price, with a lower variability in LMP. In addition, the HTC scenario had a

stronger response to congestion, which is a potential side effect of higher wind penetration levels.

6.) Discuss how the results impact the field of transmission planning - This objective is addressed in Section 7.3 to follow.

In conclusion, the PLF and HTC methods result in more realistic hydrogeneration in a PCM simulation, based on the criteria defined in this thesis. Specifically, they provide a more accurate input of the hydro plant's ability to follow load, by using the monthly *K* value unique to the plant's operation to dispatch generation in response to the forecasted load. The load-following hydrogeneration is in itself a more real-time representation than that modeled by HD or PS, since the basic function of any generator is to produce energy in response to the load, within its capabilities. Next, the hydrogeneration dispatch is further optimized in response to system energy prices with the HTC method. By using the fraction of the plant's hydrogeneration (based on the p factor) to react expressly to the variations in energy prices, as would also occur in real-time, the overall system simulation effectiveness is increased. Based on the results presented here, the use of combined PLF and HTC provides a more realistic representation of the WI system in a PCM simulation.

7.2 Further Studies

Based on the results of the 2019 case study, it would be valuable to confirm the results with a forecast comparison study. This would involve modeling the system operation from a past year in the PCM using PLF and HTC modeling methods, and comparing the results with the actual hydrogeneration dispatch, LMP values, and congestion levels. While a PCM simulation is never an exact replica of system operation due to the many assumptions and generalities that are present, a forecast/actual comparison would at least provide a measure of how effective

these models are at representing the hydrogeneration of the plants they are applied to, as well as how the modeling affects the system as a whole. In addition, since the PLF method is considered a valid interim model, more research on how to incorporate more extensive hydrogeneration models into a PCM-type simulation would also be valuable. While there is a lot of academic activity on this front, little of this has actually been incorporated into the commercially available packages that many planners use.

7.3 Industry Implications

Many planning entities use PCMs to compare future transmission options, as discussed in Section 2.2. However, many PCMs do not cost-optimize the hydrogeneration, and therefore may not provide an effective simulation of its future dispatch. This is of particular importance in operating systems with a high level of hydrogeneration production, since a significant portion of the total generation of the system may be misrepresented. The modeling methods presented here provide some measure of confidence that they are able to better forecast the realistic dispatch, for applicable plants, of hydrogeneration in a PROMOD simulation, as compared to the methods used previously. While the HTC method is PROMOD-specific, the PLF methods may be applicable to any PCM and be of use to any planning entity that uses PCM simulations in its transmission studies. The HTC concept could also be adopted by other PCM packages, so that the generation of plants that have the flexibility to respond to load and/or energy price variation can be more effectively reflected in a system simulation. This would lead to more informed transmission planning decisions, which represents an important factor for ensuring the reliability of the electricity grid in the future.

BIBLOGRAPHY

About NERC: Company Overview. (2011). Retrieved January 24, 2011, from North American Electric Reliability Corporation: http://www.nerc.com/page.php?cid=1|7

About WECC. (2011). Retrieved January 24, 2011, from Western Electricity Coordinating Council: http://www.wecc.biz/About/Pages/default.aspx

Acker, T. (2007). *Arizona Public Service Wind Integration Cost Impact Study*. Phoenix: Arizona Public Service Company.

Acker, T. (2005). Characterization of Wind and Hydropower. *Windpower*. Denver.

Acker, T. (2010). *Hydroelectric Industry's Role in Integrating Wind Energy*. Montreal: CEATI International Inc.

Acker, T. (2010). *Results of IEA Wind Implementing Agreement Task 24 on the Integration of Wind and Hydropower Systems*. Golden: NREL.

Acker, T., & Pete, C. (2011). *Western Wind and Solar Integration Study: Hydropower Analysis*. Golden: NREL.

Acker, T., Buechler, J., Knitter, K., & Conway, K. (2007). Impacts of Integrating Wind Power into the Grant County PUD Balancing Area. *Windpower 2007*. Los Angeles.

Alguacil, N., Motto, A., & Conejo, A. (2003). Transmission Expansion Planning: A Mixed-Integer LP Approach. *IEEE Transactions on Power Systems , 18* (3), 1070-1077.

Ancona, D., Krau, S., Lafrance, G., & Bezrukihk, P. (2003). . Operational Constraints and Economic Benefits of Wind-Hydro Hybrid Systems Analysis of Systems in the U.S./Canada and Russia. *European Wind Energy Conference*. Madrid.

Ancona, D., Krau, S., Lafrance, G., & Bezrukikh, P. (2003). Operational Constraints and Economic Benefits of Wind-Hydro Hybrid Systems Analysis of Systems in the U.S./Canada and Russia. *European Wind Energy Conference*. Madrid.

Borges, C., & Pinto, R. (2008). Small Hydro Power Plants Energy Availability Modeling for Generation Reliability Evaluation. *IEEE Transactions of Power Systems , 23* (3), 1125-1135.

Bunn, D., & Paschentis, S. (1986). Development of a Stochastic Model for the Economic Dispatch of Electric Power. *European Journal of Operational REsearch , 27*, 179-191.

Carrion, M., & Arroyo, J. (2006). A Computationally Efficient Mixed-Integer Linear Formulation for the Thermal Unit Commitment Problem. *IEEE Transactions on Power Systems , 21* (3), 1371-1378.

Chang, G., Aganagic, M., Waight, J., Medina, J., Reeves, S., & Christoforidis, M. (2001). Experiences with Mixed-Integer Linear Programming Based Approaches on Short-Term Hydro Scheduling. *IEEE Transactions on Power Systems , 16* (4), 743-749.

Chisholm, T. (2010). Personal Communication.

Chisholm, T., Miller, T., & Davies, D. (2008). *Hydrogeneration Modeling by the WECC Transmission Expansion Planning and Policy Committee*. WECC.

Cohen, J., Lafrance, G., Krau, S., & Saulnier, B. (2003). Analysis of Wind-Hydro Integration Value in Vermont. *Windpower 2003*.

Dennis, C., Walish, R., Pacini, H., Chisholm, T., & Acker, T. (2011). Improving Hydrogeneration in a Production Cost Model Used for Long-Term Transmission Studies in the Western Interconnection. *IEEE PES Conference*. Phoenix.

Diniz, A., & Maceira, M. (2008). A Four-Dimensional Model of Hydro Generation for the Short-Term Hydrothermal Dispatch Problem Considering Head and Spillage Effects. *IEEE Transactions on Power Systemsd , 23* (3), 1298-1308.

Drayton, G., McCoy, M., Pereira, M., Cazalet, E., Johannis, M., & Phillips, D. (2004). Transmission Expansion Planning in the Western Interconnection - The Planning Process and the Analytical Tools that will be Needed to do the Job. *IEEE Power Eng. Soc. Power Systems Conf. and Exp.*, (pp. 1556-1561).

EnerNex. (2010). *Eastern Wind Integration and Transmission Study*. NREL.

GE Energy. (2010). *Western Wind and Solar Integration Study*. NREL.

Georgilakis, P. (2008). Technical Challenges Associated with the Integration of Wind Power into Power Systems. *Renewable and Sustainable Energy Reviews , 12*, 852-863.

Gonzalez, J. (2002). Probabilistic Production Costing Modeled with AMPL. *IEEE Transactions on Power Systems , 17* (2), 277-282.

Gunasekara, C., Udawatt, L., & Witharana, S. (2006). Neural Network Based Optimum Model for Cascaded Hydro Power Generating System. *International Conference on Information and Automation*. Sri Lanka.

Hamilton, R., Lehr, R., Olsen, D., Nielson, J., Acker, T., Milligan, M., et al. (2004). *Integrating Wind into Transmission Planning: The Rocky Mountain Area Transmission Study (RMATS)*. Golden: NREL.

Hamlet, A., Huppert, D., & Lettenmaier, D. (2002). Economic Value of Long-Lead Streamflow Forecasts for Columbia River Hydropower. *Journal of Water Resources Planning and Management , 128* (2), 91-101.

Hirst, E. (2002). *Integrating Wind Energy with the BPA Power System: Preliminary Study*. Portland: Bonneville Power Administration.

Hirst, E., & Kirby, B. (2001). *Transmission Planning for a Restructuring U.S. Electric Industry*. Washington, D.C.: Edison Electric Institute.

Hiskens, I. (2006). Significance of Load Modeling in Power System Dynamics. *10th Symposium of Specialists in Electric Operational adn Expansion Planning*. Florianopolis.

Jaramillo, O., Borja, M., & Huacuz, J. (2004). Using Hydropower to Complement Wind Energy: A Hybrid System to Provide Firm Power. *Renewable Energy , 29*, 1887-1909.

Kahn, E. (1995). Regulation by Simulation: The Role of Production Cost Models in Electricity Planning and Pricing. *Operations Research , 43* (3), 388-398.

Kahn, E. (2010). Wind Integration Studies: Optimization vs. Simulation. *The Electricity Journal , 23* (9), 51-64.

Latorr, G., Cruz, R., Areiza, J., & Villegas, A. (2003). Classification of Publications and Models on Transmission Expansion Planning. *IEEE Transactions on Power Systems , 18* (2), 938-946.

Leevongwat, I., Rastgoufard, P., & Kaminsky, E. (2008). Status of Deregulation and Locational Marginal Pricing in Power Markets. *Southeastern Symposium on System Theory*, (pp. 193-197). New Orleans.

Li, C., Hsu, E., Svoboda, A., Tseng, C., & Johnson, R. (1997). Hydro Unit Commitment in Hydro-Thermal Optimization. *IEEE Transactions on Power Systems , 12* (2), 764-769.

Li, F. (2007). Continuous Locational Marginal Pricing (CLMP). *IEEE Transactions on Power Systems , 22* (4), 1638-1646.

Li, F. (2007). DCOPF-Based LMP Simulation: Algorithm, Comparison with ACOPF, and Sensitivity. *IEEE Transactions on Power Systems , 22* (4), 1475-1485.

Li, F., Yuan, H., & Tomsovic, K. (2009). Integrated Generation and Transmission Planning Tools under Competitive Energy Markets: An Academic Perspective. *IEEE PES General Meeting*. Calgary.

Lin, M., Breipohl, A., & Lee, F. (1989). Comparison of Probabilistic Production Cost Simulation Methods. *IEEE Transactions on Power Systems , 4* (4), 1326-1334.

Madsen, H., Kariniotakis, G., Nielsen, H., Nielsen, T., & Pinson, P. (2004). *A Protocol for Standardizing the Performance Evaluation of Short-Term Wind Power Prediction Models*. Project ANEMOS.

Nakmura, S. (1984). A Review of Electric Production Simulation and Capacity Expansion Planning Programs. *Energy Research , 8*, 231-240.

NERC. (2011). *Events Analysis: Transmission Loading Relief Procedure*. Retrieved from North American Electric Reliability Corporation: http://www.nerc.com/page.php?cid=5|67

Neto, T., Cotia, C., Pereira, M., & Kelman, J. (1985). Comparison of Stochastic and Deterministic Approaches in Hydrothermal Generation Scheduling. *IFAC Symposium on Planning and Operation of Electric Energy Systems*. Rio de Janeiro.

Nordlund, P., Sjelvgren, D., Pereira, M., & Bubenko, J. (1987). Generation Expansion Planning for Systems with a High Share of Hydro Power. *IEEE Transactions on Power Systems* , 161-167.

North American Electric Reliability Corporation. (2011). Retrieved January 24, 2011, from North American Electric Reliability Corporation: http://www.nerc.com/

Oh, H., & Short, W. (2009). Optimal Expansion Planning for the Deployment of Wind Energy. *Journal of Wind Engineering , 135* (3), 83-88.

Overbye, T., Cheng, X., & Sun, Y. (2004). A Comparison of the AC and DC Power Flow Models for LMP Calculations. *Procedings of the 37th Hawaii International Conference on System Sciences*.

Pacini, H. (2010). Personal Communication.

Pete, C. (2010). *Implications on Hydropower from Large-Scale Integration of Wind and Solar Power in the West*. Flagstaff: Northern Arizona University.

Rudnick, H. (2004). The Challenges of Transmission Expansion in the Chilean Power Sector: Market of Central Plannig. *Power Engineering Society General Meeting, 2004. IEEE*, (pp. 1301-1308).

Salam, S. (2007). Unit Commitment Solution Methods. *World Academy of Science, Engineering and Technology , 35*, 320-325.

Shawwash, Z., Siu, T., & Russell, S. (2000). The B.C. Hydro Short Term Hydro Scheduling Optimization Model. *IEEE Transactions on Power Systems , 15* (3), 1125-1131.

Simopoulos, D., Kavatza, S., & Vournas, C. (2007). An Enhanced Peak Shaving Method for Short Term Hydrothermal Scheduling. *Energy Conversion and Management* (48), 3018-3024.

Siqueira, T., Zambelli, M., Cicogna, M., Andrade, M., & Soares, S. (2006). Stochastic Dynamic Programming for Long Term Hydrothermal Scheduling Considering Different Streamflow Models. *9th International Conference on Probabalistic Methods Applied to Power Systems.* Stockholm: KTH.

Smith, J., Milligan, M., DeMeo, E., & Parsons, B. (2007). Utility Wind Integration and Operating Impact State of the Art. *IEEE Transactions on Power Systems , 22* (3).

Stewart, J. (2005). *Calculus Concepts and Contexts.* Belmont: Thomson Higher Education.

TEPPC Hydromodeling Task Force. (2009). HTC Description. *Technical Advisory Subcommittee* .

U.S. Department of Energy. (2009, June 16). *EERE State Activities and Partnerships.* Retrieved April 2011, from Energy Efficiency and Renewable Energy: http://apps1.eere.energy.gov/states/maps/renewable_portfolio_states.cfm

WECC. (2009). *2008 Annual Report of the Western Electricity Coordinating Council's Transmission Expansion Planning Policy Committee.* WECC.

WECC. (2010). *Transmission Expansion Plannining Policy Committee 2009 Study Program Results Report.* Salt Lake City: WECC.

WECC. (2011). *Western Electricity Coordinating Council Library.* Retrieved January 27, 2011, from Western Electricity Coordinating Counci: http://www.wecc.biz/library/default.aspx?RootFolder=/library/WECC%20Documents/Publications/Information%20Summaries&FolderCTID=0x012000278A29140A43884799CB122F821DFD01&View={8D18396E-7F8B-4472-AB30-18D2A9576FF0}

Westrick, K., Storck, P., & Froese, G. (2003). Reliance on REnewables-The Synergistic Relationship Between Wind and Hydropower. *AWEA Windpower 2003 Conference.* Austin.

Wood, A., & Wollenberg, B. (1996). *Power Generation Operation adn Control.* New York: Wiley.

Wu, R., Lee, T., & Hill, E. (1989). An Investigation of the Accuracy and the Characteristics of the Peak-Shaving Method Applied to Production Cost Calculations. *IEEE Transactions on Power Systems , 4* (3), 1043-1049.

Zagona, E., & Magee, T. (1999). Modeling Hydropower in Riverware. *Proceedings of the International Conference on Hydropower.* Las Vegas: ASCE.

Zambelli, M., Siqueira, T., Cicogna, M., & Soares, S. (2006). Deterministic versus stochastic models for long term hydrothermal scheduling. *Power Engineering Society General Meeting.* IEEE.

8 APPENDIX

Long term Hydrothermal Scheduling Problem

This section provides a general outline of the LTHS problem, using Zambelli et al. (2006) as the primary reference. Similar to production cost modeling, the overall objective for one hydro plant is:

$$min \sum_{t=1}^{T-1} \Psi_t (D_t - Gh_t) \quad \text{(A.1)}$$

This is subject to the following constraints:

$$Gh_t = kh_{lt} q_t \quad \text{(A.2)}$$

$$h_{lt} = \varphi(x_t) - \theta(u_t) - pc \quad \text{(A.3)}$$

$$x_t = x_{t-1} + (y_t - u_t)\gamma \quad \text{(A.4)}$$

$$u_t = q_t + s_t \quad \text{(A.5)}$$

$$\underline{x_t} \leq x_t \leq \overline{x}_t \quad \text{(A.6)}$$

$$\underline{u_t} \leq u_t \leq \overline{u}_t \quad \text{(A.7)}$$

$$\underline{q_t} \leq q_t \leq \overline{q}_t \quad \text{(A.8)}$$

$$\underline{s_t} \geq 0 \quad \text{(A.9)}$$

where Ψ_t is the operational cost, $Gh_t$is the hydrogeneration, D_t is the load demand, x_t is the water storage, u_t is the release from the reservoir, s_t is the spillage, q_t is the discharge through the turbines, y_t is the inflow into the reservoir, φ is the forebay elevation function, θ is the tailrace elevation function, underbars represent minimum bounds, overbars represent maximum bounds, *t* is the time, and *T* is the total time interval. Constants *pc*, k, and γ represent the average penstock loss of the hydro plant, a product constant (water density,

gravity acceleration, average efficiency), and a flow conversion factor, respectively. The operational cost Ψ_t is obtained from a parallel cost minimization of the thermal generation in the system associated with the hydro plant. To include multiple plants, Equation A.1 would become:

$$min \sum_{t=1}^{T-1} \sum_{i=1}^{N} \Psi_t (D_t - Gh_{ti}) \quad \text{(A.10)}$$

where *i* is the individual plant, and N is the total number of plants. If a deterministic solution method is used for the inflow, initial assumptions may be made from the expected inflow values of $\tilde{y}_t$. The recursive equation:

$$\alpha_{t-1}(x_{t-1}) = min\{C_p + C_f\} \quad \text{(A.11)}$$

where:

$$C_p = \Psi_t (D_t - Gh_t) \quad \text{(A.12)}$$

$$C_f = \alpha_t (x_t) \quad \text{(A.13)}$$

$$x_t = x_{t-1} + (\tilde{y}_t - u_t)\gamma \quad \text{(A.14)}$$

is solved backwards, where at *T*, $\alpha_t(x_t)$ is known (Zambelli, Siqueira, Cicogna, & Soares, 2006).

PCM 2019 DTC Profile

This section provides a summary of the PROMOD inputs 2019 and 2019LW DTC case development. The DTC used was the PC1a case described in the TEPPC 2009 Annual Study Report. This PROMOD case was built on a 2012 case, with additions of load, generation, and transmissions to meet 2019 forecasts (WECC, 2010). The load additions were determined by a work group, and once these were set the generation additions were determined. A primary goal for determining the generation additions consisted of meeting the RPS standards for every state and province of the WI. Table A.1 summarizes the WECC-wide generation additions to the 2012 case that formed the 2019 base case.

Table A.1: Generation capacity additions to 2012 data case to make the 2019 test case

	Hydro (MW)	Thermal (MW)	Renewable (MW)	Total (MW)
Existing (2012)	67,163	132,589	13,880	213,632
Additional Generation	3,201	19,503	35,416	57,719
Total (2019)	70,364	151,692	49,297	271,352

Next, a work group determined the minimal transmission additions that would be necessary for a 2019 system, based on the load and generation. Detailed descriptions of the transmission additions are found in the TEPPC 2009 Annual Report, and therefore are not shown here. In addition, Appendix B of the 2009 Annual Report contains the Matrix of Assumptions used for the PC1, including those relating to economics, generation, reserves, outages, and fuel, as well as the sources for the load, transmission, renewable generation, and hydrogeneration profiles used.

The *K* values and *p* factors used in the PLF and HTC hydromodeling are listed in Tables A.2 and A.3 below. As described in Section 3.4, the *K* value is halved for PLF modeling to be used with HTC modification.

Table A.2: Monthly *K* values for 2019 study plants

	***K* value**											
Plant	**Jan**	**Feb**	**Mar**	**Apr**	**May**	**Jun**	**Jul**	**Aug**	**Sep**	**Oct**	**Nov**	**Dec**
John Day	1.17	1.14	0.61	1.0	0.97	0.95	1.21	1.58	1.14	1.22	1.13	1.13
The Dalles	1.19	1.11	0.63	0.90	0.50	0.50	0.76	0.98	1.22	1.19	1.04	1.13

	***K* value**											
Brownlee	3.0	3.0	3.0	3.0	3.0	3.0	3.0	3.0	3.0	3.0	3.0	3.0
Round Butte	3.0	3.0	3.0	3.0	3.0	3.0	3.0	3.0	3.0	3.0	3.0	3.0
Chief Joseph	2.58	2.41	2.41	1.32	1.49	1.47	1.57	2.04	2.91	2.73	2.48	2.17
Little Goose	2.34	2.34	0.60	1.46	1.35	0.61	1.16	1.52	1.49	0.70	0.69	3.09
Boundary	3.97	4.22	3.87	3.0	3.0	3.0	3.0	3.48	3.77	3.60	4.17	4.89
Wells	2.68	2.63	3.33	1.55	1.40	1.50	1.50	2.31	2.76	2.93	2.11	3.25
Grand Coulee	3.03	3.26	3.05	1.78	2.23	2.36	2.21	2.44	3.16	2.83	2.72	2.65
Rocky Reach	1.65	1.24	2.26	1.15	0.86	1.00	1.00	2.14	2.52	2.30	1.63	2.12
Noxon	3.00	3.00	3.00	3.00	3.00	3.00	3.00	3.00	3.00	3.00	3.00	3.00
Lower Monumental	2.15	2.12	0.53	1.01	0.68	0.32	1.38	1.77	1.50	0.70	0.43	2.93

Table A.3: Monthly p factors for 2019 study plants

	***p* factor**											
Plant	**Jan**	**Feb**	**Mar**	**Apr**	**May**	**Jun**	**Jul**	**Aug**	**Sep**	**Oct**	**Nov**	**Dec**
John Day	0.06	0.05	0.03	0.06	0.05	0.04	0.04	0.04	0.02	0.03	0.03	0.05
The Dalles	0.06	0.06	0.03	0.05	0.02	0.02	0.02	0.02	0.02	0.03	0.03	0.05
Brownlee	0.10	0.10	0.10	0.10	0.10	0.10	0.10	0.10	0.10	0.10	0.10	0.10
Round Butte	0.10	0.10	0.10	0.10	0.10	0.10	0.10	0.10	0.10	0.10	0.10	0.10
Chief Joseph	0.11	0.11	0.11	0.10	0.08	0.09	0.08	0.10	0.08	0.09	0.11	0.12
Little Goose	0.06	0.08	0.02	0.05	0.06	0.03	0.03	0.03	0.02	0.01	0.01	0.05
Boundary	0.11	0.11	0.11	0.11	0.11	0.11	0.11	0.05	0.04	0.11	0.11	0.11
Wells	0.13	0.11	0.11	0.09	0.06	0.07	0.07	0.09	0.07	0.09	0.08	0.11
Grand Coulee	0.11	0.11	0.12	0.12	0.11	0.13	0.11	0.09	0.07	0.08	0.11	0.12
Rocky Reach	0.08	0.06	0.09	0.07	0.04	0.05	0.04	0.08	0.06	0.07	0.06	0.10
Noxon	0.07	0.08	0.06	0.11	0.11	0.11	0.11	0.03	0.03	0.04	0.08	0.07
Lower Monumental	0.06	0.08	0.01	0.04	0.03	0.02	0.04	0.03	0.02	0.01	0.00	0.05

2019 DTC Load and Wind Profiles

To present a picture of the 2019 load for the study BAs used in the PCM study, the yearly load profile used for both the 2019 DTC and the 2019LW DTC is shown in Figure A.1 below. In addition, the yearly wind profiles for both DTCs are shown in Figures A.2 and A.3.

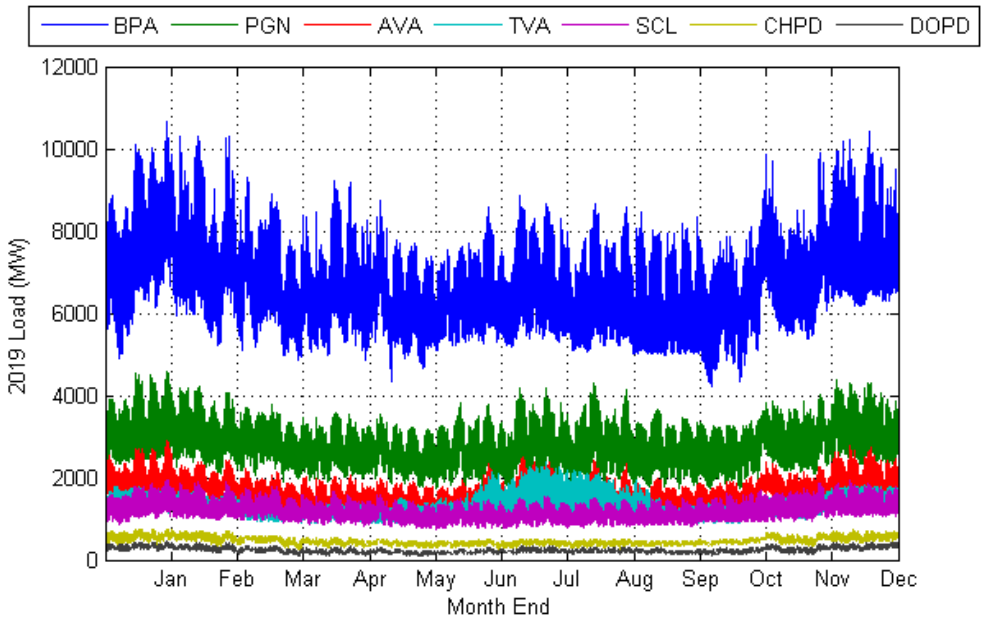

Figure A.1: 2019 yearly load profiles for study BAs

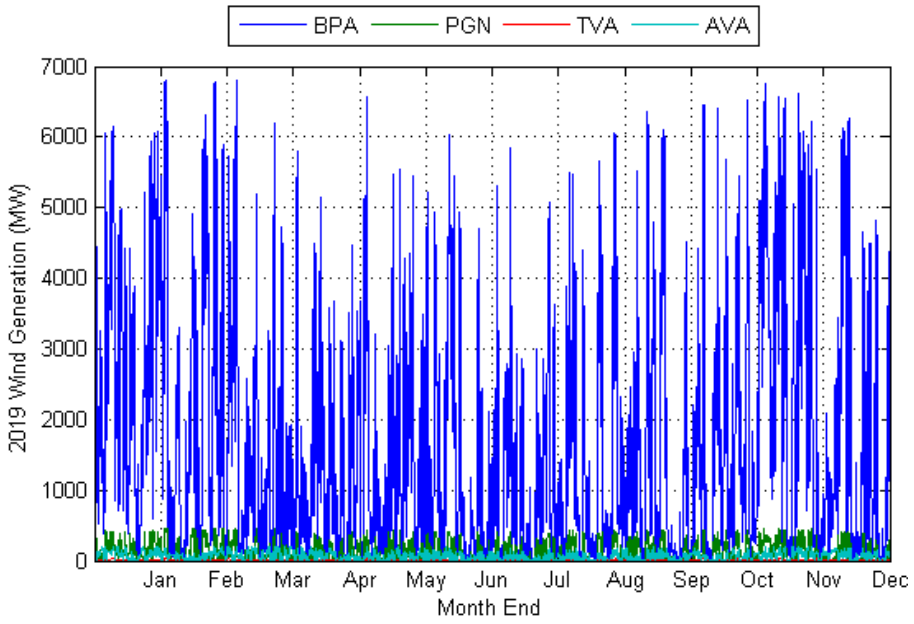

Figure A.2: 2019 DTC yearly wind profiles for study BAs

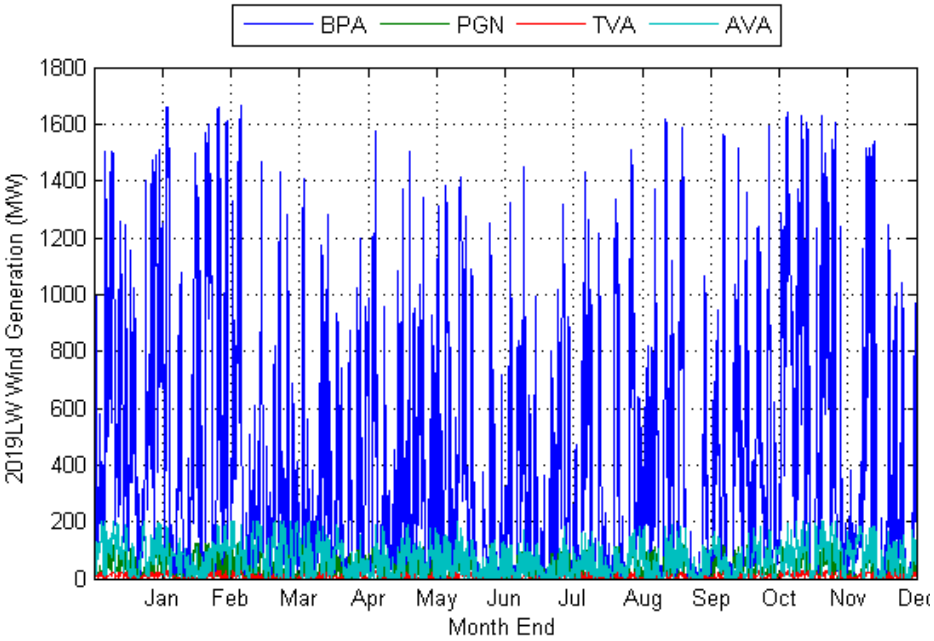

Figure A.3: 2019LW yearly wind profiles for study BAs

The transmission flow duration curves for the study paths are shown in the following figures. As discussed, the 2019LW DTC transmission duration curves did not differ from the 2019 DTC, with the exception of the COI and the PDCI, shown in Section 6.3.

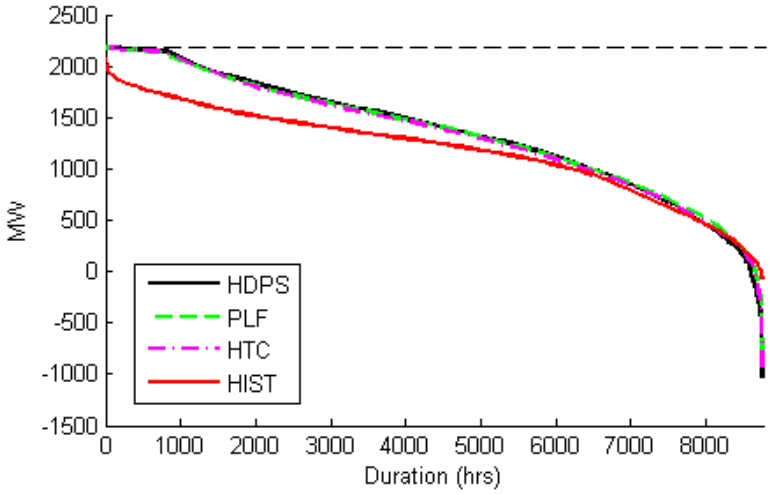

Figure A.4: 2019 MNW transmission duration curve. Black dashed line is the TTC of 2,200 MW

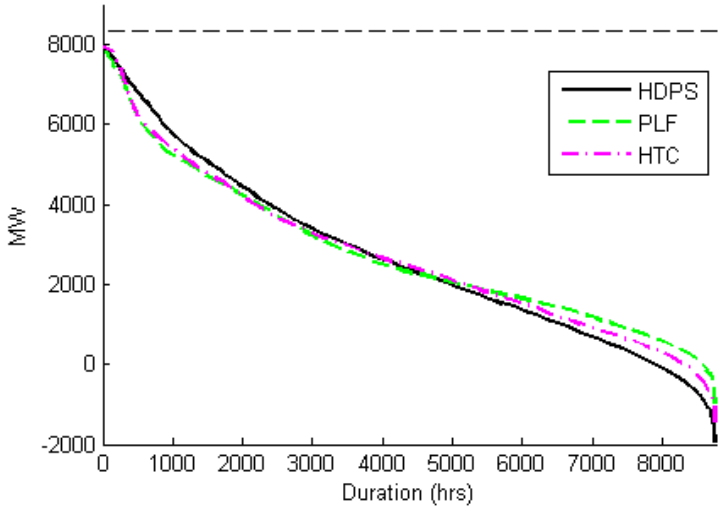

Figure A.5: 2019 NJD transmission duration curve. Black dashed line is TTC of 8,400 MW

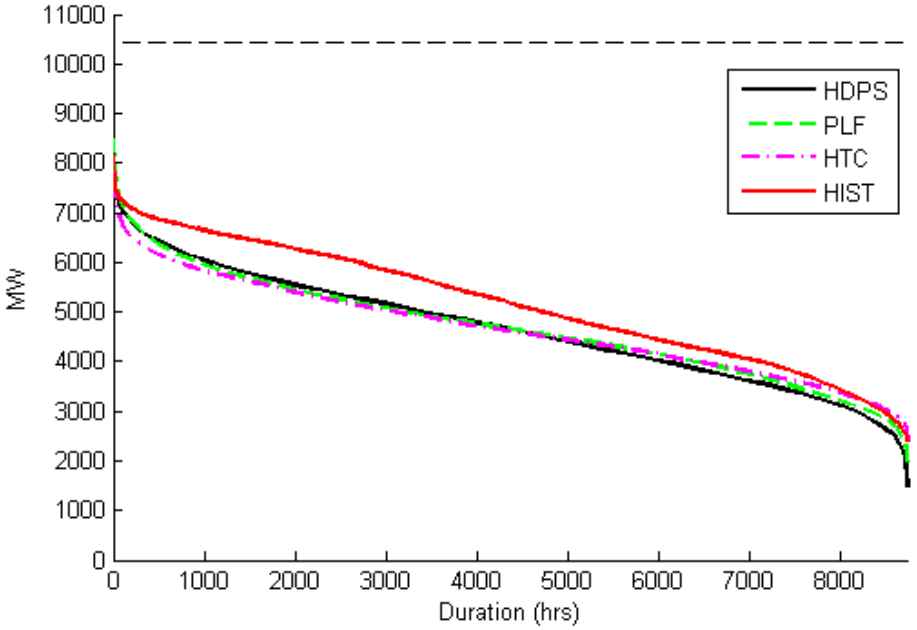

Figure A.6: 2019 WCN transmission duration curve. Black dashed line is TTC of 10,500 MW

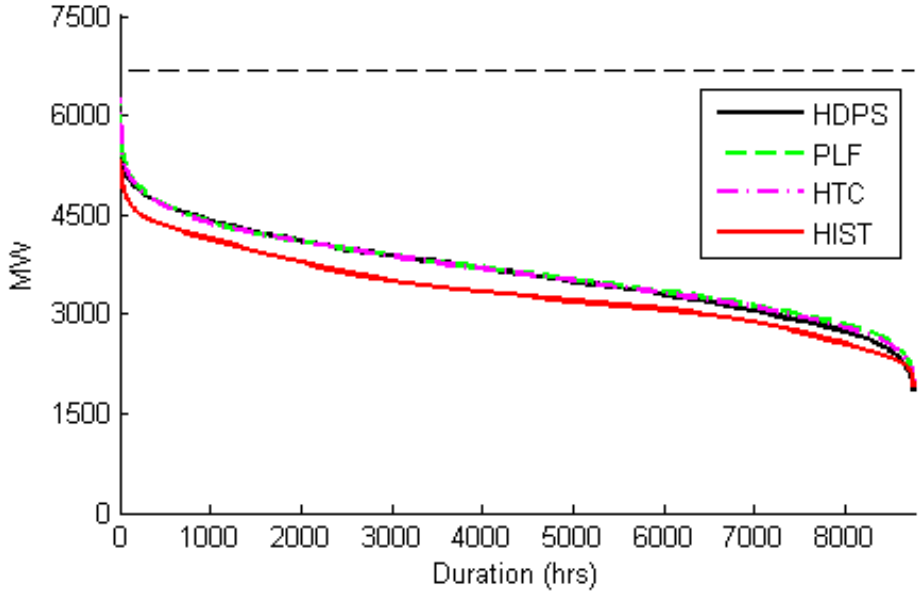

Figure A.7: 2019 WCS transmission duration curve. Black dashed line is TTC of 7,000 MW